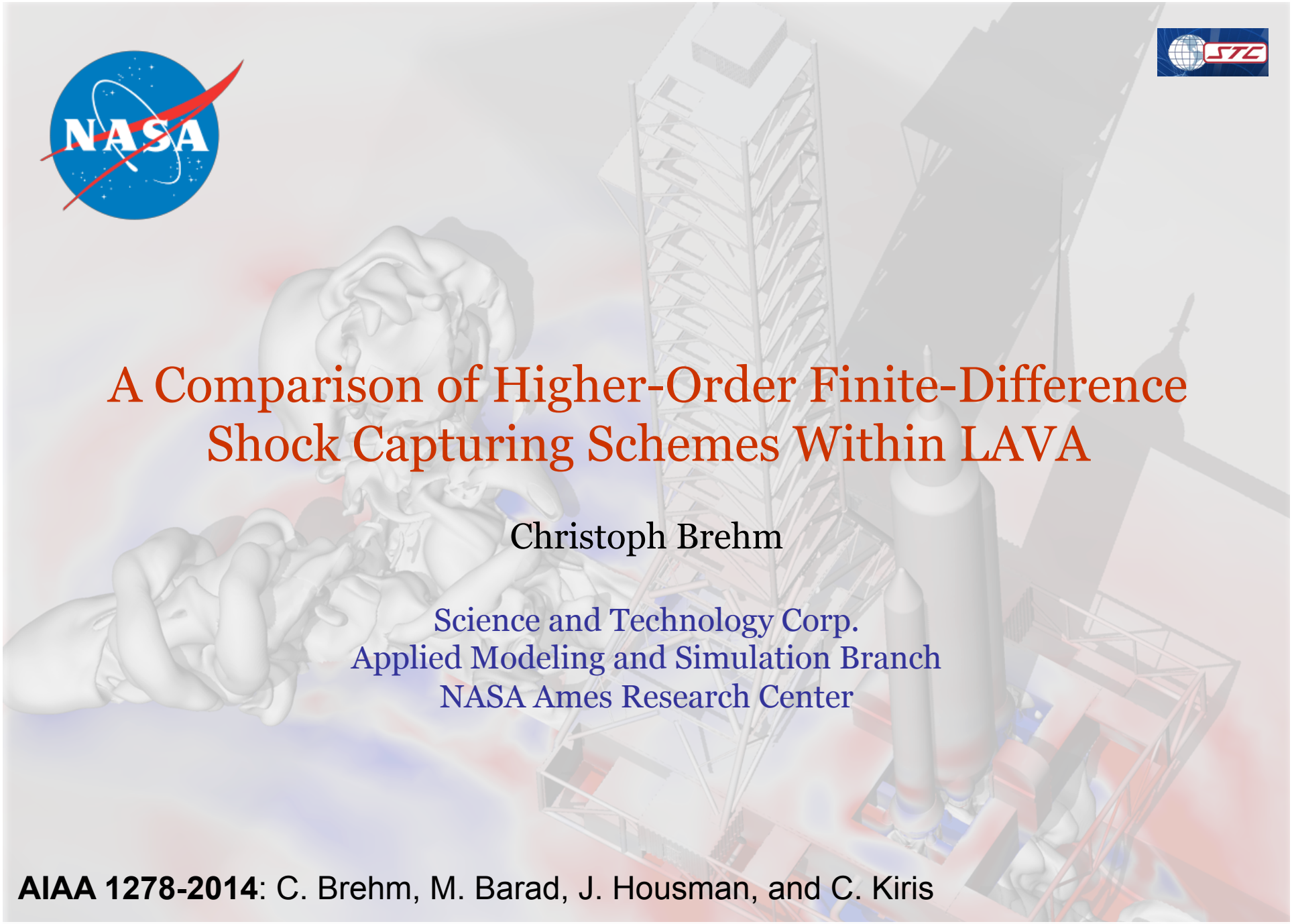


# A Comparison of Higher-Order Finite-Difference Shock Capturing Schemes Within LAVA

Christoph Brehm

Science and Technology Corp.
Applied Modeling and Simulation Branch
NASA Ames Research Center

**AIAA 1278-2014**: C. Brehm, M. Barad, J. Housman, and C. Kiris

# Outline

## Motivation
*Motivation of higher-order schemes for LAVA.*

## Higher-Order Shock Capturing Schemes
*Overview of different higher-order shock capturing schemes in LAVA.*

## Accuracy
*Accuracy study including nonlinear weights, filtering, and dissipation terms.*

## Test Problems
*Various test problems: 1D shock problems to isotropic turbulence.*

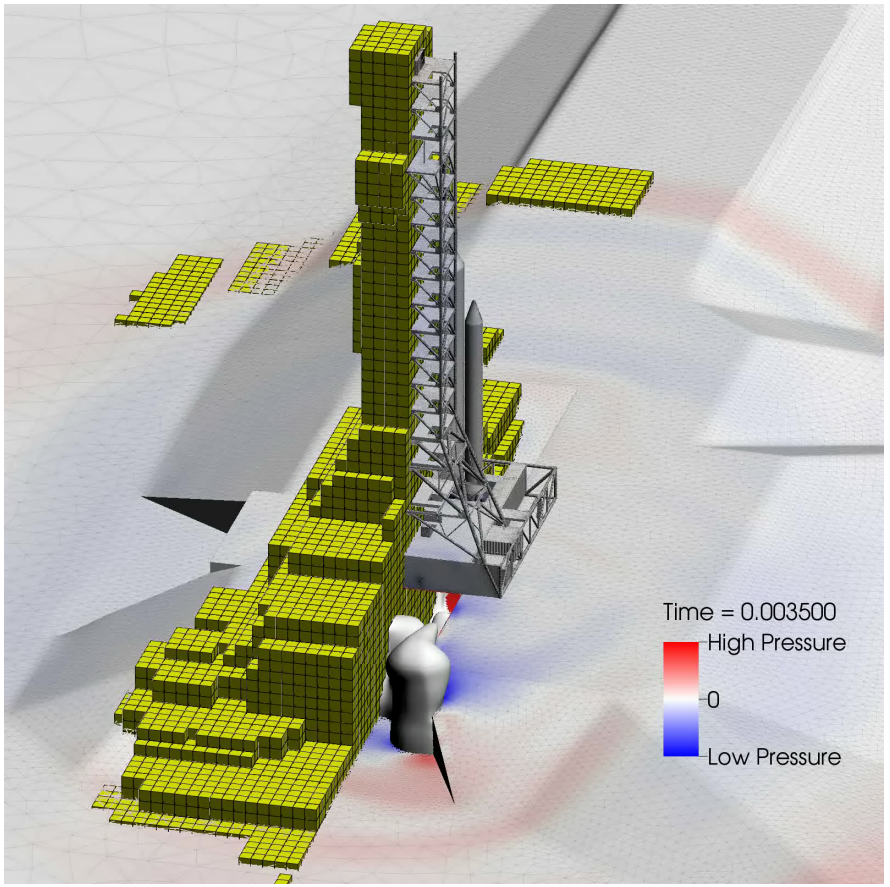
## Computational Performance
*Analysis and comparison of computational cost.*

## Summary & Future Work
*Summary of results and what tasks lie ahead.*

Motivation:

# Launch Ascent & Vehicle Aerodynamics

- Developed by the authors* at NASA Ames Research Center
- Supports Cartesian AMR, block structured-curvilinear overset, and unstructured arbitrary polyhedral cells




Block-Structured Cartesian Solver:

- For accuracy and efficiency
- Adaptive mesh refinement (AMR) for tracking flow features with local refinement (gradient, entropy adjoint, and geometry based)
- High-performance MPI-parallel AMR data-structures and inter-level operators from Chombo library.

*Kiris et al.(2014), Sozer et al. (2014)

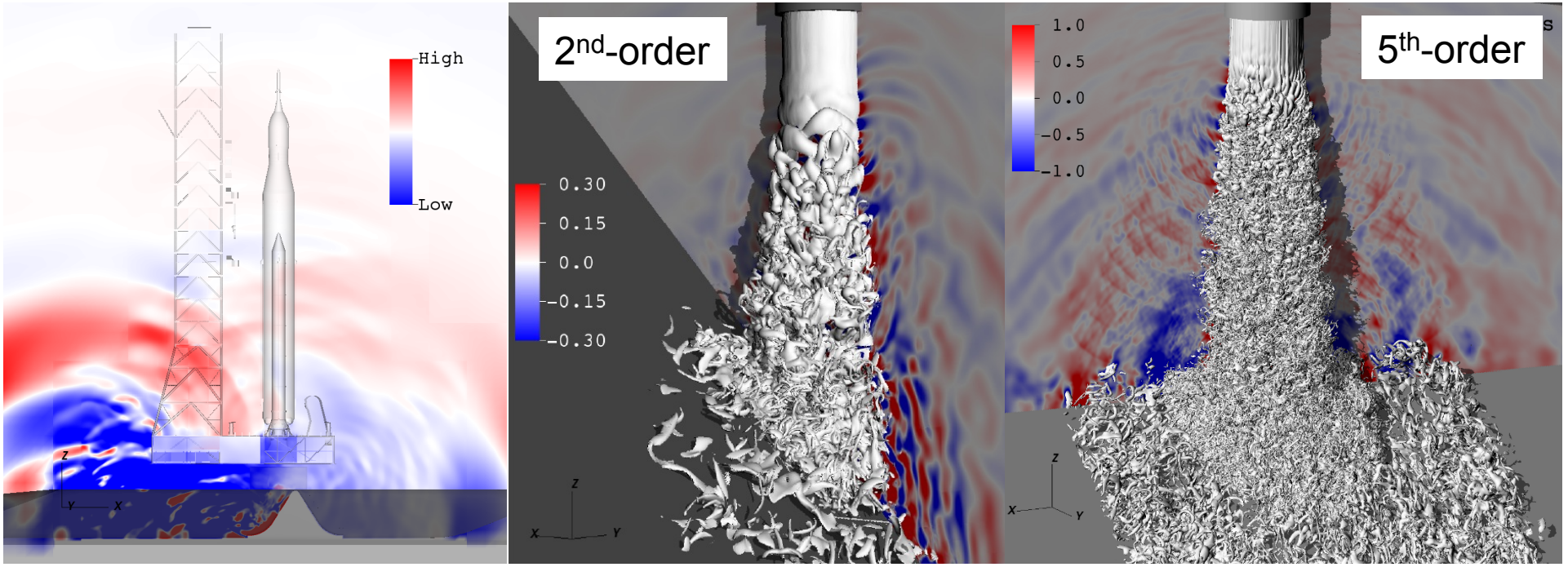
Motivation:

# Why Higher-Order Methods?

- Initial stage of rocket launch involves highly unsteady flow fields:

IOP

Launch Acoustics




- Rocket launch CFD simulations involve highly unsteady and shocked flows
- Unsteady jet impingement simulations* require high-fidelity computations to correctly capture noise signature

*Brehm et al.(2013)

# Outline

Motivation/Introduction

Higher-Order Shock Capturing Schemes

*Overview of different higher-order shock capturing schemes in LAVA.*

Accuracy

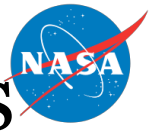
Test Problems

Computational Performance

Summary & Future Work

Numerical Methods:

# Higher-Order Shock Capturing Schemes







- Central FD with Explicit Artificial Dissipation (Central)
  - Lowest computational cost of all higher-order schemes considered here
  - Relies on explicit second-difference dissipation term for shocked flows

- Localized Artificial Diffusivity (LAD)
  - Add artificial transport properties to regularize equations
  - Promises low computational cost (not as cheap as Central)
  - High spectral resolution is achieved with compact finite-differences
  - High artificial viscosities may reduce $\Delta t$ limit especially on stretched grids

- Weighted Essentially Non-Oscillatory (WENO)
  - Well established method for shock capturing
  - Relies on non-linear smoothness indicator, locally reduces order-of-accuracy
  - Very robust and provides sharply resolved shocks
  - Steady-state convergence issues reported in the literature
  - Characteristic variable transform is most expensive component
  - Recent developments on improving spectral resolution accuracy

# Central FD with Artificial Dissipation

- Basic Scheme:

$$\frac{\partial F}{\partial x} \approx D_x^{(n)} + AD,$$

- Sixth-Order Explicit Finite-Difference Scheme:

$$D_x^{(6)} F_i = \frac{F_{i+3} - 9F_{i+2} + 45F_{i+1} - 45F_{i-1} + 9F_{i-2} - F_{i-3}}{60\Delta x}$$

- Explicit Artificial Dissipation:

$$AD = \frac{1}{\Delta x}(F^{AD}_{i+\frac{1}{2}} - F^{AD}_{i-\frac{1}{2}})$$

$$\begin{aligned} F^{AD}_{i+\frac{1}{2}} &= \alpha_6 \sigma_{i+\frac{1}{2}} \Gamma_{p,i+\frac{1}{2}} \left[10(Q_i - Q_{i+1}) - 5(Q_{i-1} - Q_{i+2}) + (Q_{i-2} - Q_{i+3})\right] \\ &- \alpha_2 \sigma_{i+\frac{1}{2}} \Gamma_{p,i+\frac{1}{2}} \left[Q_i - Q_{i+1}\right], \end{aligned}$$

  - Pressure gradient switch and spectral radius scaling identifies discontinuities and large gradients in the flow field

$$\begin{aligned} \alpha_2 &= \frac{\epsilon_2}{4}\left(\frac{1}{2}(\Psi_{i+1} + \Psi_i)\right), \quad \alpha_6 = \epsilon_6 - \min\left(\alpha_2, \epsilon_6\right), \text{ and} \\ \Psi_i &= \frac{|p_{i+1} - 2p_i + p_{i-1}|}{\frac{1}{4}|p_{i+1} + 2p_i + p_{i-1}|}. \end{aligned}$$

*Buning and Pulliam (2011), Pulliam (2011), Jameson (1981)

Numerical Methods:

# Localized Artificial Diffusivity Method







- Idea:
  Locally add artificial shear viscosity, bulk viscosity, thermal conductivity, and species diffusivity to the fluid properties to smooth out discontinuities

- Cook and Cabot (2004):
  Introduced this method as an alternative for LES of flows involving shocks
  - referred to Artificial-Fluid Large-Eddy Simulation (AFLES)

- Artificial Shear Viscosity: $\mu^* = C_\mu \overline{\rho |\nabla^r F_\mu|} \Delta^{r+2}$ and $\nabla^r \sim \sum_{k=1}^{D} \partial^r / \partial x_k^r$ (polyhamonic operator)

  $F_\mu = (\underline{\mathbf{S}}:\underline{\mathbf{S}})^{1/2}$ … treats unresolved turbulence

- Artificial Thermal conductivity: $\kappa^* = C_\kappa \overline{\frac{\rho c_s}{T} |\nabla^r F_\kappa|} \Delta^{r+1}$

  $F_\kappa = e = p/(\rho(\kappa-1))$… addresses contact discontinuity and unresolved turbulence

- Artificial Bulk Viscosity: $\beta^* = C_\beta \overline{\rho f_{sw} |\nabla^r F_\beta|} \Delta^{r+2}$

  $F_\beta$ = S or Div($\mathbf{u}$)… smoothes shock waves

  $f_{sw}$ … localizes bulk viscosity near shocks (Ducros type sensor × H(-Div($\mathbf{u}$)))

*Cook and Cabot (2004, 2005), Cook (2007), Fiorina and Lele (2007), Mani et al. (2009), Kawai et al. (2008, 2010), Olson et al. (2013) Gaitonde and Visbal (2000)

# Localized Artificial Diffusivity Method

- Flux derivative … Sixth-Order Compact/Explicit Finite-Difference

$$\beta\frac{\partial\phi}{\partial x_k}\bigg|_{i-2}+\alpha\frac{\partial\phi}{\partial x_k}\bigg|_{i-1}+\frac{\partial\phi}{\partial x_k}\bigg|_{i}+\alpha\frac{\partial\phi}{\partial x_k}\bigg|_{i+1}+\beta\frac{\partial\phi}{\partial x_k}\bigg|_{i+2}$$
$$=a\frac{\phi_{i+1}-\phi_{i-1}}{2\Delta x_k}+b\frac{\phi_{i+2}-\phi_{i-2}}{4\Delta x_k}+c\frac{\phi_{i+3}-\phi_{i-3}}{6\Delta x_k}.$$

- Fourth derivative … Sixth-Order Compact/Explicit Finite-Difference

$$\alpha\frac{\partial^4\phi}{\partial x_k^4}\bigg|_{i-1}+\frac{\partial^4\phi}{\partial x_k^4}\bigg|_{i}+\alpha\frac{\partial^4\phi}{\partial x_k^4}\bigg|_{i+1}=$$
$$\frac{b(\phi_{i+3}+\phi_{i-3})+6a(\phi_{i+2}+\phi_{i-2})-(24a+9b)(\phi_{i+1}+\phi_{i-1})+(36a+16b)\phi_i}{6\Delta x^4}$$

- Truncated Gaussian Filter … stencil widths= 3 & 4

$$\overline{\phi}_i=\sum_{m=1}^{N_f}d_m\left(\phi_{i+m-1}+\phi_{i-m+1}\right)$$

- Eight-Order accurate Compact/Explicit filter …

$$\alpha_f\hat{\phi}_{i-1}+\hat{\phi}_i+\alpha_f\hat{\phi}_{i+1}=\sum_{m=0}^{N_f}a_m\frac{\phi_{i+m}+\phi_{i-m}}{2}$$

# Weighted Essentially Non-Oscillatory




- WENO (FD): $\frac{\partial f}{\partial x} = \frac{1}{\Delta x}(h_{i+1/2} - h_{i-1/2}) = \frac{1}{\Delta x}(\hat{f}_{i+1/2} - \hat{f}_{i-1/2}) + \mathcal{O}\left(\Delta x^{2n-1}\right)$
- Final interface ϕ (q or f): $\hat{\phi}_{i+1/2} = \sum_{k=1}^{n} \omega_k \phi_{i+1/2}^k$
- Standard smoothness indicator: $\beta_k = \sum_{j=1}^{2} \Delta x^{2j-1} \int_{x_{i-1/2}}^{x_{i+1/2}} \left(\frac{d^j}{dx^j}\hat{f}_k(x)\right)^2 dx$
- WENO-JS (Jiang & Shu 1996): $\alpha_k = \frac{c_k}{(\beta_k + \epsilon)^p}$ and $\omega_k = \frac{\alpha_k}{\sum_k^n \alpha_k}$
- WENO-M (Henrick 2005): mapping function f($w_k$) increases accuracy at crit. pts.
- WENO-Z (Borges 2008): mimic WENO-M with reduced cost (~25%)
- WENO6 (Hu *et al.* 2010): centered finite-difference, additional candidate stencil
- WENO5B (LAVA): basically a blend with WENO5 and WENO6
- CWENO5 (Ghosh & Baeder 2012): compact finite-difference, tri-diagonal solve, block/domain treatment

# Weighted Essentially Non-Oscillatory




- WENO (FD): $\frac{\partial f}{\partial x} = \frac{1}{\Delta x}(h_{i+1/2} - h_{i-1/2}) = \frac{1}{\Delta x}(\hat{f}_{i+1/2} - \hat{f}_{i-1/2}) + \mathcal{O}\left(\Delta x^{2n-1}\right)$
- Final interface ϕ (q or f): $\hat{\phi}_{i+1/2} = \sum_{k=1}^{n} \omega_k \phi_{i+1/2}^k$
- Standard smoothness indicator: $\beta_k = \sum_{j=1}^{2} \Delta x^{2j-1} \int_{x_{i-1/2}}^{x_{i+1/2}} \left(\frac{d^j}{dx^j}\hat{f}_k(x)\right)^2 dx$
- WENO-JS (Jiang & Shu 1996): $\alpha_k = \frac{c_k}{(\beta_k + \epsilon)^p}$ and $\omega_k = \frac{\alpha_k}{\sum_k^n \alpha_k}$

**nonlinear weights**

- WENO-M (Henrick 2005): mapping function f($w_k$) increases accuracy at crit. pts.
- WENO-Z (Borges 2008): mimic WENO-M with reduced cost (~25%)
- WENO6 (Hu *et al.* 2010): centered finite-difference, additional candidate stencil
- WENO5B (LAVA): basically a blend with WENO5 and WENO6
- CWENO5 (Ghosh & Baeder 2012): compact finite-difference, tri-diagonal solve, block/domain treatment

# Weighted Essentially Non-Oscillatory




- WENO (FD): $\frac{\partial f}{\partial x} = \frac{1}{\Delta x}(h_{i+1/2} - h_{i-1/2}) = \frac{1}{\Delta x}(\hat{f}_{i+1/2} - \hat{f}_{i-1/2}) + \mathcal{O}\left(\Delta x^{2n-1}\right)$
- Final interface ϕ (q or f): $\hat{\phi}_{i+1/2} = \sum_{k=1}^{n} \omega_k \phi_{i+1/2}^k$
- Standard smoothness indicator: $\beta_k = \sum_{j=1}^{2} \Delta x^{2j-1} \int_{x_{i-1/2}}^{x_{i+1/2}} \left(\frac{d^j}{dx^j}\hat{f}_k(x)\right)^2 dx$
- WENO-JS (Jiang & Shu 1996): $\alpha_k = \frac{c_k}{(\beta_k + \epsilon)^p}$ and $\omega_k = \frac{\alpha_k}{\sum_k^n \alpha_k}$
- WENO-M (Henrick 2005): mapping function f($w_k$) increases accuracy at crit. pts.

**underlying optimal scheme (+ nonlinear weights)**

- ...himic WENO-M with reduced cost (~25%)
- WENO6 (Hu *et al.* 2010): centered finite-difference, additional candidate stencil
- WENO5B (LAVA): basically a blend with WENO5 and WENO6
- CWENO5 (Ghosh & Baeder 2012): compact finite-difference, tri-diagonal solve, block/domain treatment

# Weighted Essentially Non-Oscillatory

- WENO in Finite-Difference Form: $f(x) = \frac{1}{\Delta x}\int_{x-\Delta x/2}^{x+\Delta x/2} h(\xi)d\xi$

$$\frac{\partial f}{\partial x} = \frac{1}{\Delta x}(h_{i+1/2} - h_{i-1/2}) = \frac{1}{\Delta x}(\hat{f}_{i+1/2} - \hat{f}_{i-1/2}) + \mathcal{O}\left(\Delta x^{2n-1}\right)$$

- Final interface ϕ (q or f): $\hat{\phi}_{i+1/2} = \sum_{k=1}^{n} \omega_k \phi_{i+1/2}^k$
- WENO-JS: $\alpha_k = \frac{c_k}{(\beta_k + \epsilon)^p}$ and $\omega_k = \frac{\alpha_k}{\sum_k^n \alpha_k}$
- WENO-M: $\tilde{\omega}_k = \frac{\omega'(c_k + (c_k)^2 - 3c_k\omega' + \omega'^2)}{c_k^2 + (1-2c_k)\omega'}$
- WENO-Z: $\beta_k^Z = \frac{\beta_k + \epsilon}{\beta_k + \tau_5 + \epsilon}$, $\alpha_r^Z = \frac{c_k}{\beta_k^Z} = c_k\left(1 + \frac{\tau_5}{\beta_k + \epsilon}\right)$ and $\omega_k^Z = \frac{\alpha_k^Z}{\sum_{i=0}^{2}\alpha_i^Z}$
- Standard smoothness indicator: $\beta_k = \sum_{j=1}^{2} \Delta x^{2j-1} \int_{x_{i-1/2}}^{x_{i+1/2}} \left(\frac{d^j}{dx^j}\hat{f}_k(x)\right)^2 dx$

# Weighted Essentially Non-Oscillatory







Candidate Stencils

Flux Derivative

- **WENO5** (f):

$$\hat{f}^0_{i+1/2} = \frac{1}{3}f_{i-2} - \frac{7}{6}f_{i-1} + \frac{11}{6}f_i,$$

$$\hat{f}^1_{i+1/2} = -\frac{1}{6}f_{i-1} + \frac{5}{6}f_i + \frac{1}{3}f_{i+1}, \text{and}$$

$$\hat{f}^2_{i+1/2} = \frac{1}{3}f_i + \frac{5}{6}f_{i+1} - \frac{1}{6}f_{i+2}.$$

with $c_0$=1/10, $c_1$=6/10, and $c_2$=3/10

$$\left.\frac{\partial f}{\partial x}\right|_i = \frac{1}{\Delta x}\left(\hat{f}_{i+1/2} - \hat{f}_{i-1/2}\right)$$

Can only use flux vector splitting schemes.

- **WCNS5** (Nonomura 2010):

$$\hat{q}^0_{i+1/2} = \frac{3}{8}q_{i-2} - \frac{5}{4}q_{i-1} + \frac{15}{8}q_i,$$

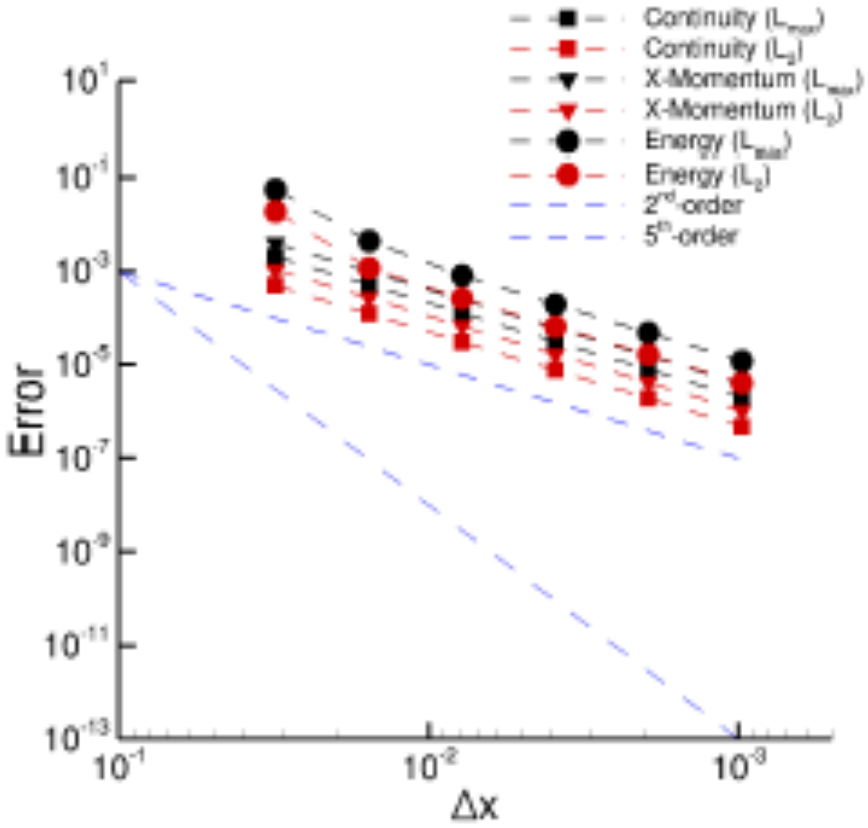
$$\hat{q}^1_{i+1/2} = -\frac{1}{8}q_{i-1} + \frac{3}{4}q_i + \frac{3}{8}q_{i+1}, \text{ and}$$

$$\hat{q}^2_{i+1/2} = \frac{3}{8}q_i + \frac{3}{4}q_{i+1} - \frac{1}{8}q_{i+2}.$$

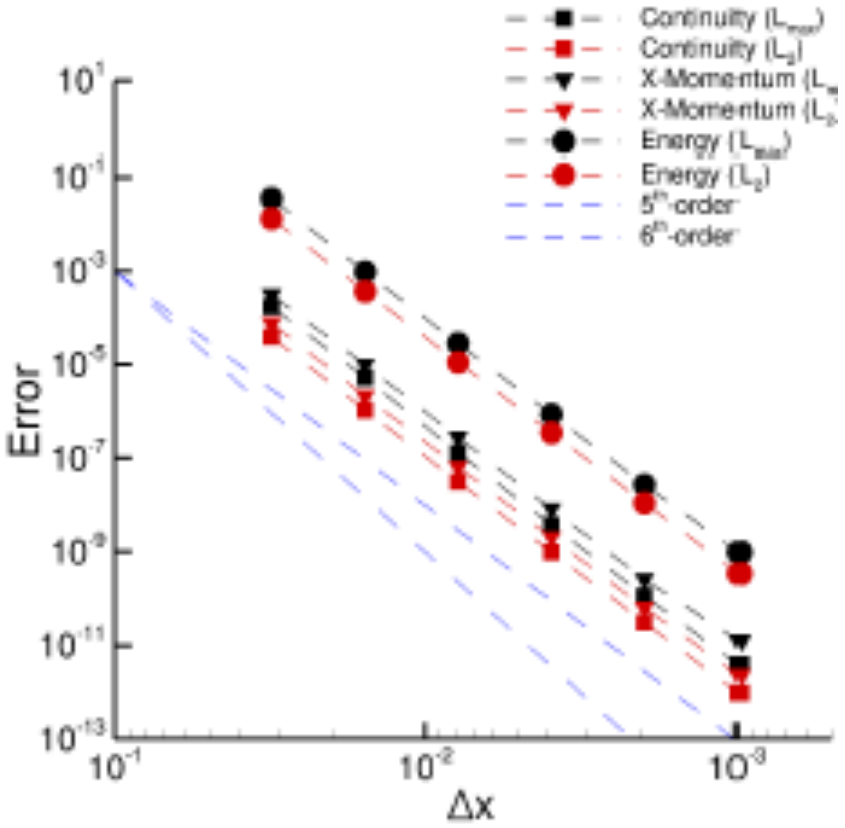
with $c_0$=1/10, c1=6/10, and c2=3/10

$$\left.\frac{\partial f}{\partial x}\right|_{i-1} + b\left.\frac{\partial f}{\partial x}\right|_i + c\left.\frac{\partial f}{\partial x}\right|_{i+1} = \frac{1}{\Delta x}\sum_{k=0}^{N}\alpha_k\left(\hat{f}_{i+k+1/2} - \hat{f}_{i+k-1/2}\right)$$

# Weighted Essentially Non-Oscillatory




Fifth-order accurate WENO variable extrapolation with simple midpoint rule




WCNS: Fifth-order accurate WENO variable extrapolation with higher-order differentiation (Nonomura et al.,2010)

# Improved WENO Schemes





**WENO6**, Hu et al.(2010):

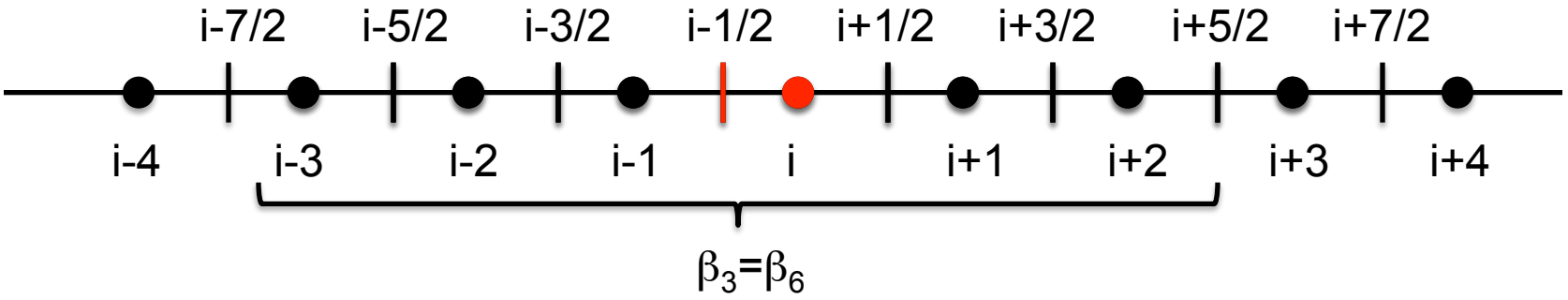
- Additional candidate stencil to obtain 6th-order centered scheme

$$\hat{f}^3_{i+1/2} = \frac{11}{6} f_{i+1} - \frac{7}{6} f_{i+2} + \frac{2}{6} f_{i+3}$$

linear weights: $c_0$=1/20, $c_1$=9/20, $c_2$=9/20, and $c_3$=1/20

- Nonlinear weights $\omega_k = \dfrac{\alpha_k}{\sum_{k=0}^{3} \alpha_k}$, and $\alpha_k = c_k \left( C + \dfrac{\tau_6}{\beta_k + \epsilon} \right)$ with C=20

- Smoothness indicator $\tau_6 = \beta_6 - \dfrac{1}{6} (\beta_0 + \beta_2 + 4\beta_1)$




**WENO5B**, LAVA:

- basically a blend with WENO5 and WENO6

# Improved WENO Schemes







**CWENO5**, Ghosh and Baeder (2012):

- Compact reconstruction stencils

$$\frac{2}{3}\hat{f}^0_{i-1/2} + \frac{1}{3}\hat{f}^0_{i+1/2} = \frac{1}{6}\left(f_{i-1} + 5f_i\right),$$
$$\frac{1}{3}\hat{f}^1_{i-1/2} + \frac{2}{3}\hat{f}^1_{i+1/2} = \frac{1}{6}\left(5f_i + f_{i+1}\right), \text{ and}$$
$$\frac{2}{3}\hat{f}^2_{i+1/2} + \frac{1}{3}\hat{f}^2_{i+3/2} = \frac{1}{6}\left(f_i + 5f_{i+1}\right).$$

- Tri(-block)-diagonal implicit system of equations

$$\left(\frac{2}{3}\omega_0 + \frac{1}{3}\omega_1\right)\hat{f}_{i-1/2} + \left(\frac{1}{3}\omega_0 + \frac{2}{3}\left(\omega_1 + \omega_2\right)\right)\hat{f}_{i+1/2} + \frac{1}{3}\omega_2\hat{f}_{i+3/2} =$$
$$\frac{\omega_0}{6}f_{i-1} + \frac{5\left(\omega_0 + \omega_1\right) + \omega_2}{6}f_i + \frac{\omega_1 + 5\omega_2}{6}f_{i+1}$$

- Explicit block/domain boundary treatment reduces order of accuracy

$$\left.\frac{\partial f}{\partial x}\right|_{x=x_j} = \frac{h_{j+1/2} - h_{j-1/2}}{\Delta x} - \frac{3}{200}\left.\frac{\partial^5 f}{\partial x^5}\right|_{x=x_j}\Delta x^4.$$

# CWENO: Block Boundary Treatment

- Numerical flux derivative at $x_i$:

$$\left.\frac{\partial f}{\partial x}\right|_{x=x_i} = \frac{h_{i+1/2} - h_{i-1/2}}{\Delta x} \approx \frac{\hat{f}_{i+1/2} - \hat{f}_{i-1/2}}{\Delta x}$$

- Truncation error of explicit optimal numerical flux at $x_{i+1/2}$:

$$\hat{f}_{i+1/2} = h_{i+1/2} - \frac{1}{60}\left.\frac{\partial^5 f}{\partial x^5}\right|_{x=x_i} \Delta x^5$$

- Compact scheme at $x_{i-1/2}$:

$$\hat{f}_{i-1/2} = h_{i-1/2} - \frac{1}{600}\left.\frac{\partial^5 f}{\partial x^5}\right|_{x=x_i} \Delta x^5$$

- Substituting (2) and (3) in (1) leads to:

$$\left.\frac{\partial f}{\partial x}\right|_{x=x_i} = \frac{h_{i+1/2} - h_{i-1/2}}{\Delta x} - \frac{3}{200}\left.\frac{\partial^5 f}{\partial x^5}\right|_{x=x_i} \Delta x^4$$

# Block/Domain Boundary Treatment

$$h(x) = h_0 + h_1 x + h_2 \frac{x^2}{2!} \quad \longrightarrow \quad \hat{f} = \frac{1}{\Delta x} \int_{x-\Delta x/2}^{x+\Delta x/2} h(\xi) d\xi = h_0 + \ldots..$$

- Candidate Boundary Stencil (left)

$$\frac{11}{16}\hat{f}^0_{i-1/2} + \frac{5}{16}\hat{f}^0_{i+1/2} = -\frac{1}{96}f_{i-2} + \frac{5}{24}f_{i-1} + \frac{77}{96}f_i$$

$$\frac{1}{3}\hat{f}^1_{i-1/2} + \frac{2}{3}\hat{f}^1_{i+1/2} = \frac{5}{6}f_i + \frac{1}{6}f_{i+1}$$

$$\hat{f}^2_{i+1/2} = \frac{1}{3}f_i + \frac{5}{6}f_{i+1} - \frac{1}{6}f_{i+2}$$

with $c_0$=2/5, $c_1$=21/40, and $c_2$=3/40

- Candidate Boundary Stencil (right)

$$\hat{f}^0_{i-1/2} = \frac{1}{3}f_{i-3} - \frac{7}{6}f_{i-2} + \frac{11}{6}f_{i-1}$$

$$\hat{f}^1_{i-1/2} = \frac{-1}{6}f_{i-2} + \frac{5}{6}f_{i-1} + \frac{1}{3}f_i$$

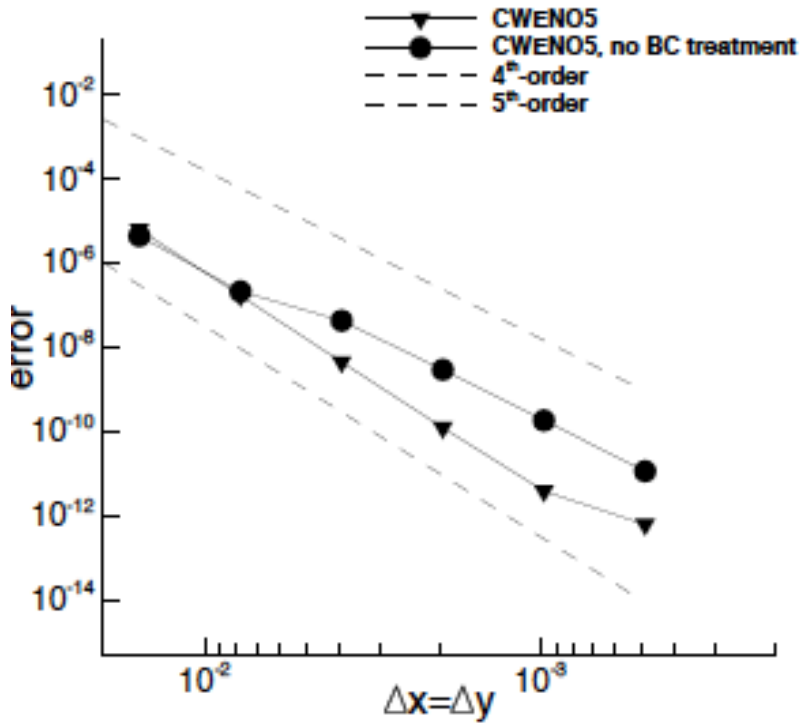
$$\frac{3}{5}\hat{f}^2_{i-1/2} + \frac{2}{5}\hat{f}^2_{i+1/2} = \frac{4}{30}f_{i-1} + \frac{5}{6}f_i + \frac{1}{30}f_{i+1}$$

with $c_0$=1/40, $c_1$=9/40, and $c_2$=30/40

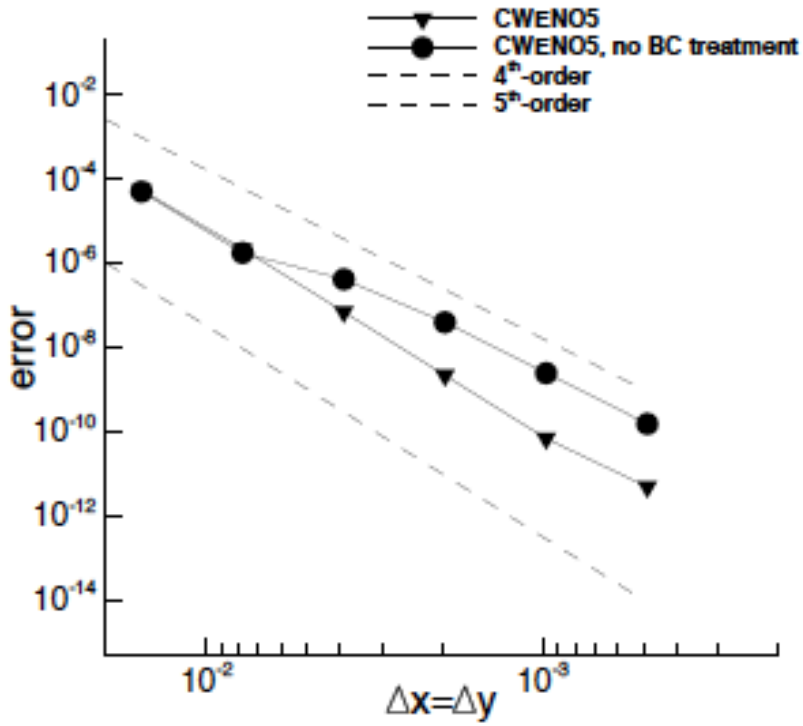
# Block/Domain Boundary Treatment

- Error Convergence Study with and without boundary treatment

X-momentum $L_2$-norm




X-momentum $L_\infty$-norm

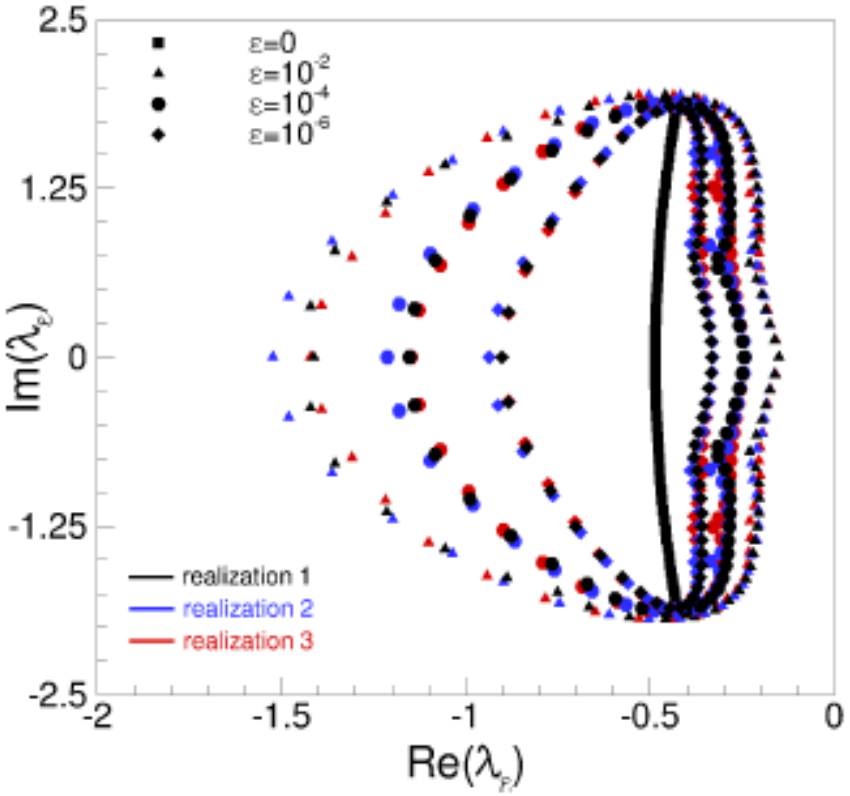


# Block/Domain Boundary Treatment

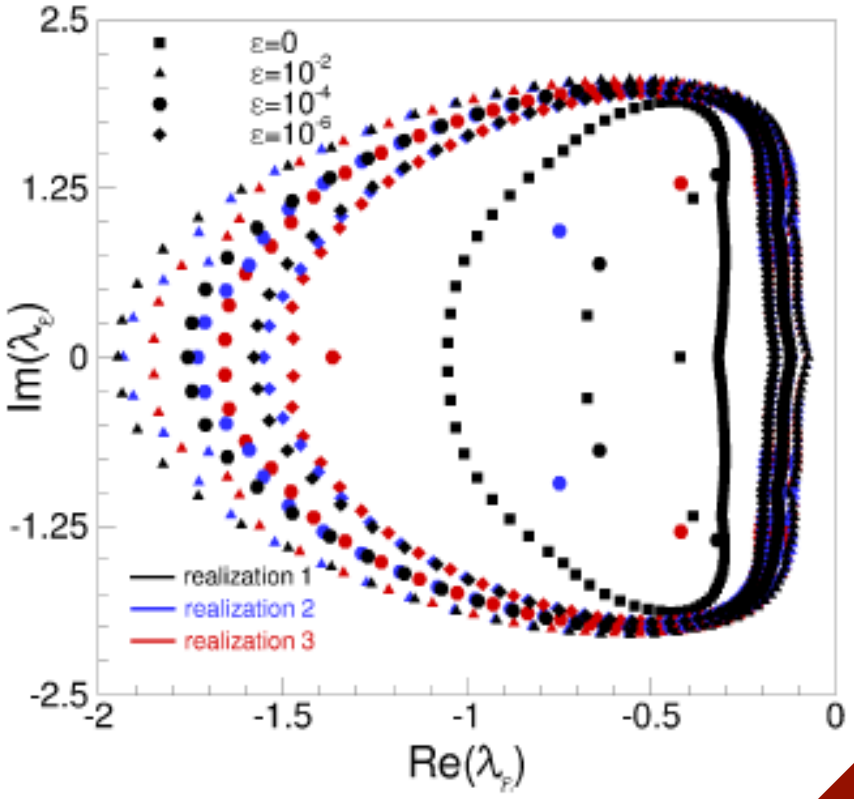
- Pseudo Spectral Analysis

$$\left(\underline{\boldsymbol{A}}\lambda_\epsilon + \frac{1}{\Delta x}\underline{\boldsymbol{B}} - \underline{\boldsymbol{AD}}\right)\boldsymbol{v} = 0$$

N=60



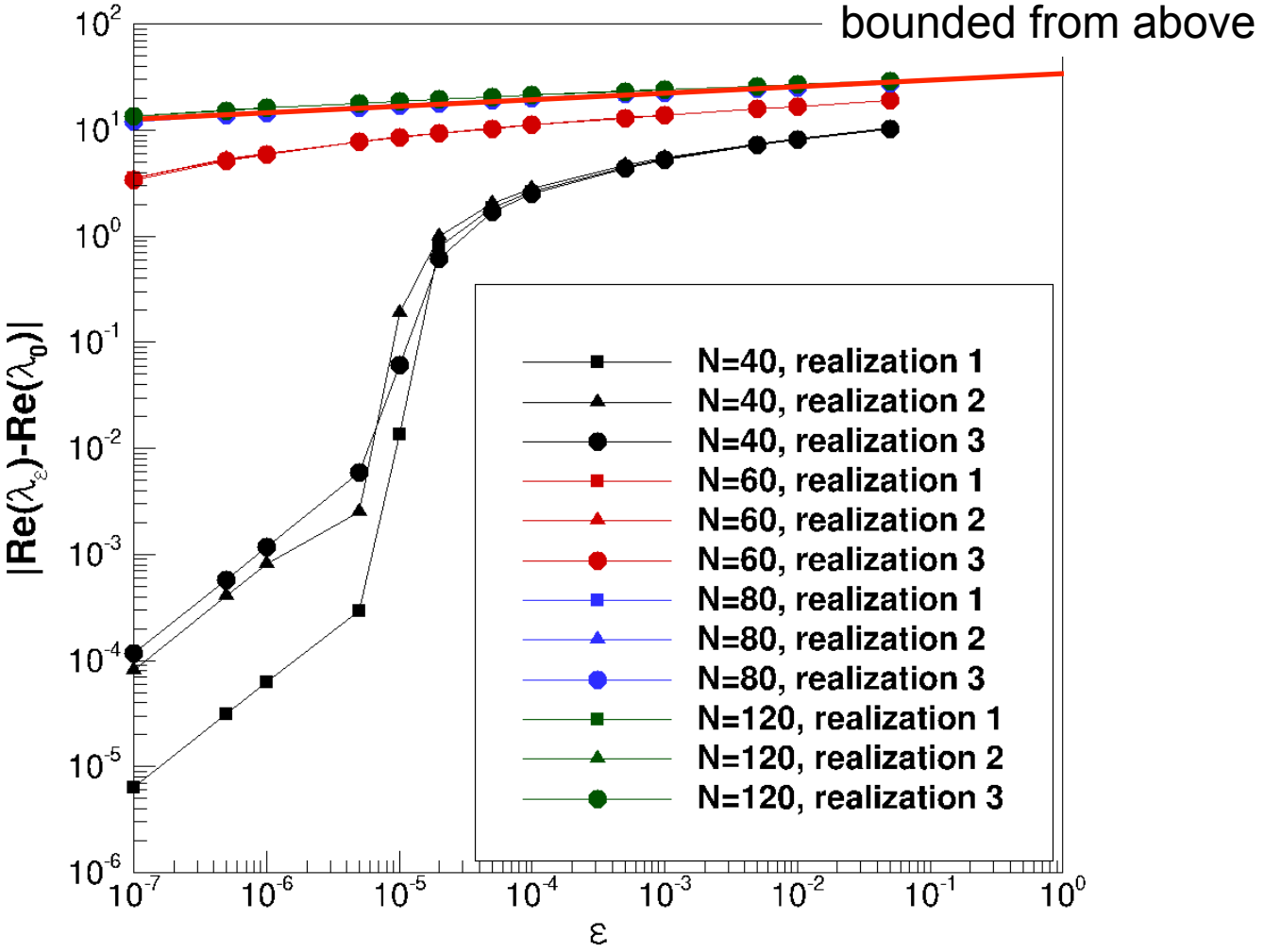

N=120



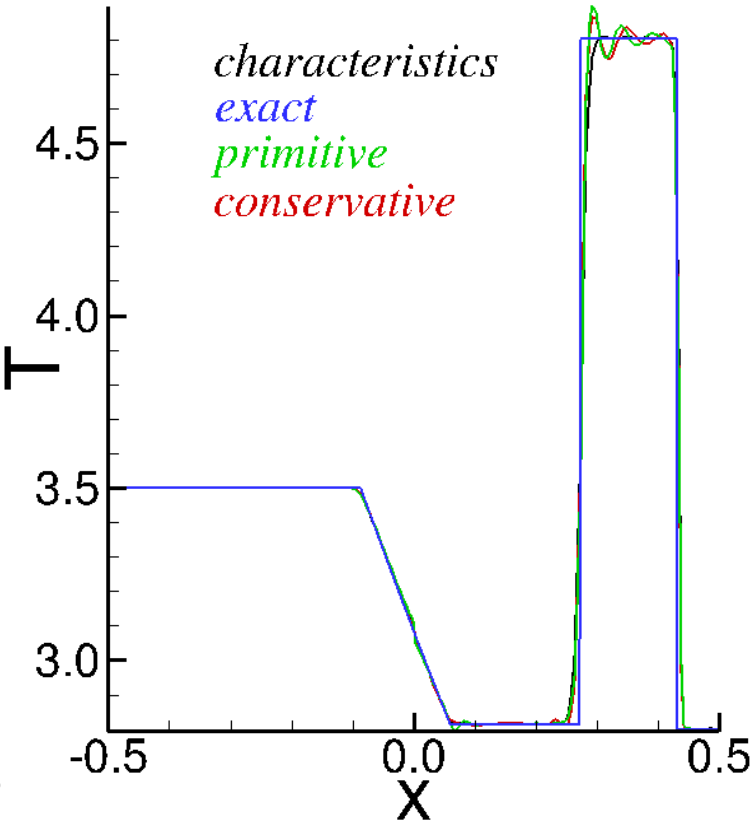
# Block/Domain Boundary Treatment

- Pseudo Spectral Analysis

$$\lambda_{\epsilon,real} \leq s + K_0\epsilon \qquad \forall \epsilon \geq 0$$



# Weighted Essentially Non-Oscillatory




- Characteristic Variable Transform:

$$\mathbf{\Phi} = \underline{\boldsymbol{L}}\boldsymbol{\phi}$$

with $\underline{\boldsymbol{L}}$, left eigenvectors, of $\underline{\mathbf{A}} = \partial\mathbf{F}/\partial\mathbf{Q}$

- Even higher computational cost for CWENO5
  - Tri(-block)-diagonal implicit system of equations

$$\left(\frac{2}{3}\omega_0 + \frac{1}{3}\omega_1\right)\hat{f}_{i-1/2} + \left(\frac{1}{3}\omega_0 + \frac{2}{3}\left(\omega_1 + \omega_2\right)\right)\hat{f}_{i+1/2} + \frac{1}{3}\omega_2\hat{f}_{i+3/2} =$$

$$\frac{\omega_0}{6}f_{i-1} + \frac{5\left(\omega_0 + \omega_1\right) + \omega_2}{6}f_i + \frac{\omega_1 + 5\omega_2}{6}f_{i+1}$$

# Outline







Motivation/Introduction

Higher-Order Shock Capturing Schemes

Accuracy

*Accuracy study including nonlinear weights, filtering, and dissipation terms.*

Test Problems

Computational Performance

Summary & Future Work

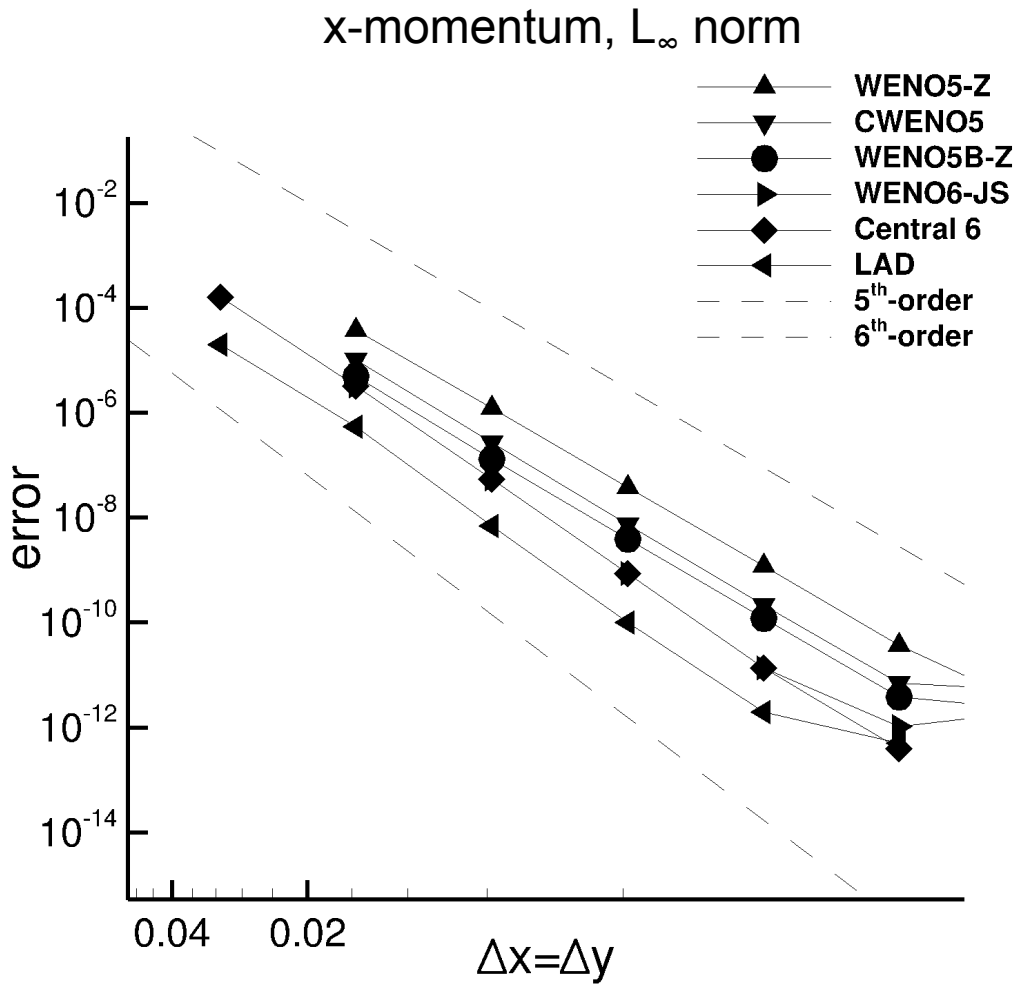
Accuracy:

# Method of Manufactured Solution

$$p = 4 + \frac{1}{30}\left(\cos(2\pi x) + \cos(2\pi y)\right),$$
$$u = v = \cos(2\pi(x+y)),$$
$$T = \frac{1}{2} + \frac{1}{10}\left(\cos(4\pi x) + \cos(4\pi y)\right)$$
$$C_p = 1005, \text{ and}$$
$$\gamma = 1.4.$$

Setup:

- use blocks with 16×16
- includes boundary treatment
- r.h.s. term added to make solution satisfy Euler equations

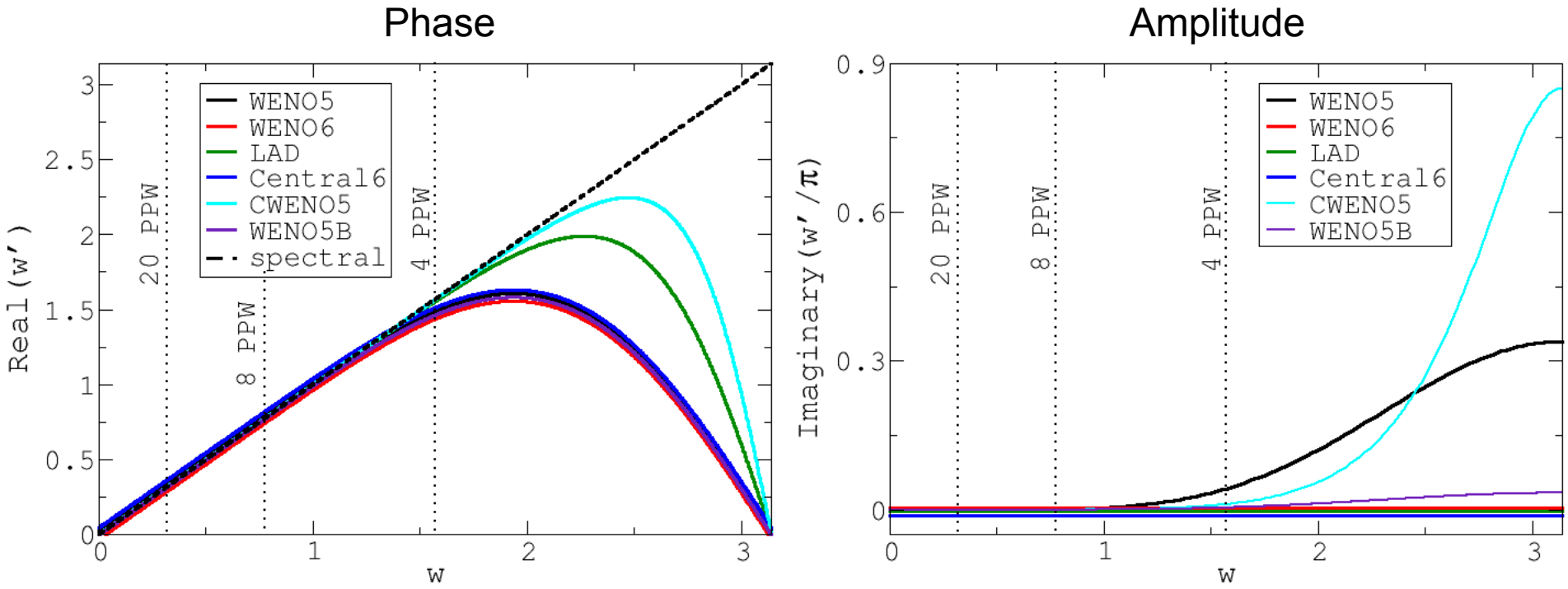



Leading order truncation error term:

| MUSCL | WENO5 | WENO6 | CWENO5 | Central6 | LAD |
|---|---|---|---|---|---|
| $-\frac{\Delta x^2}{3} f^{(3)}$ | $-\frac{\Delta x^5}{60} f^{(6)}$ | $-\frac{\Delta x^6}{140} f^{(7)}$ | $-\frac{\Delta x^5}{600} f^{(6)}$ | $-\frac{\Delta x^6}{140} f^{(7)}$ | $-\frac{\Delta x^6}{2100} f^{(7)}$ |

Accuracy:

# Spectral Resolution Accuracy

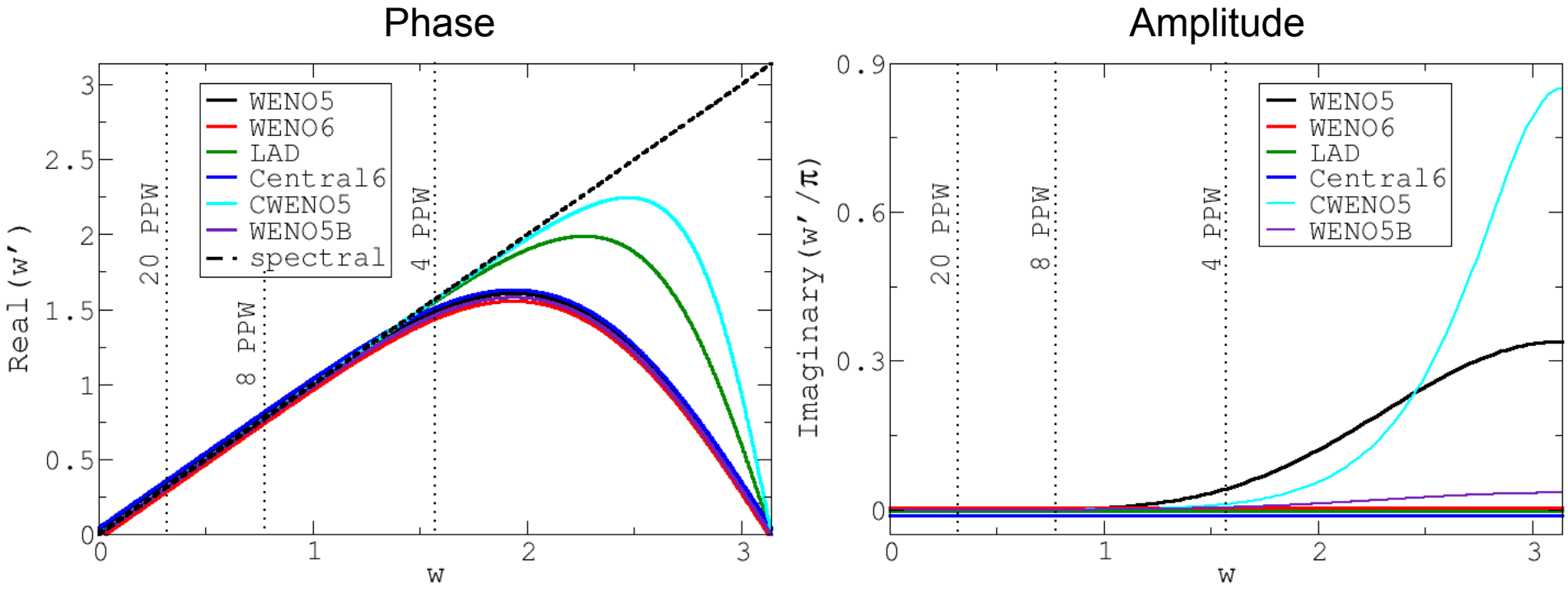



❑ Modified wavenumber (expanded around w=0):

| | MUSCL | WENO5 | WENO6 | CWENO5 | Central6 | LAD |
|---|---|---|---|---|---|---|
| $Im(w')$ | $w+\frac{w^3}{3}$ | $w-\frac{w^7}{140}$ | $w-\frac{w^7}{140}$ | $w-\frac{w^7}{7000}$ | $w-\frac{w^7}{140}$ | $w-\frac{w^7}{2100}$ |
| $Re(w')$ | $-\frac{w^4}{4}$ | $\frac{w^6}{60}$ | - | $\frac{w^6}{600}$ | - | - |

Accuracy:

# Spectral Resolution Accuracy




❑ Spectral resolution efficiency:

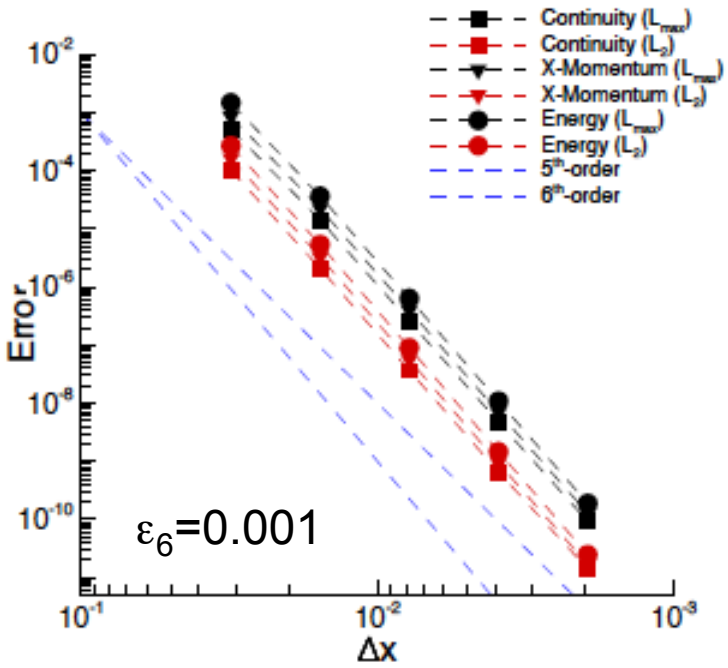
| | WENO5 | WENO6 | WENO5B | CWENO5 | Central6D6 | LAD |
|---|---|---|---|---|---|---|
| $\xi$ | 0.3503 | 0.3503 | 0.3503 | 0.6065 | 0.3503 | 0.5023 |
| $N_{min}$ | 5.7100 | 5.7100 | 5.7100 | 3.2974 | 5.7100 | 3.9813 |

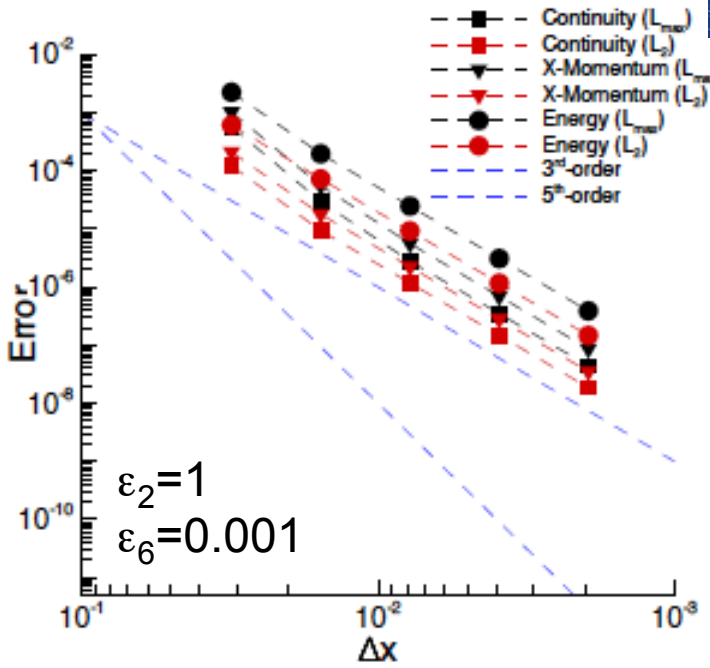
$\xi=w_s/\pi$: bandwidth-resolving efficiency parameter (at $w_s$ relative phase error exceeds 1%)

$N_{min}$: points per wavelength

Accuracy:

# Central: Effect of Artificial Dissipation




Explicit Artificial Dissipation: $$AD = \alpha_2 \sigma \Gamma_p \frac{Q_{i+1} - 2Q_i + Q_{i-1}}{\Delta x} \approx \alpha_2 \overline{\sigma} \overline{\Gamma}_p \frac{\partial^2 Q}{\partial x^2}\bigg|_i \Delta x$$

TE for Pressure Switch: $$\Psi_i = \Delta x^2 \frac{\frac{\partial^2 p}{\partial x^2}\Big|_i + \mathcal{O}(\Delta x^2)}{\overline{p}_i + \mathcal{O}(\Delta x^2)}$$

Scaling in smooth flow region: $$AD \propto \frac{\Delta x^2}{\overline{p}_i} \frac{\partial^2 p}{\partial x^2} \Delta x \frac{\partial^2 Q}{\partial x^2}$$

Accuracy:

# WENO5: Effect of Nonlinear Weights



Necessary and sufficient conditions for 5th-order accuracy:

$$\sum_{k=0}^{2}(\omega_{k,i\pm\frac{1}{2}} - c_k) = \mathcal{O}(\Delta x^6),\ \sum_{k=0}^{2} A_k(\omega_{k,i+\frac{1}{2}} - \omega_{k,i-\frac{1}{2}}) = \mathcal{O}(\Delta x^3),\ \text{and}\ (\omega_{k,i\pm\frac{1}{2}} - c_k) = \mathcal{O}(\Delta x^2).$$

with WENO weights, ω, optimal weights, c, and A from: $\hat{f}_{k,i\pm\frac{1}{2}} = h_{i\pm\frac{1}{2}} + \Delta x^3 A_k + \mathcal{O}(\Delta x^4)$

Smoothness indicator: $\beta_k = \sum_{j=1}^{n-1} \Delta x^{2j-1} \int_{x-\frac{1}{2}}^{x+\frac{1}{2}} \left(\frac{d^j \hat{f}_k(x)}{dx^j}\right)^2 dx$

$$\beta_0 = f_i'^2\Delta x^2 + \left(\frac{13}{12}f_i''^2 - \frac{2}{3}f_i' f_i'''\right)\Delta x^4 - \left(\frac{13}{6}f_i'' f_i''' - \frac{1}{2}f_i' f_i''''\right)\Delta x^5 + \mathcal{O}(\Delta x^6),$$

$$\beta_1 = f_i'^2\Delta x^2 + \left(\frac{13}{12}f_i''^2 + \frac{1}{3}f_i' f_i'''\right)\Delta x^4 + \mathcal{O}(\Delta x^6),\ \text{and}$$

$$\beta_2 = f_i'^2\Delta x^2 + \left(\frac{13}{12}f_i''^2 - \frac{2}{3}f_i' f_i'''\right)\Delta x^4 + \left(\frac{13}{6}f_i'' f_i''' - \frac{1}{2}f_i' f_i''''\right)\Delta x^5 + \mathcal{O}(\Delta x^6).$$

with: $\beta_k = (f'_{k,i}\Delta x)^2(1 + \mathcal{O}(\Delta x^2))$ and $\omega_k = \frac{\alpha_k}{\sum_k^n \alpha_k}$

$$\alpha_k = \frac{c_k}{(C(1+\mathcal{O}(\Delta x^2)))^p} = \frac{c_k}{C^p}\left(1 + \mathcal{O}(\Delta x^2)\right)$$

Accuracy:

# WENO5: Effect of Nonlinear Weights



Necessary and sufficient conditions for 5th-order accuracy:

$$\sum_{k=0}^{2}(\omega_{k,i\pm\frac{1}{2}} - c_k) = \mathcal{O}(\Delta x^6),\ \sum_{k=0}^{2} A_k(\omega_{k,i+\frac{1}{2}} - \omega_{k,i-\frac{1}{2}}) = \mathcal{O}(\Delta x^3),\ \text{and}\ (\omega_{k,i\pm\frac{1}{2}} - c_k) = \mathcal{O}(\Delta x^2).$$

with WENO weights, ω, optimal weights, c, and A from: $\hat{f}_{k,i\pm\frac{1}{2}} = h_{i\pm\frac{1}{2}} + \Delta x^3 A_k + \mathcal{O}(\Delta x^4)$

Smoothness indicator: $\beta_k = \sum_{j=1}^{n-1} \Delta x^{2j-1} \int_{x-\frac{1}{2}}^{x+\frac{1}{2}} \left(\frac{d^j \hat{f}_k(x)}{dx^j}\right)^2 dx$

$$\beta_0 = f_i'^2\Delta x^2 + \left(\frac{13}{12}f_i''^2 - \frac{2}{3}f_i' f_i'''\right)\Delta x^4 - \left(\frac{13}{6}f_i'' f_i''' - \frac{1}{2}f_i' f_i''''\right)\Delta x^5 + \mathcal{O}(\Delta x^6),$$

$$\beta_1 = f_i'^2\Delta x^2 + \left(\frac{13}{12}f_i''^2 + \frac{1}{3}f_i' f_i'''\right)\Delta x^4 + \mathcal{O}(\Delta x^6),\ \text{and}$$

$$\beta_2 = f_i'^2\Delta x^2 + \left(\frac{13}{12}f_i''^2 - \frac{2}{3}f_i' f_i'''\right)\Delta x^4 + \left(\frac{13}{6}f_i'' f_i''' - \frac{1}{2}f_i' f_i''''\right)\Delta x^5 + \mathcal{O}(\Delta x^6).$$

with: $\beta_k = 13/12(f''_{k,i}\Delta x^2)^2(1 + \mathcal{O}(\Delta x^{\ }))$ and $\omega_k = \frac{\alpha_k}{\sum_k^n \alpha_k}$

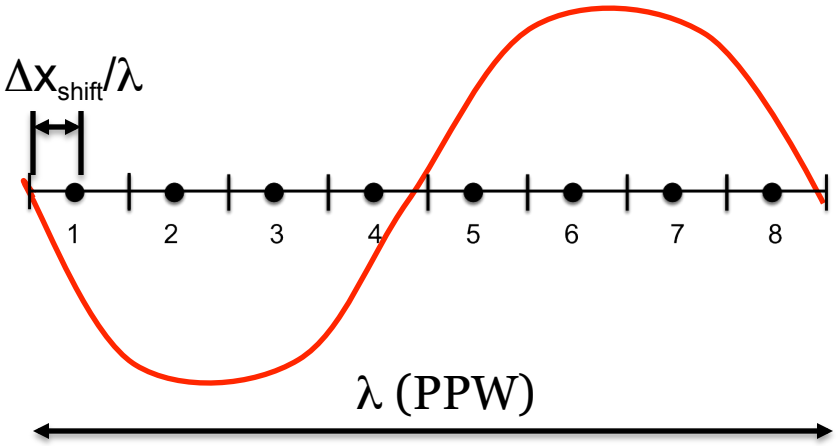
$$\alpha_k = \frac{c_k}{(C(1+\mathcal{O}(\Delta x^{\ })))^p} = \frac{c_k}{C^p}(1 + \mathcal{O}(\Delta x^{\ }))$$

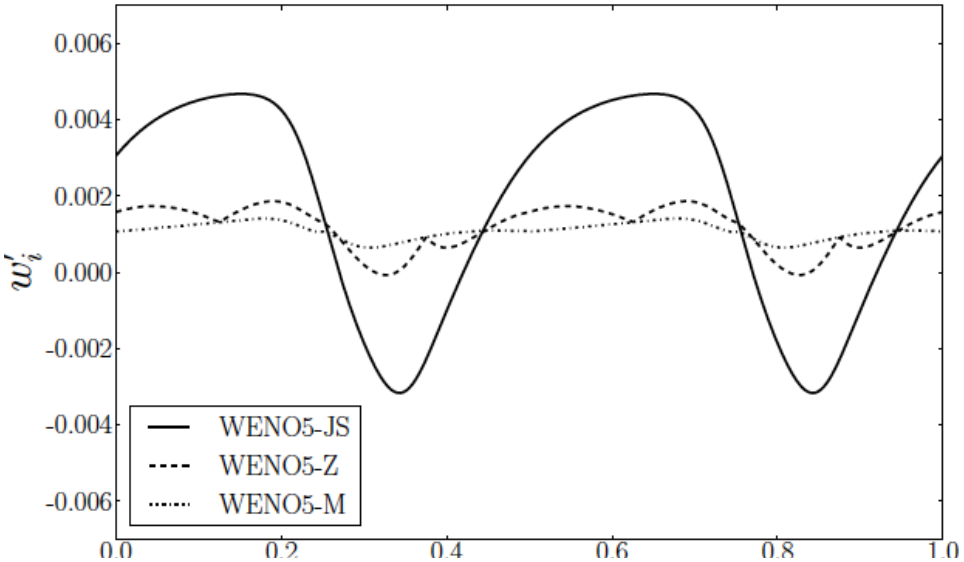
**reduces to 3rd-order accuracy!**

Accuracy:

# Smoothness Indicator

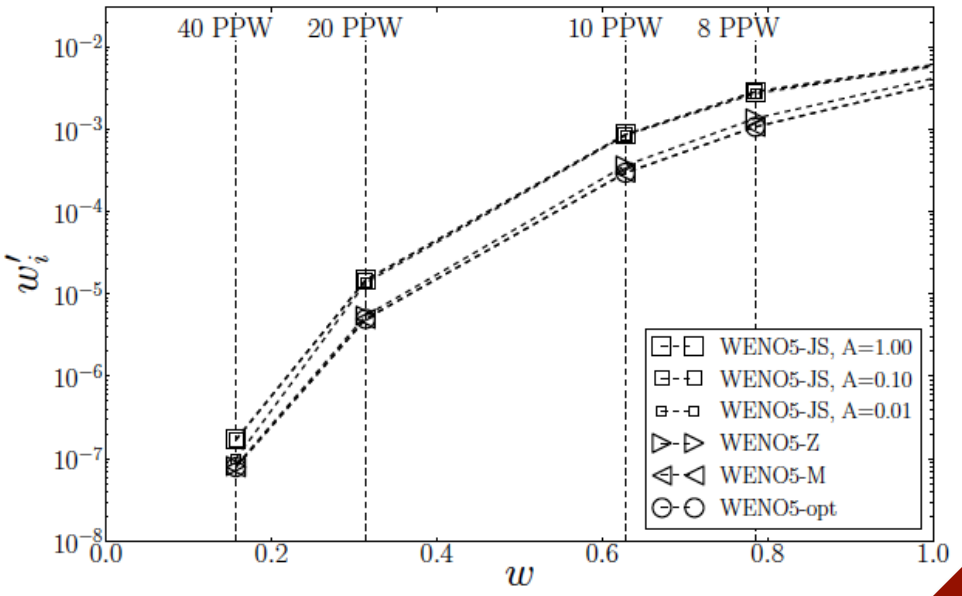
- Amplitude factor:




- Phase Error:

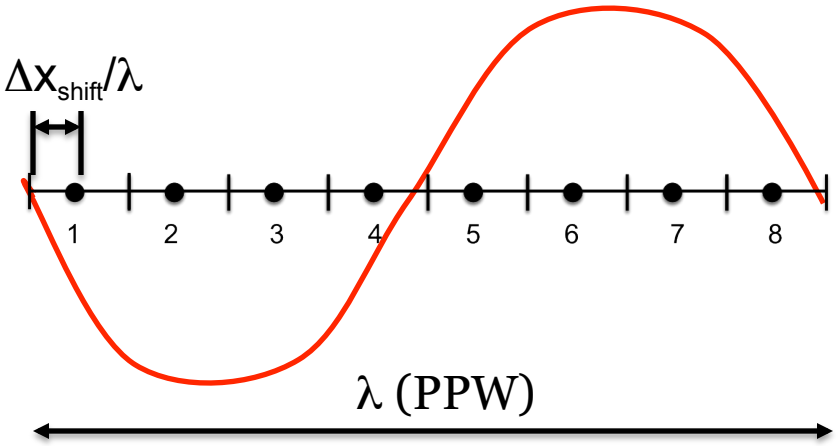
- Solve linear advection equation to determine decay rate
- Strong effect of smoothness indicator

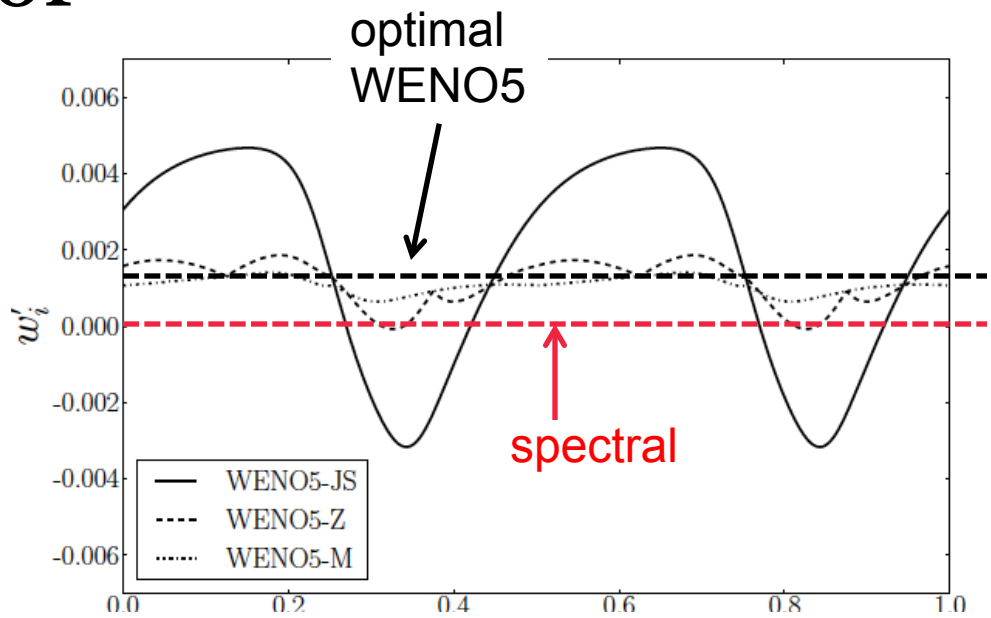


Accuracy:

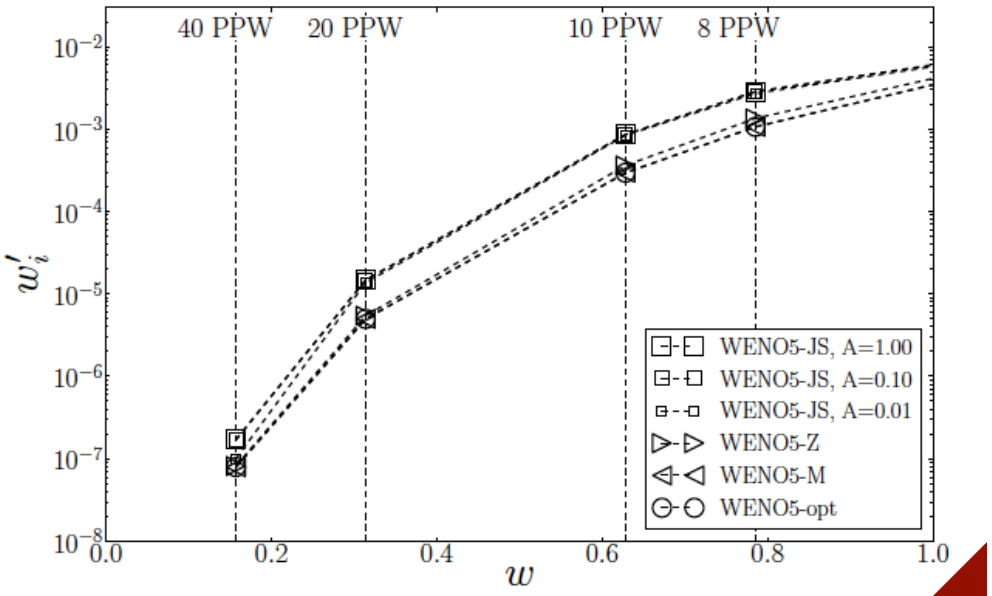
# Smoothness Indicator

- Amplitude factor:



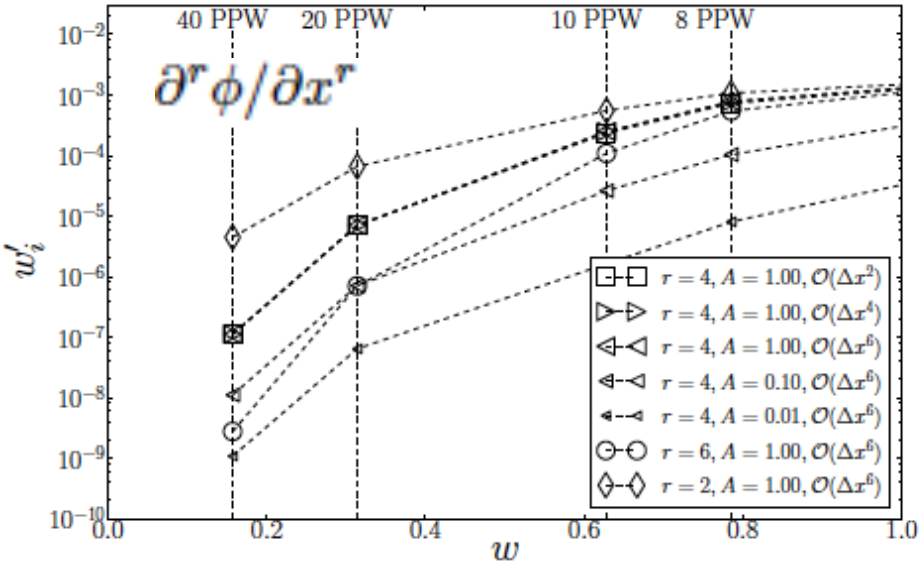

- Phase Error:

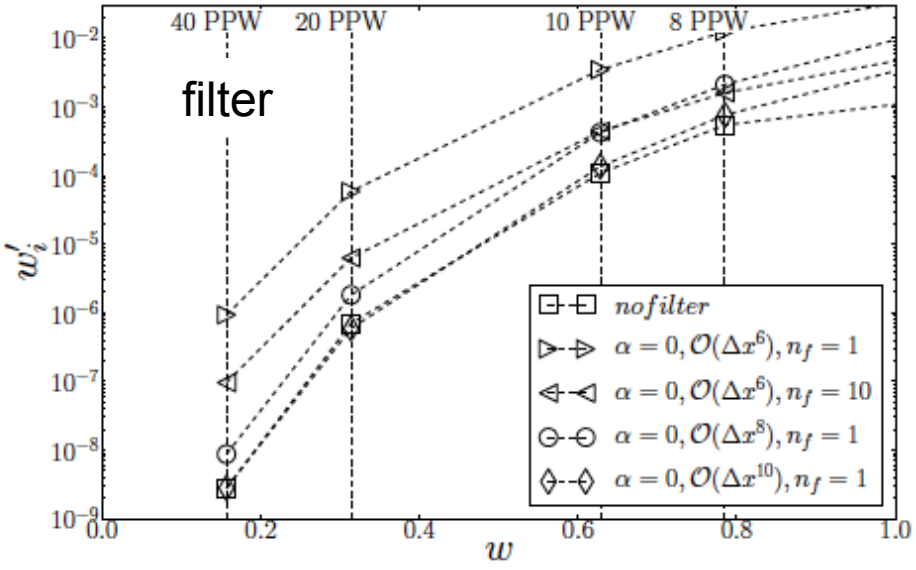



- Solve linear advection equation to determine decay rate
- Strong effect of smoothness Indicator
- Results for WENO5 depend on amplitude of disturbance

Accuracy:

# LAD: Effect of Localized Artificial Diffusivity

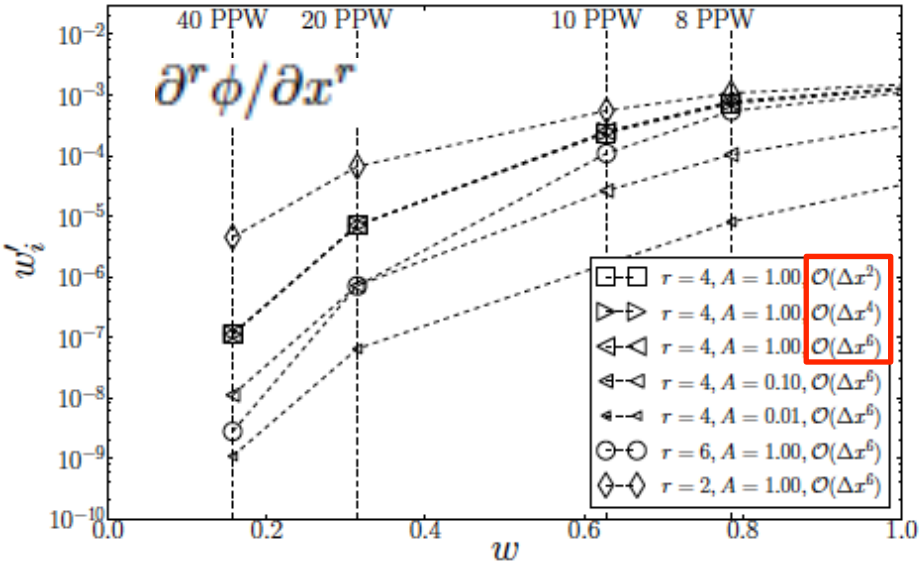


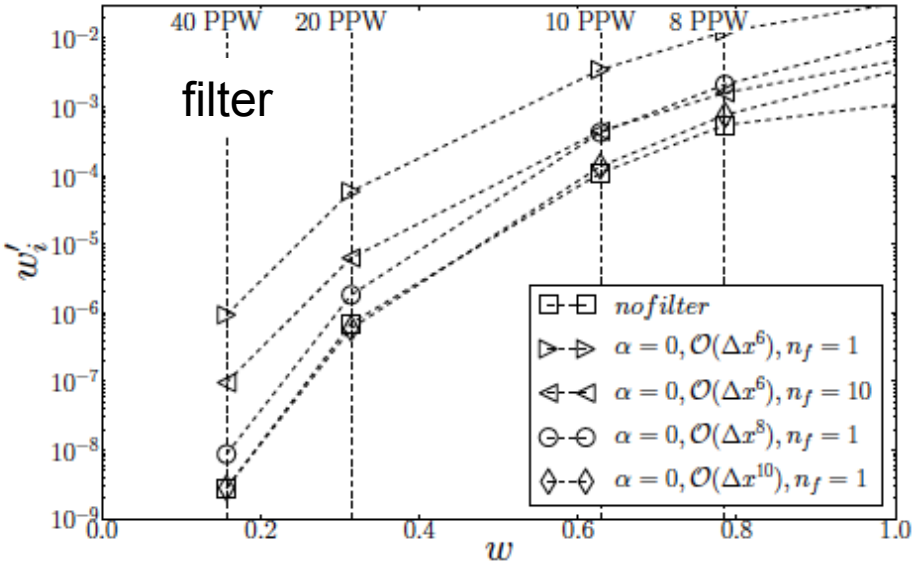




- adding $\partial\tau/\partial x$ with $\tau = \mu^* \partial\phi/\partial x$ and $\mu^* \propto \partial^r \phi / \partial x^r$
- effective at high wavenumbers: $k^r$
- artificial viscosity $\mu^* = C_\mu \overline{|\partial^r \phi / \partial x^r|} \Delta x^s$ with $C_\mu = 1$
- Consistently used s=r+2
- Partial derivative $\partial^r \phi / \partial x^r$ was approximated with central FD of $O(\Delta x^p)$

Accuracy:

# LAD: Effect of Localized Artificial Diffusivity

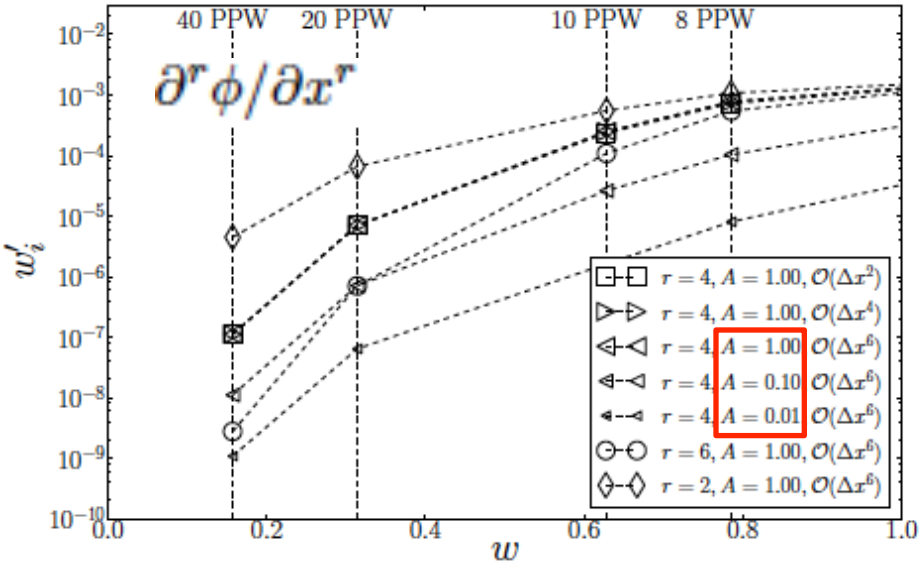


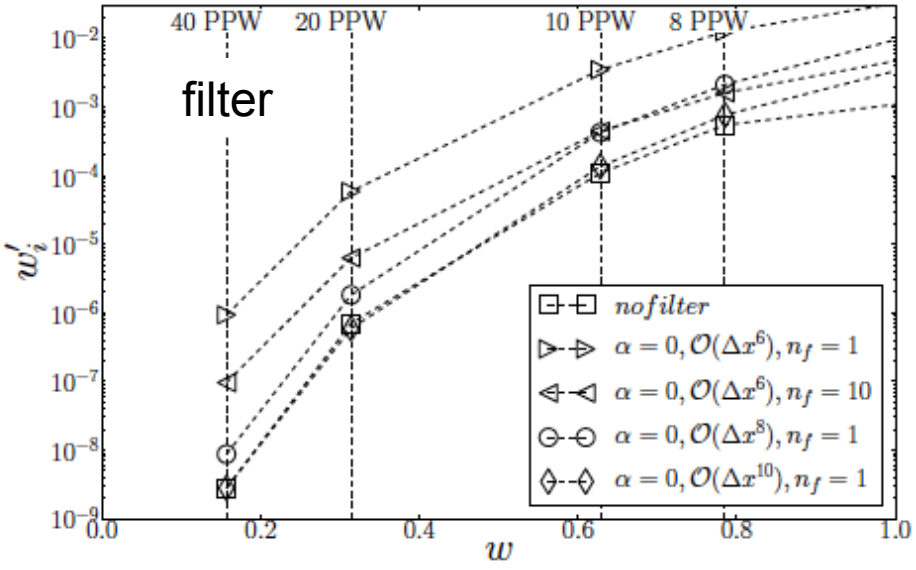




- adding $\partial\tau/\partial x$ with $\tau = \mu^* \partial\phi/\partial x$ and $\mu^* \propto \partial^r \phi / \partial x^r$
- effective at high wavenumbers: $k^r$
- artificial viscosity $\mu^* = C_\mu \overline{|\partial^r \phi / \partial x^r|} \Delta x^s$ with $C_\mu = 1$
- Consistently used s=r+2
- Partial derivative $\partial^r \phi / \partial x^r$ was approximated with central FD of $O(\Delta x^p)$

Accuracy:

# LAD: Effect of Localized Artificial Diffusivity

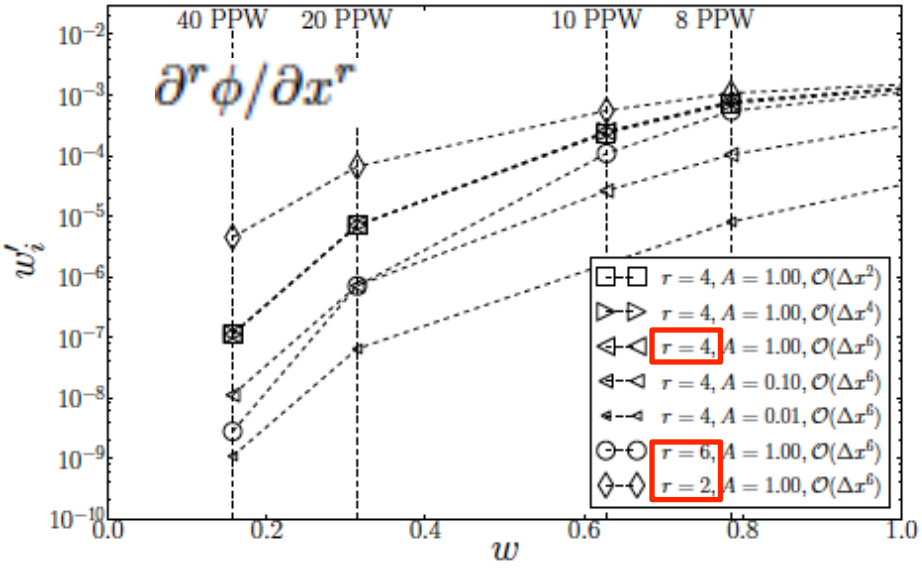


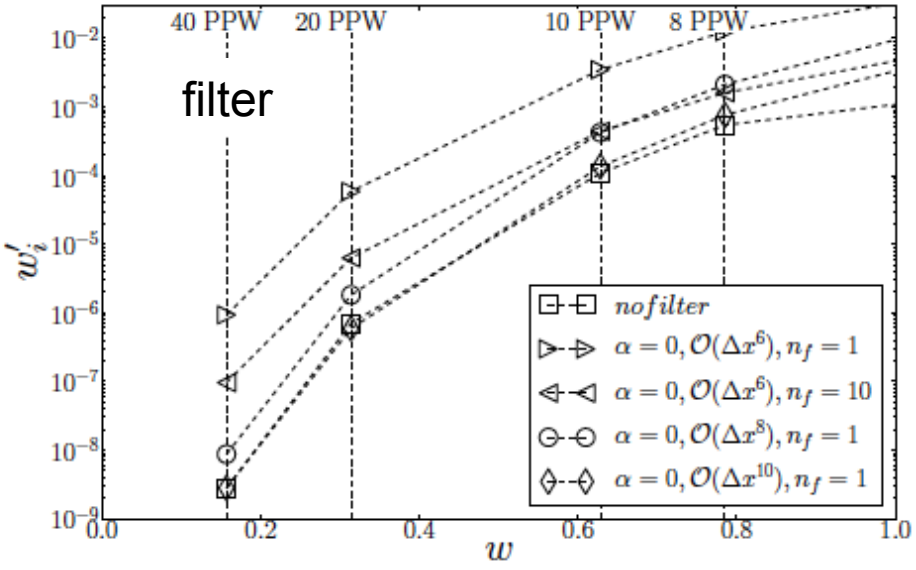




- adding $\partial\tau/\partial x$ with $\tau = \mu^* \partial\phi/\partial x$ and $\mu^* \propto \partial^r \phi / \partial x^r$
- effective at high wavenumbers: $k^r$
- artificial viscosity $\mu^* = C_\mu \overline{|\partial^r \phi / \partial x^r|} \Delta x^s$ with $C_\mu = 1$
- Consistently used s=r+2
- Partial derivative $\partial^r \phi / \partial x^r$ was approximated with central FD of $O(\Delta x^p)$

Accuracy:

# LAD: Effect of Localized Artificial Diffusivity

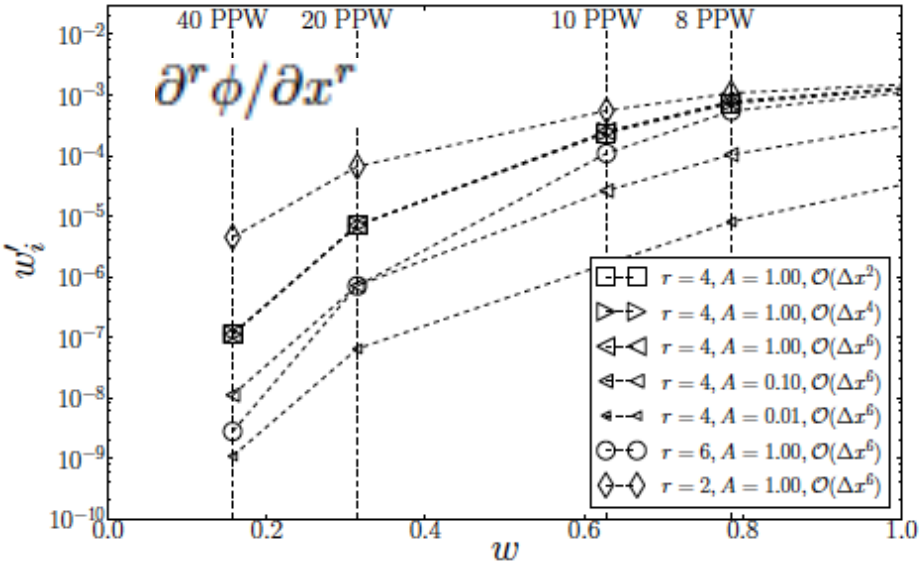


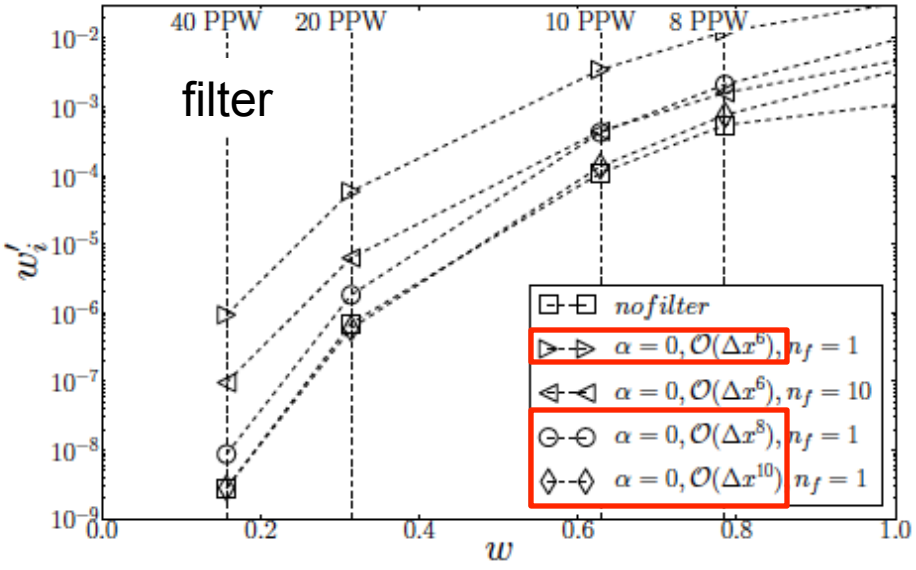




- adding $\partial\tau/\partial x$ with $\tau = \mu^* \partial\phi/\partial x$ and $\mu^* \propto \partial^r \phi / \partial x^r$
- effective at high wavenumbers: $k^r$
- artificial viscosity $\mu^* = C_\mu \overline{|\partial^r \phi / \partial x^r|} \Delta x^s$ with $C_\mu = 1$
- Consistently used s=r+2
- Partial derivative $\partial^r \phi / \partial x^r$ was approximated with central FD of $O(\Delta x^p)$

Accuracy:

# LAD: Effect of Localized Artificial Diffusivity



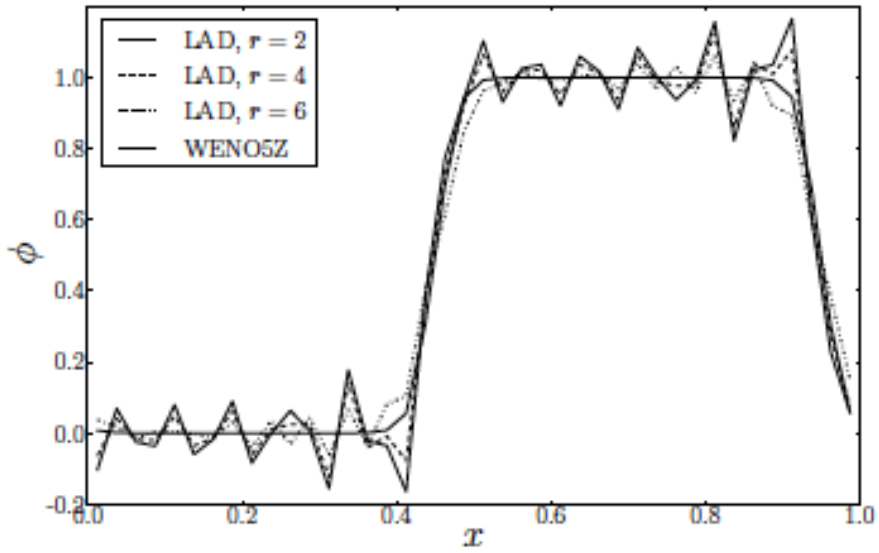




- adding $\partial\tau/\partial x$ with $\tau = \mu^* \partial\phi/\partial x$ and $\mu^* \propto \partial^r \phi / \partial x^r$
- effective at high wavenumbers: $k^r$
- artificial viscosity $\mu^* = C_\mu \overline{|\partial^r \phi / \partial x^r|} \Delta x^s$ with $C_\mu = 1$
- Consistently used s=r+2
- Partial derivative $\partial^r \phi / \partial x^r$ was approximated with central FD of $O(\Delta x^p)$

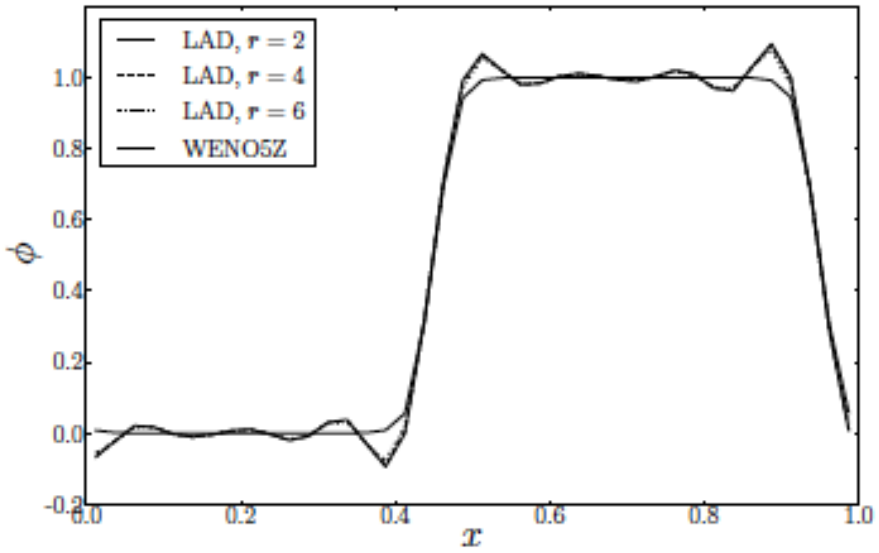
Accuracy:

# LAD

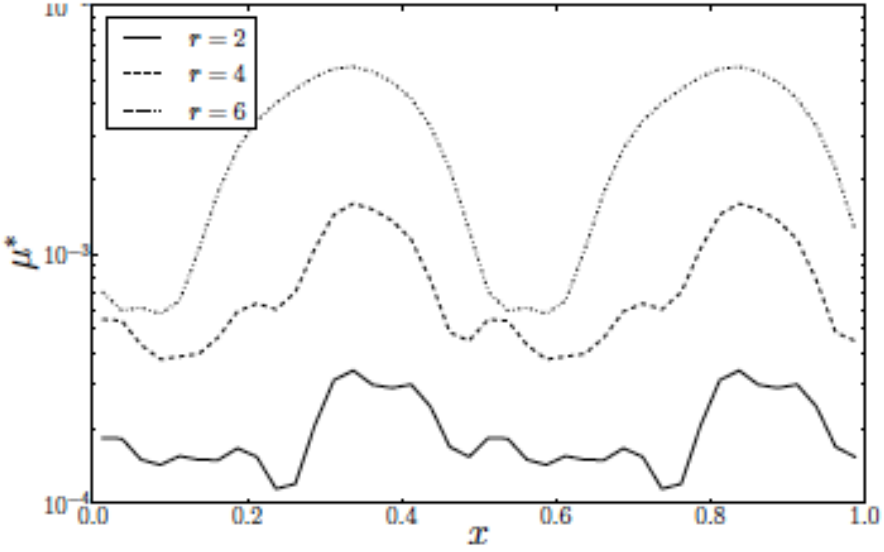
unfiltered solution



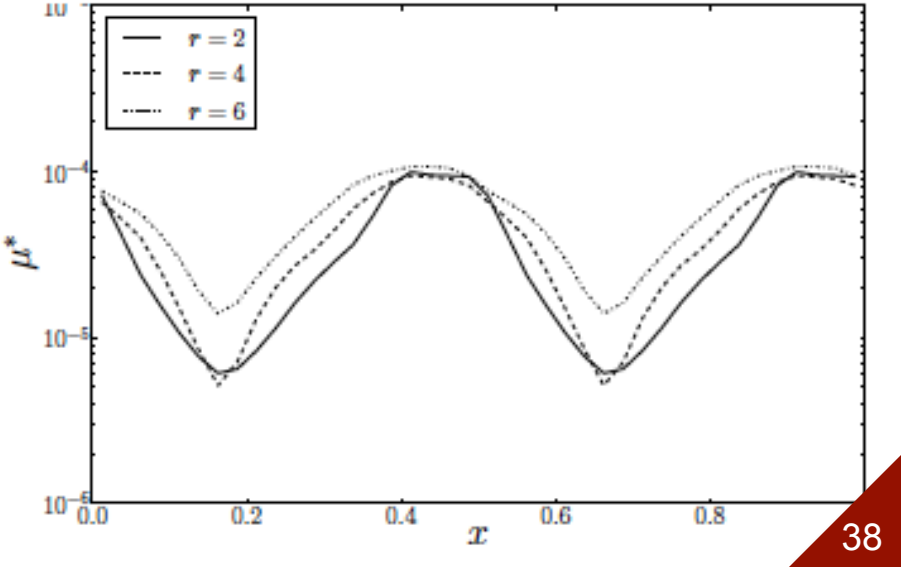

filtered solution




artificial viscosity for unfiltered solution




artificial viscosity for filtered solution



# Outline



Motivation/Introduction

Higher-Order Shock Capturing Schemes

Accuracy

Test Problems

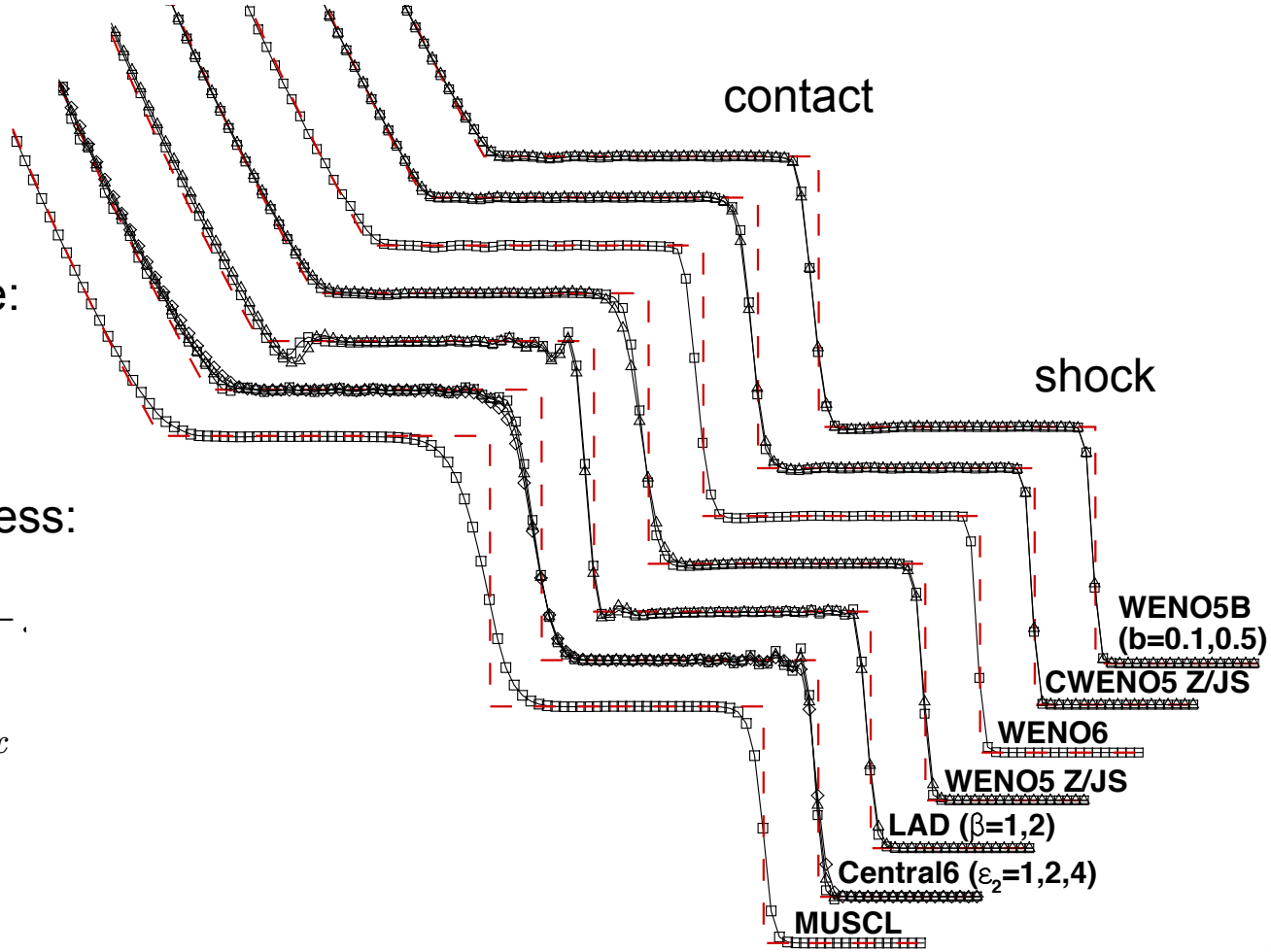
*Various test problems: 1D shock problems to isotropic turbulence.*

Computational Performance

Summary & Future Work

1D Unsteady Shock Problem:

# Sod Problem




- wiggle amplitude:

$$\Delta p_{max}/\Delta p$$

- discontinuity thickness:

$$\frac{\delta}{\Delta x} = \frac{\Delta p}{\Delta x \frac{\partial p}{\partial x}\Big|_{max}}.$$

200 points on L=1



| | WENO5 Z/JS | WENO6 | WENO5B b = 0.1, 0.5 | CWENO5 Z/JS | LAD $\beta = 1.5$ | Central6 $\epsilon_2 = 1, 2, 4$ |
|---|---|---|---|---|---|---|
| contact | | | | | | |
| $\frac{\Delta\rho_{max}}{\Delta\rho}$ | 0.0079\|0.0060 | 0.0082 | 0.0081\|0.0121 | 0.0073\|0.0058 | 0.0666 | 0.0320\|0.0112\|0.0101 |
| $\frac{\delta}{\Delta x}$ | 3.7540\|4.7821 | 3.1872 | 3.2166\|3.4060 | 2.9421\|3.4263 | 2.6616 | 4.8374\|5.1386\|5.6107 |

1D Unsteady Shock Problem:

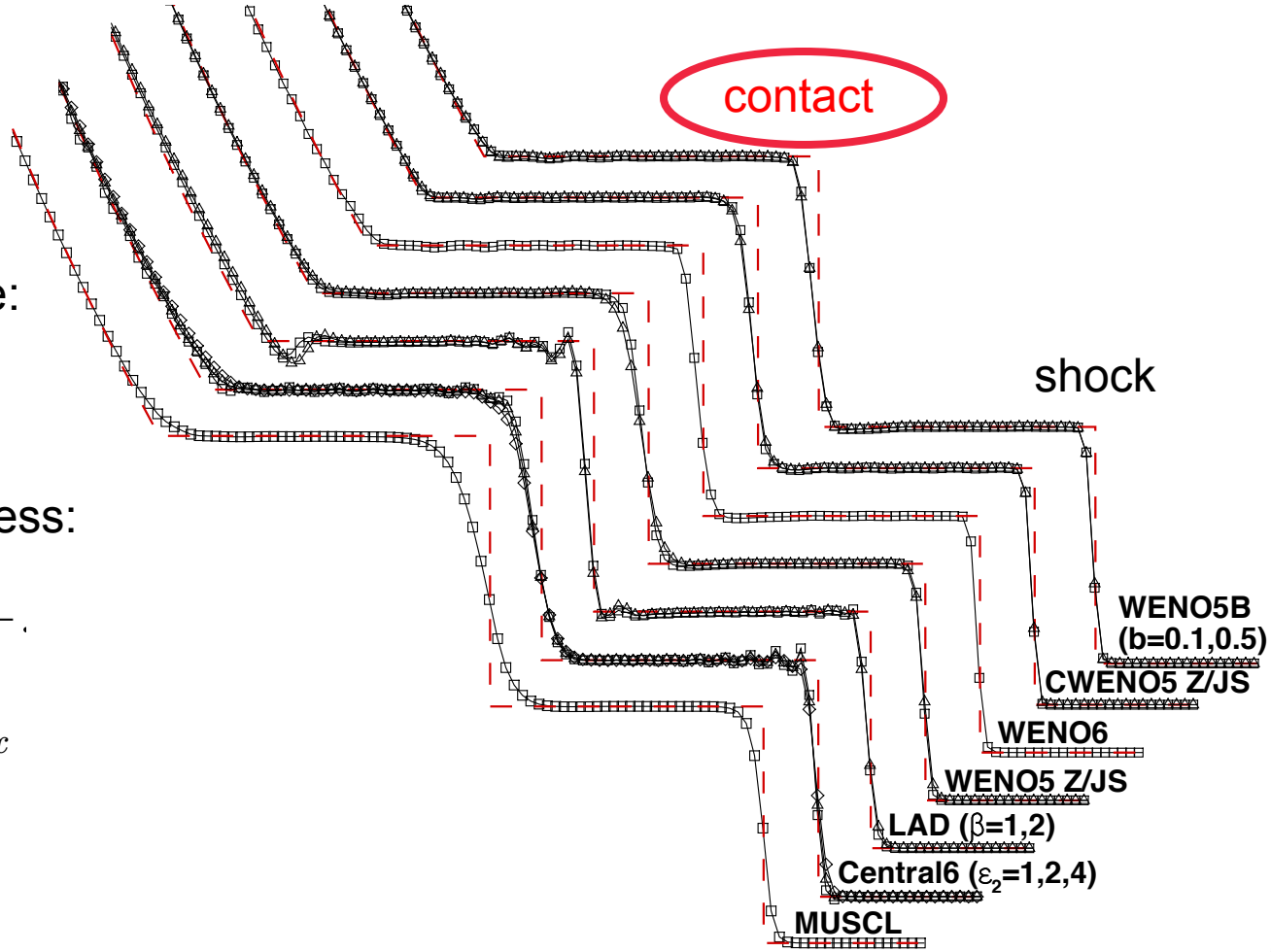
# Sod Problem

- wiggle amplitude:

$$\Delta p_{max}/\Delta p$$

- discontinuity thickness:

$$\frac{\delta}{\Delta x} = \frac{\Delta p}{\Delta x \frac{\partial p}{\partial x}\Big|_{max}}.$$

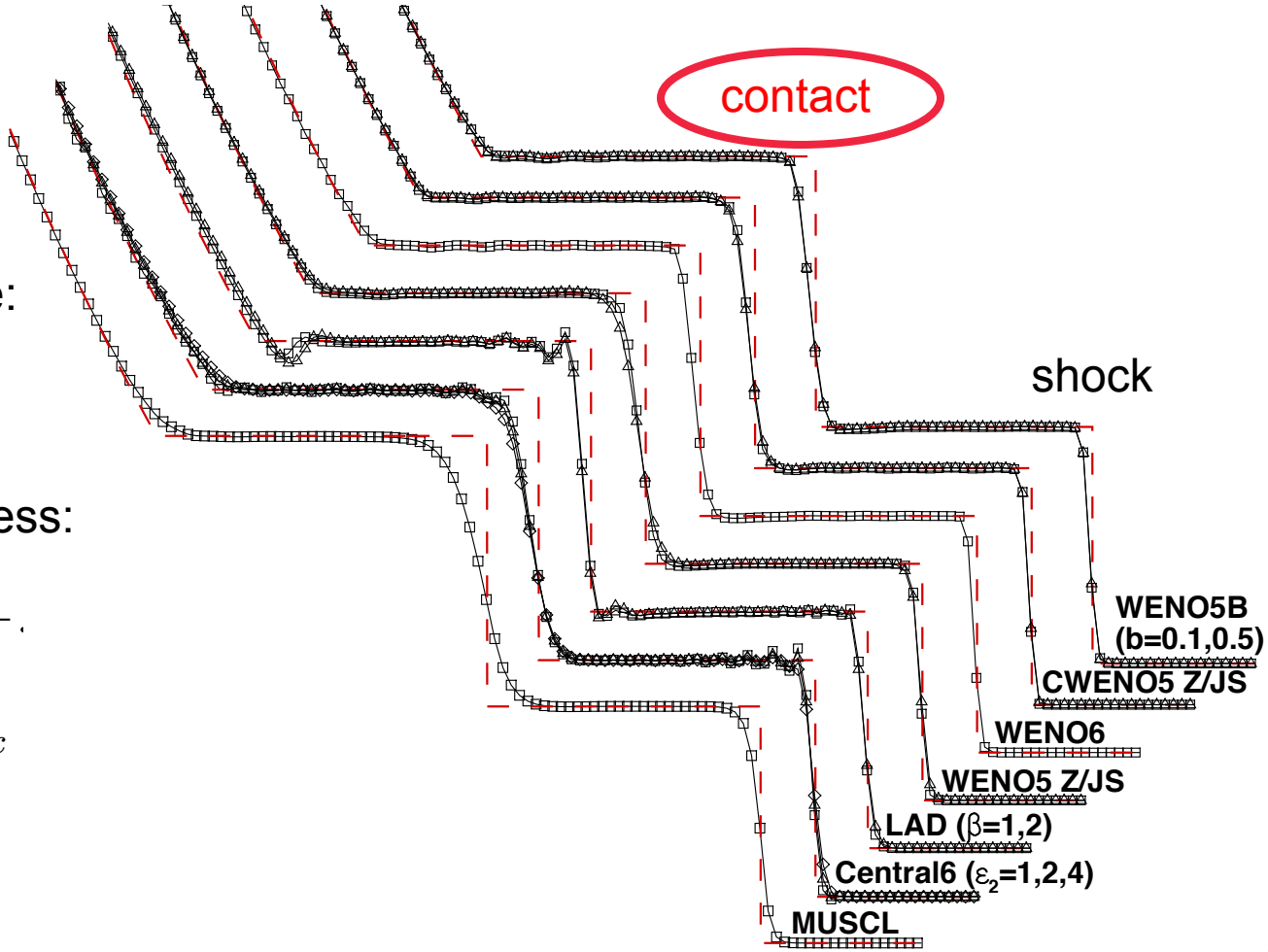



200 points on L=1

| | WENO5 Z/JS | WENO6 | WENO5B b = 0.1, 0.5 | CWENO5 Z/JS | LAD $\beta = 1.5$ | Central6 $\epsilon_2 = 1, 2, 4$ |
|---|---|---|---|---|---|---|
| contact | | | | | | |
| $\frac{\Delta\rho_{max}}{\Delta\rho}$ | 0.0079\|0.0060 | 0.0082 | 0.0081\|0.0121 | 0.0073\|0.0058 | 0.0666 | 0.0320\|0.0112\|0.0101 |
| $\frac{\delta}{\Delta x}$ | 3.7540\|4.7821 | 3.1872 | 3.2166\|3.4060 | 2.9421\|3.4263 | 2.6616 | 4.8374\|5.1386\|5.6107 |

1D Unsteady Shock Problem:

# Sod Problem




- wiggle amplitude:

$$\Delta p_{max}/\Delta p$$

- discontinuity thickness:

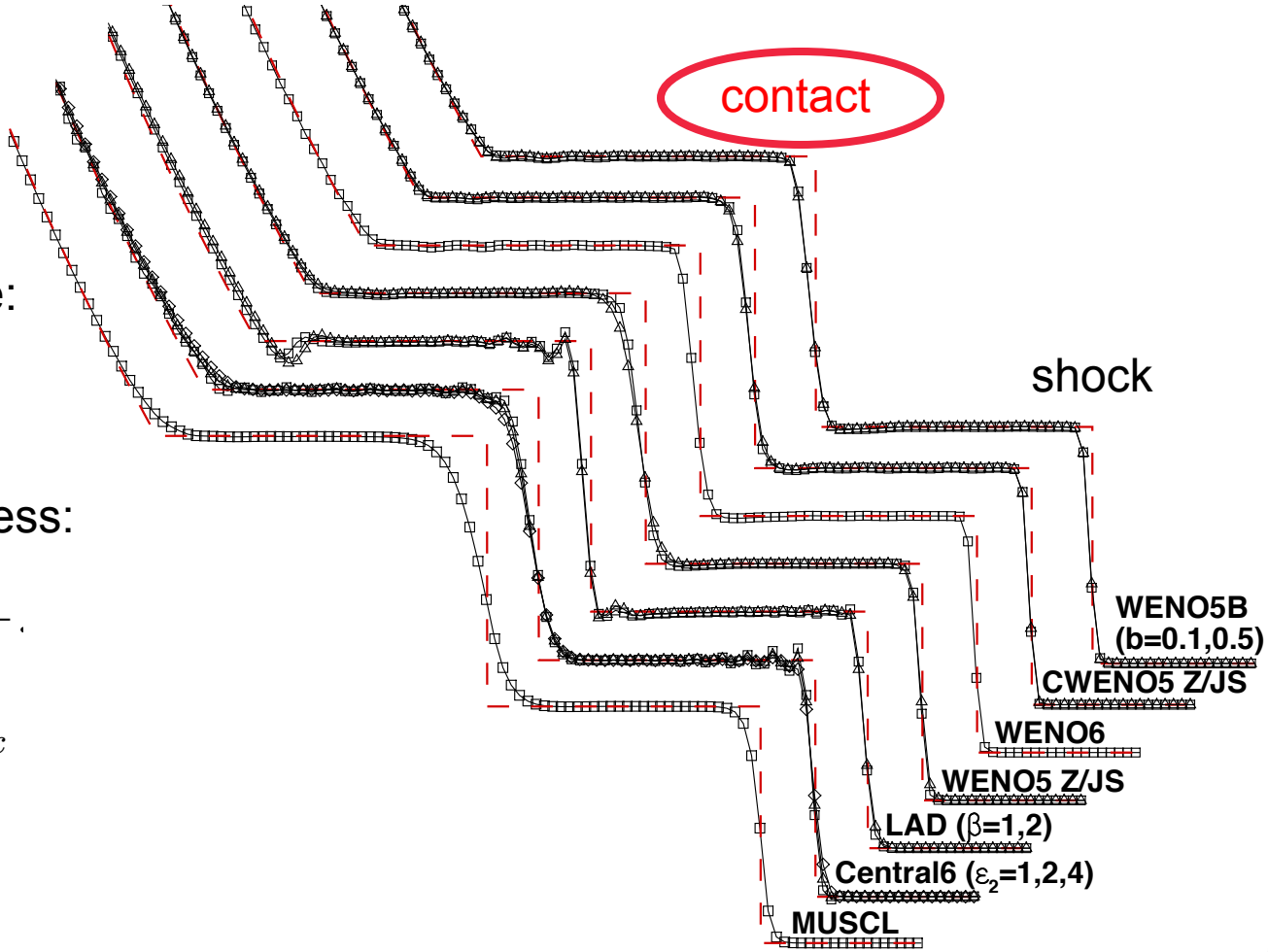
$$\frac{\delta}{\Delta x} = \frac{\Delta p}{\Delta x \frac{\partial p}{\partial x}\Big|_{max}}.$$

200 points on L=1

| | WENO5 Z/JS | WENO6 | WENO5B b = 0.1, 0.5 | CWENO5 Z/JS | LAD $\beta = 1.5$ | Central6 $\epsilon_2 = 1, 2, 4$ |
|---|---|---|---|---|---|---|
| contact | | | | | | |
| $\frac{\Delta\rho_{max}}{\Delta\rho}$ | 0.0079\|0.0060 | 0.0082 | 0.0081\|0.0121 | 0.0073\|0.0058 | 0.0666 | 0.0320\|0.0112\|0.0101 |
| $\frac{\delta}{\Delta x}$ | 3.7540\|4.7821 | 3.1872 | 3.2166\|3.4060 | 2.9421\|3.4263 | 2.6616 | 4.8374\|5.1386\|5.6107 |

1D Unsteady Shock Problem:

# Sod Problem




- wiggle amplitude:

$$\Delta p_{max}/\Delta p$$

- discontinuity thickness:

$$\frac{\delta}{\Delta x} = \frac{\Delta p}{\Delta x \frac{\partial p}{\partial x}\Big|_{max}}.$$

200 points on L=1



| | WENO5 Z/JS | WENO6 | WENO5B b = 0.1, 0.5 | CWENO5 Z/JS | LAD $\beta = 1.5$ | Central6 $\epsilon_2 = 1, 2, 4$ |
|---|---|---|---|---|---|---|
| contact | | | | | | |
| $\frac{\Delta\rho_{max}}{\Delta\rho}$ | 0.0079\|0.0060 | 0.0082 | 0.0081\|0.0121 | 0.0073\|0.0058 | 0.0666 | 0.0320\|0.0112\|0.0101 |
| $\frac{\delta}{\Delta x}$ | 3.7540\|4.7821 | 3.1872 | 3.2166\|3.4060 | 2.9421\|3.4263 | 2.6616 | 4.8374\|5.1386\|5.6107 |

1D Unsteady Shock Problem:

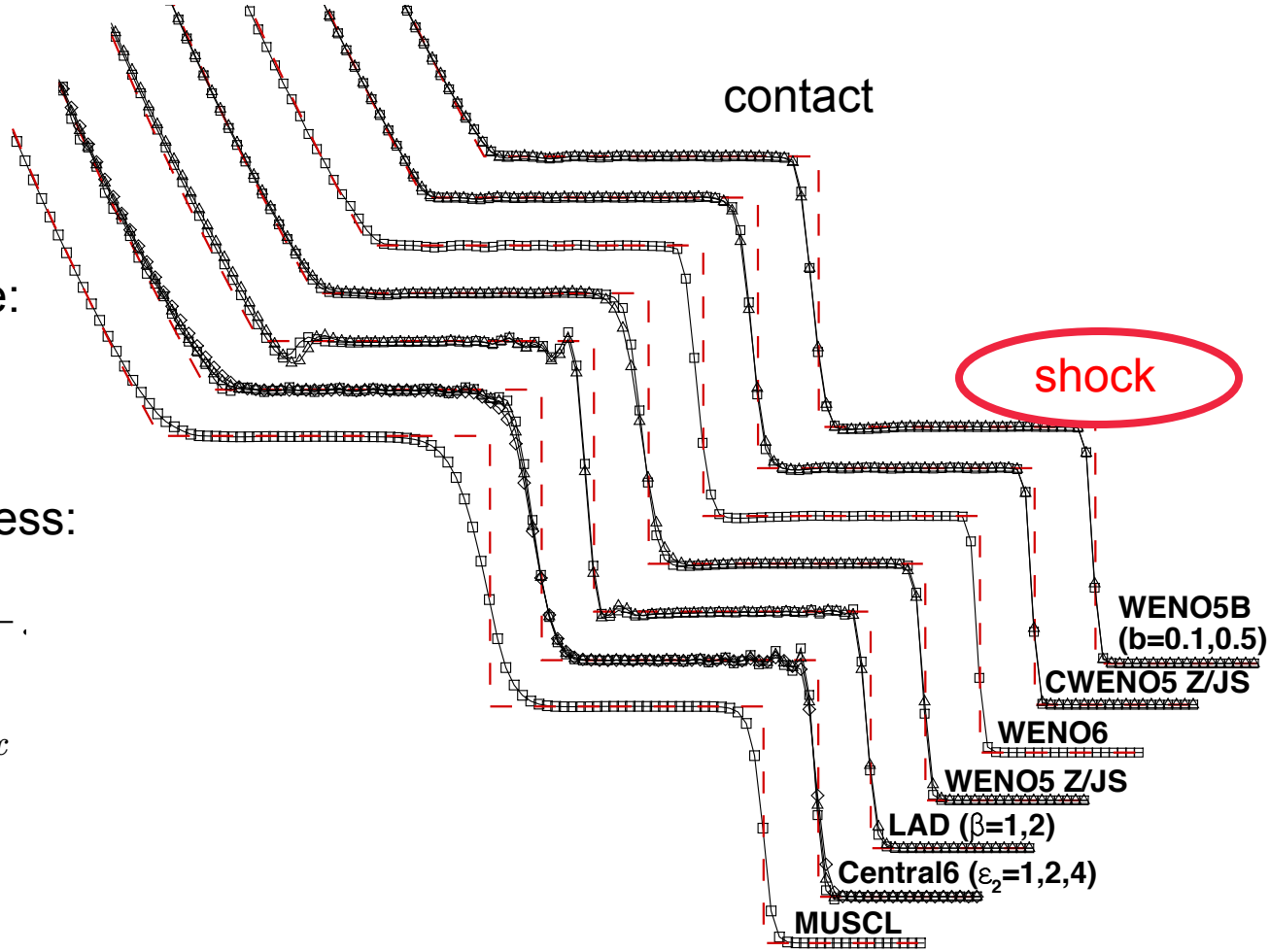
# Sod Problem

- wiggle amplitude:

$$\Delta p_{max}/\Delta p$$

- discontinuity thickness:

$$\frac{\delta}{\Delta x} = \frac{\Delta p}{\Delta x \frac{\partial p}{\partial x}\Big|_{max}}.$$

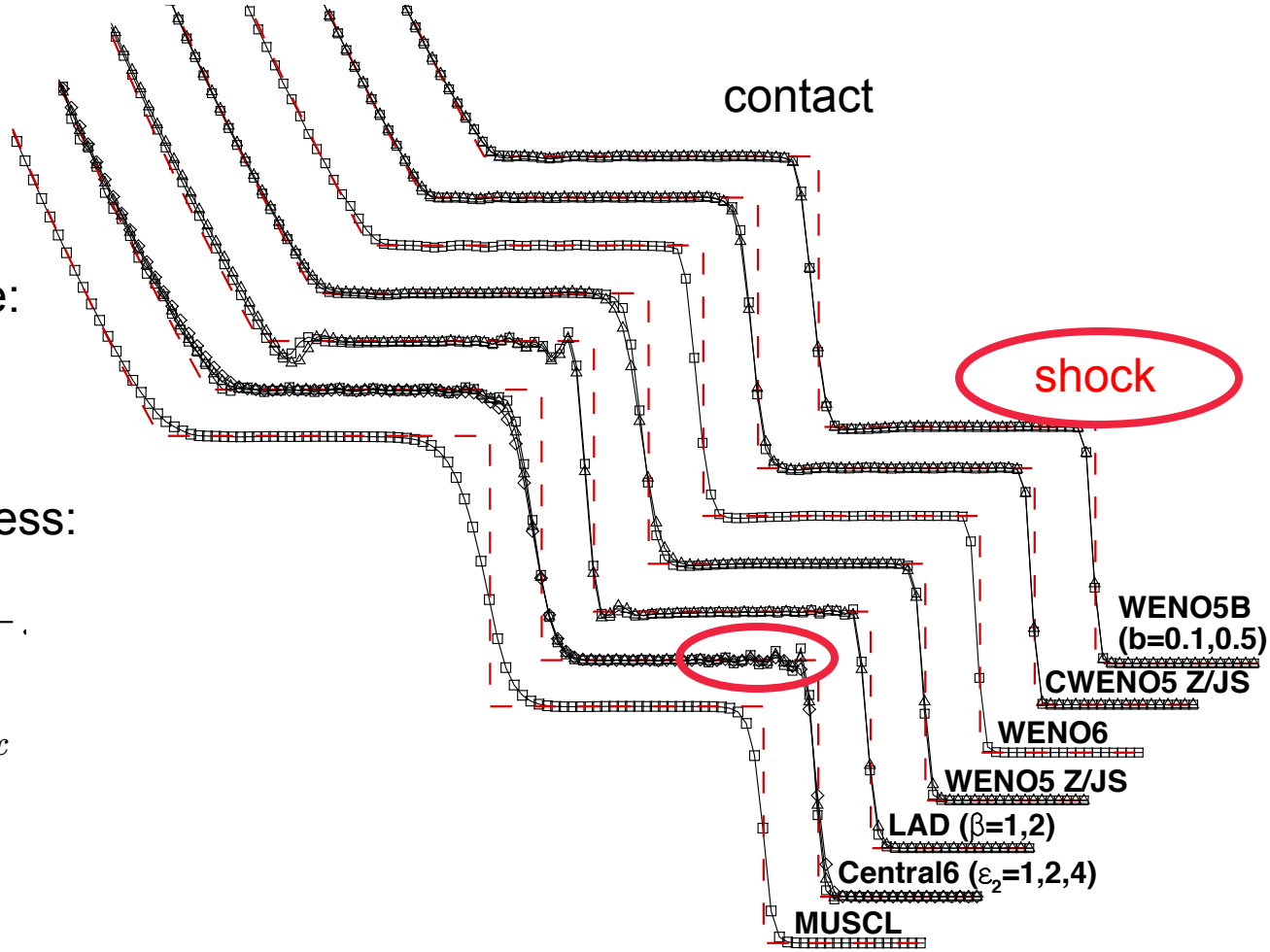



200 points on L=1

| | WENO5 Z/JS | WENO6 | WENO5B b = 0.1, 0.5 | CWENO5 Z/JS | LAD $\beta = 1.5$ | Central6 $\epsilon_2 = 1, 2, 4$ |
|---|---|---|---|---|---|---|
| shock | | | | | | |
| $\frac{\Delta p_{max}}{\Delta p}$ | 0.0161\|0.0163 | 0.0169 | 0.0165\|0.0171 | 0.0183\|0.0161 | 0.0223 | 0.0592\|0.0416\|0.0281 |
| $\frac{\delta}{\Delta x}$ | 1.8873\|2.1939 | 1.6945 | 1.7078\|1.7629 | 1.6191\|1.6772 | 2.2301 | 1.8984\|2.1989\|2.6284 |

1D Unsteady Shock Problem:

# Sod Problem




- wiggle amplitude:

$$\Delta p_{max}/\Delta p$$

- discontinuity thickness:

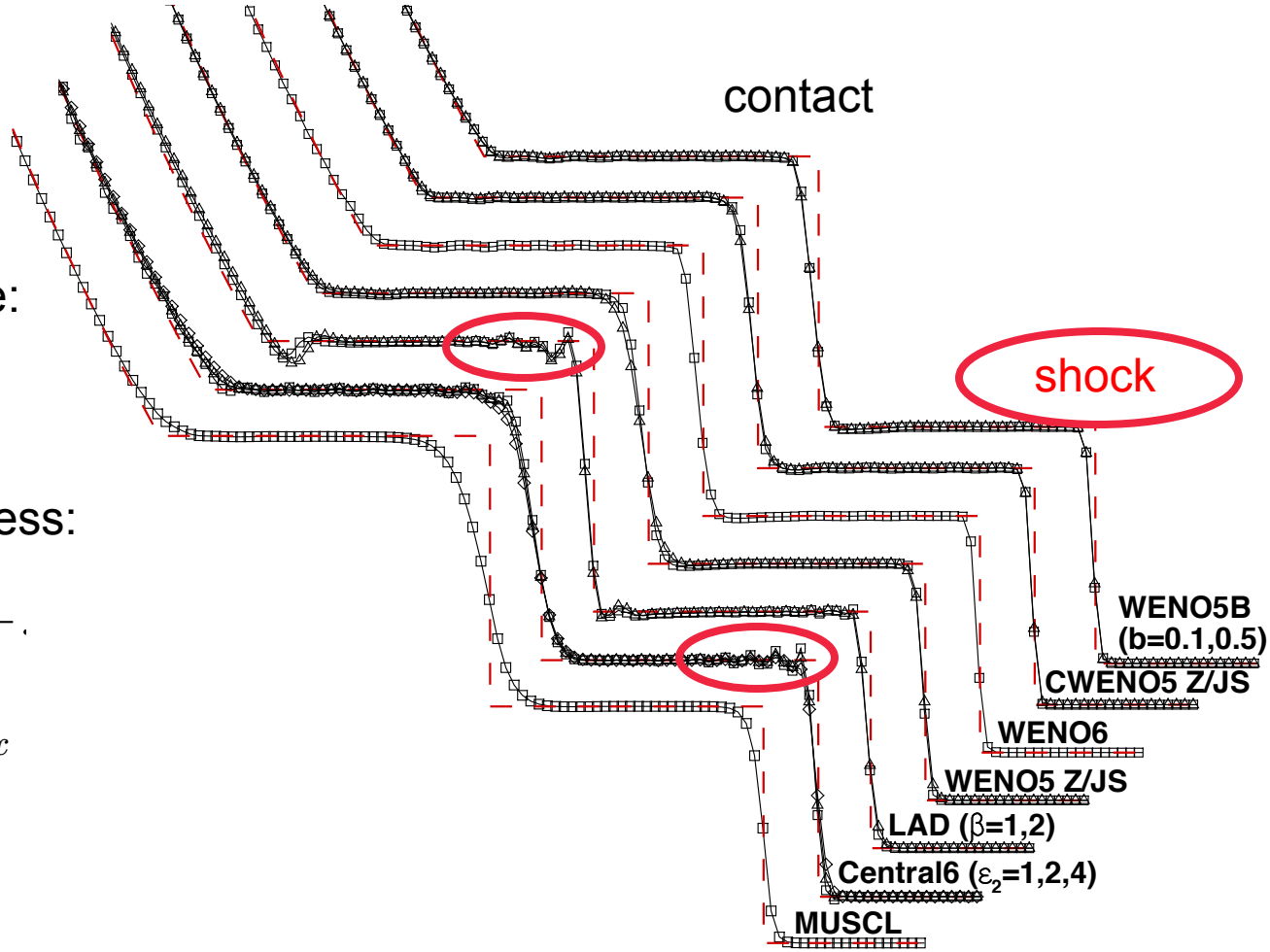
$$\frac{\delta}{\Delta x} = \frac{\Delta p}{\Delta x \frac{\partial p}{\partial x}\Big|_{max}}.$$

200 points on L=1

| | WENO5 Z/JS | WENO6 | WENO5B b = 0.1, 0.5 | CWENO5 Z/JS | LAD $\beta = 1.5$ | Central6 $\epsilon_2 = 1, 2, 4$ |
|---|---|---|---|---|---|---|
| shock | | | | | | |
| $\frac{\Delta p_{max}}{\Delta p}$ | 0.0161\|0.0163 | 0.0169 | 0.0165\|0.0171 | 0.0183\|0.0161 | 0.0223 | 0.0592\|0.0416\|0.0281 |
| $\frac{\delta}{\Delta x}$ | 1.8873\|2.1939 | 1.6945 | 1.7078\|1.7629 | 1.6191\|1.6772 | 2.2301 | 1.8984\|2.1989\|2.6284 |

1D Unsteady Shock Problem:

# Sod Problem




- wiggle amplitude:

$$\Delta p_{max}/\Delta p$$

- discontinuity thickness:

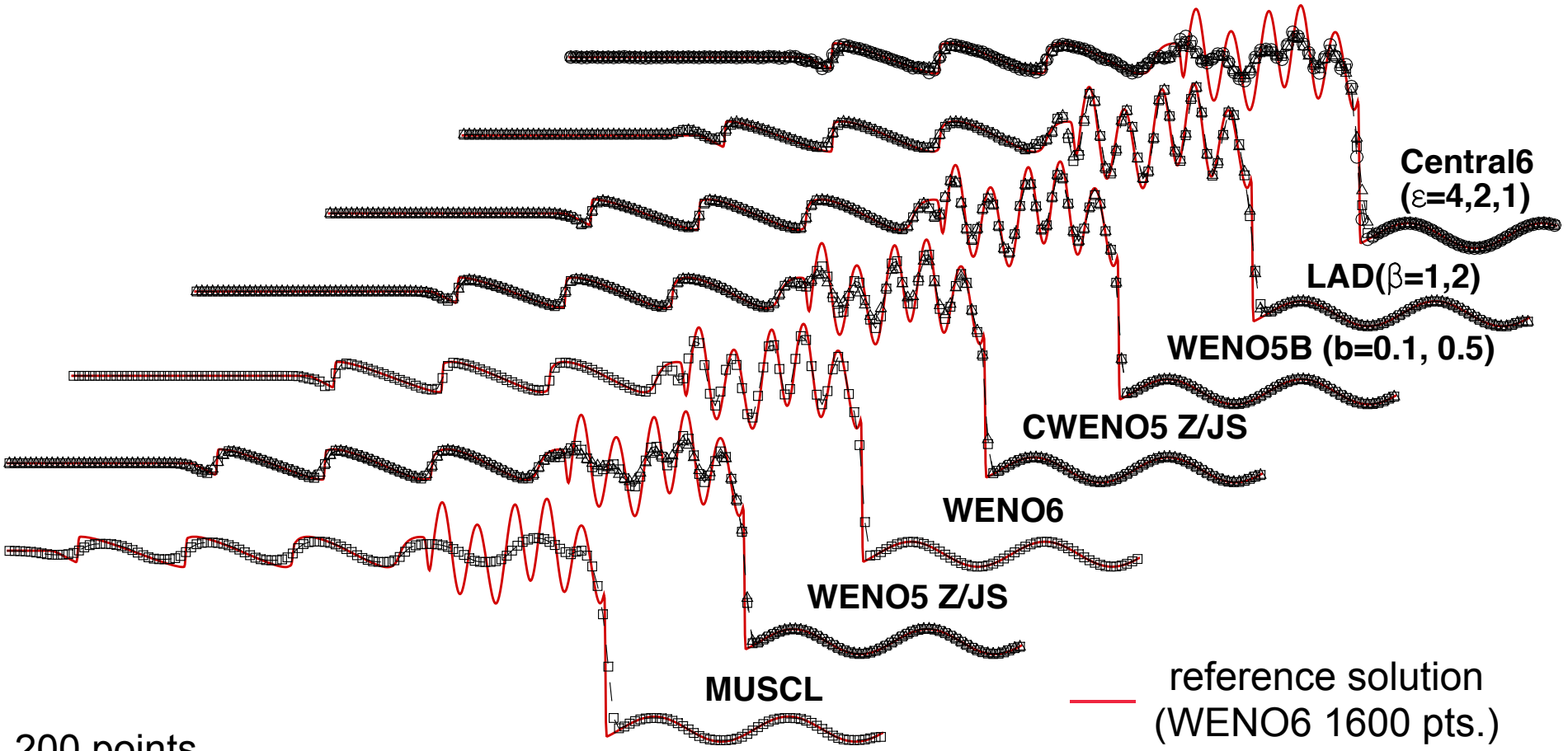
$$\frac{\delta}{\Delta x} = \frac{\Delta p}{\Delta x \frac{\partial p}{\partial x}\Big|_{max}}.$$

200 points on L=1

| | WENO5 Z/JS | WENO6 | WENO5B b = 0.1, 0.5 | CWENO5 Z/JS | LAD $\beta = 1.5$ | Central6 $\epsilon_2 = 1, 2, 4$ |
|---|---|---|---|---|---|---|
| shock | | | | | | |
| $\frac{\Delta p_{max}}{\Delta p}$ | 0.0161\|0.0163 | 0.0169 | 0.0165\|0.0171 | 0.0183\|0.0161 | 0.0223 | 0.0592\|0.0416\|0.0281 |
| $\frac{\delta}{\Delta x}$ | 1.8873\|2.1939 | 1.6945 | 1.7078\|1.7629 | 1.6191\|1.6772 | 2.2301 | 1.8984\|2.1989\|2.6284 |

Shock-Turbulence Interaction Model Problem:

# Shu-Osher Problem

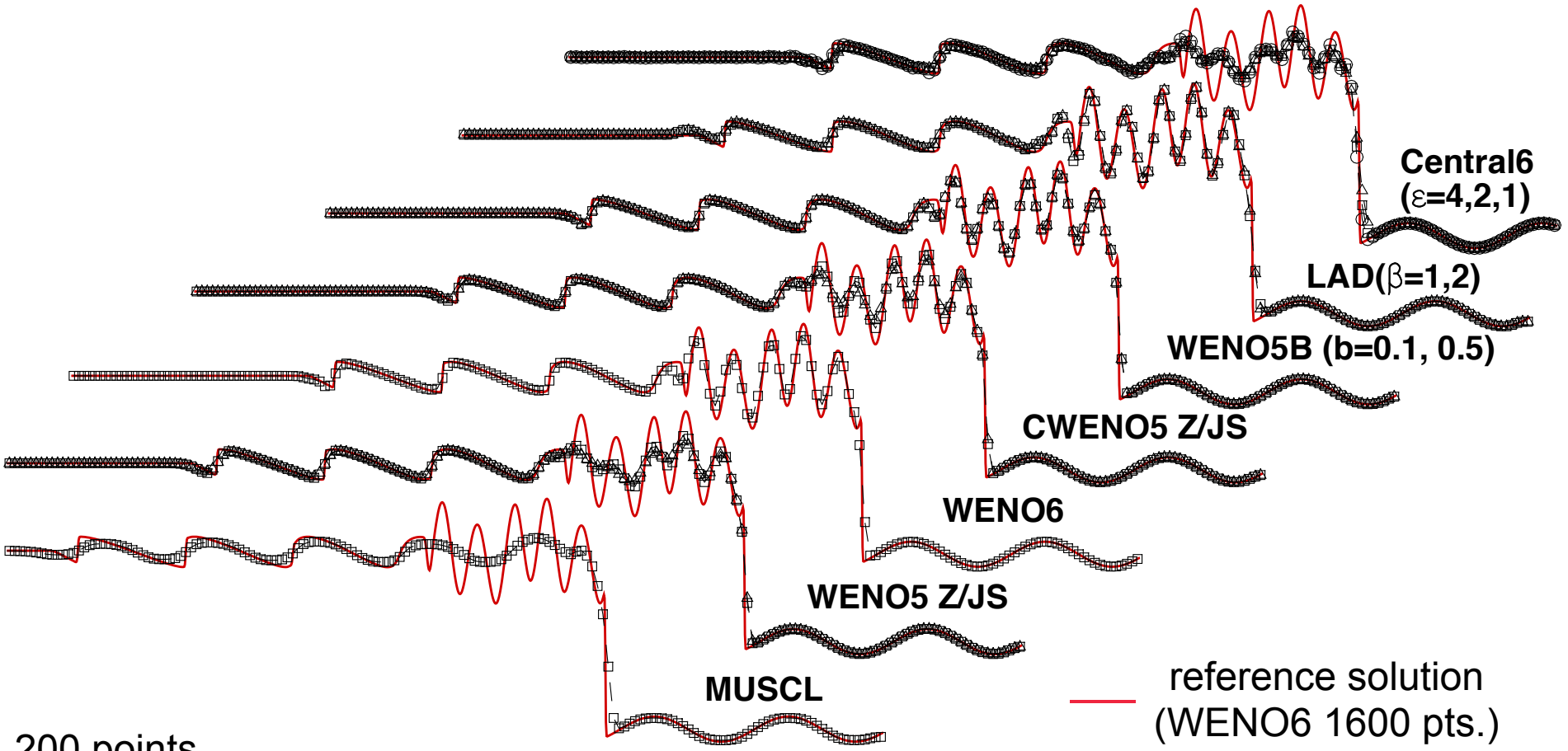



200 points
Solution error:

| | WENO5 Z/JS | WENO6 | WENO5B b=0.1 | CWENO5 Z/JS | LAD $\beta = 1, 2$ | Central6 $\epsilon_2 = 1, 1.5, 2$ |
|---|---|---|---|---|---|---|
| $\|\|\epsilon_\rho\|\|_2$ | 0.0467\|0.05550 | 0.0254 | 0.0266 | 0.0269\|0.0392 | 0.0244\|0.0268 | 0.0607\|0.0619\|0.0632 |
| $\|\|\epsilon_\rho\|\|_\infty$ | 0.1701\|0.19780 | 0.1034 | 0.0983 | 0.1036\|0.1515 | 0.0872\|0.1044 | 0.2022\|0.2107\|0.217 |

Shock-Turbulence Interaction Model Problem:

# Shu-Osher Problem




200 points
Solution error:

| | WENO5 Z/JS | WENO6 | WENO5B b=0.1 | CWENO5 Z/JS | LAD $\beta = 1, 2$ | Central6 $\epsilon_2 = 1, 1.5, 2$ |
|---|---|---|---|---|---|---|
| $\|\|\epsilon_\rho\|\|_2$ | 0.0467\|0.05550 | 0.0254 | 0.0266 | 0.0269\|0.0392 | 0.0244\|0.0268 | 0.0607\|0.0619\|0.0632 |
| $\|\|\epsilon_\rho\|\|_\infty$ | 0.1701\|0.19780 | 0.1034 | 0.0983 | 0.1036\|0.1515 | 0.0872\|0.1044 | 0.2022\|0.2107\|0.217 |

Propagation of Vortical Structures:

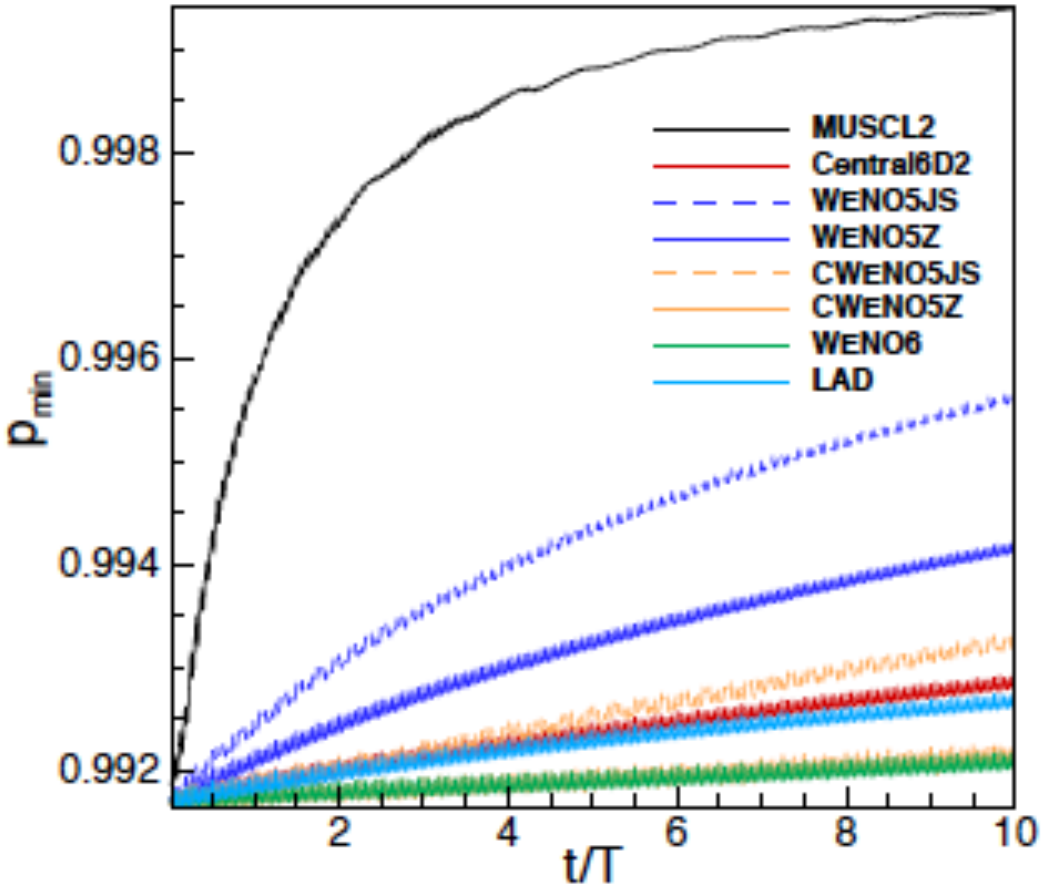
# Vortex-Propagation

- Isentropic vortex

$$
\begin{aligned}
T &= T_\infty - \frac{V_s^2(\gamma-1)}{16 G_s \gamma \pi^2} e^{2G_s(1-r^2)} \\
\rho &= T^{\frac{1}{(\gamma-1)}} \\
u &= M_\infty - \frac{V_s}{2\pi}(y-y_0) e^{G_s(1-r^2)} \\
v &= \frac{V_s}{2\pi}(x-x_0) e^{G_s(1-r^2)}
\end{aligned}
$$

- small amplitude ($V_s$=0.5)
- smooth flow (!!)
- larger amplitudes used in performance study
- 32×32 on 10×10 domain
- periodic BCs

$p_{min}$ versus Time



Propagation of Vortical Structures:

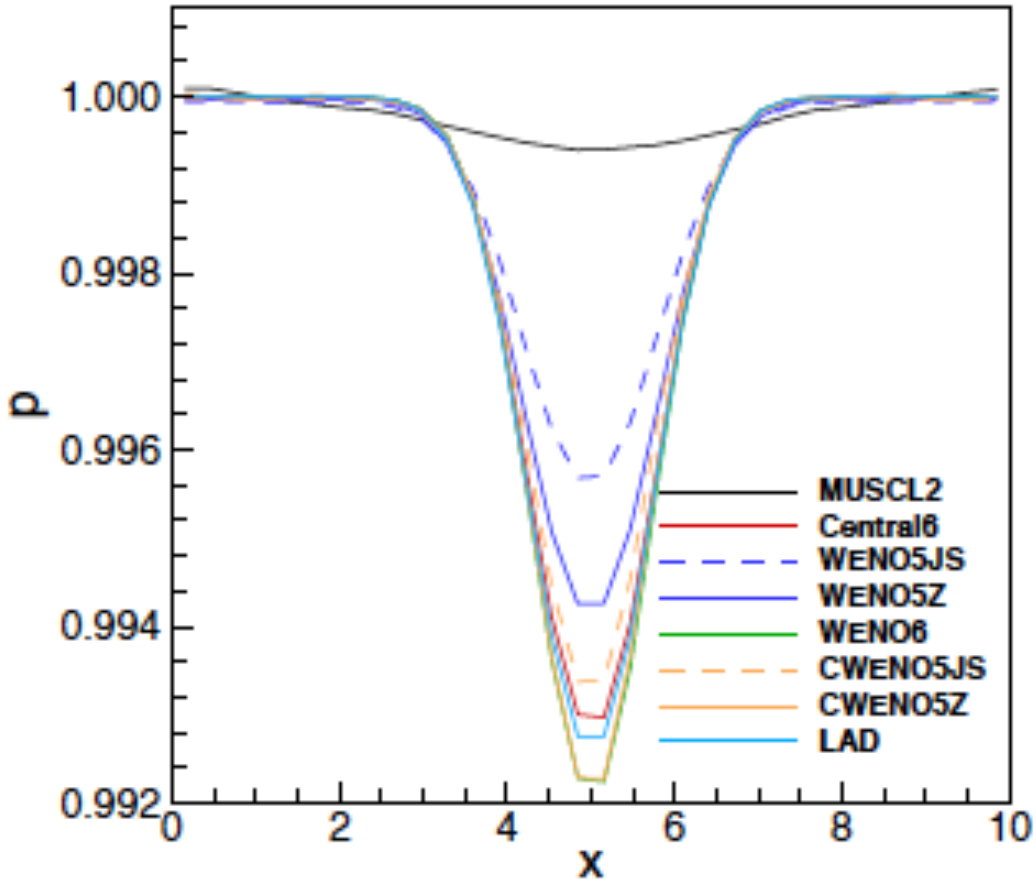
# Vortex-Propagation

- Isentropic vortex

$$
\begin{aligned}
T &= T_\infty - \frac{V_s^2(\gamma-1)}{16 G_s \gamma \pi^2} e^{2G_s(1-r^2)} \\
\rho &= T^{\frac{1}{(\gamma-1)}} \\
u &= M_\infty - \frac{V_s}{2\pi}(y-y_0) e^{G_s(1-r^2)} \\
v &= \frac{V_s}{2\pi}(x-x_0) e^{G_s(1-r^2)}
\end{aligned}
$$

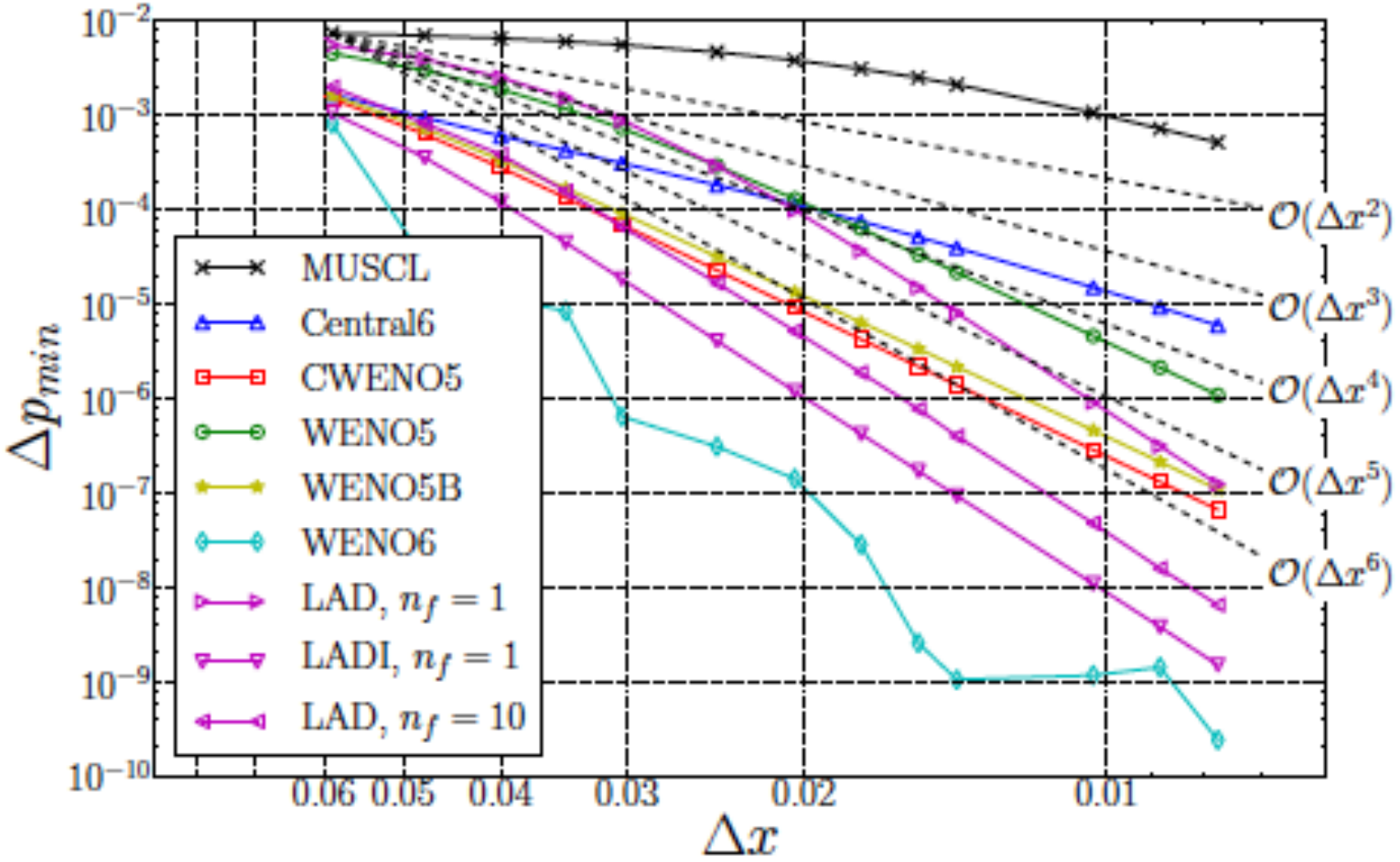
- small amplitude ($V_s$=0.5)
- smooth flow
- larger amplitudes used in performance study
- 32×32 on 10×10 domain
- periodic BCs

Final $p_{min}$ Distribution



# Vortex-Propagation

Error convergence study for minimum pressure extracted at t/T=2:

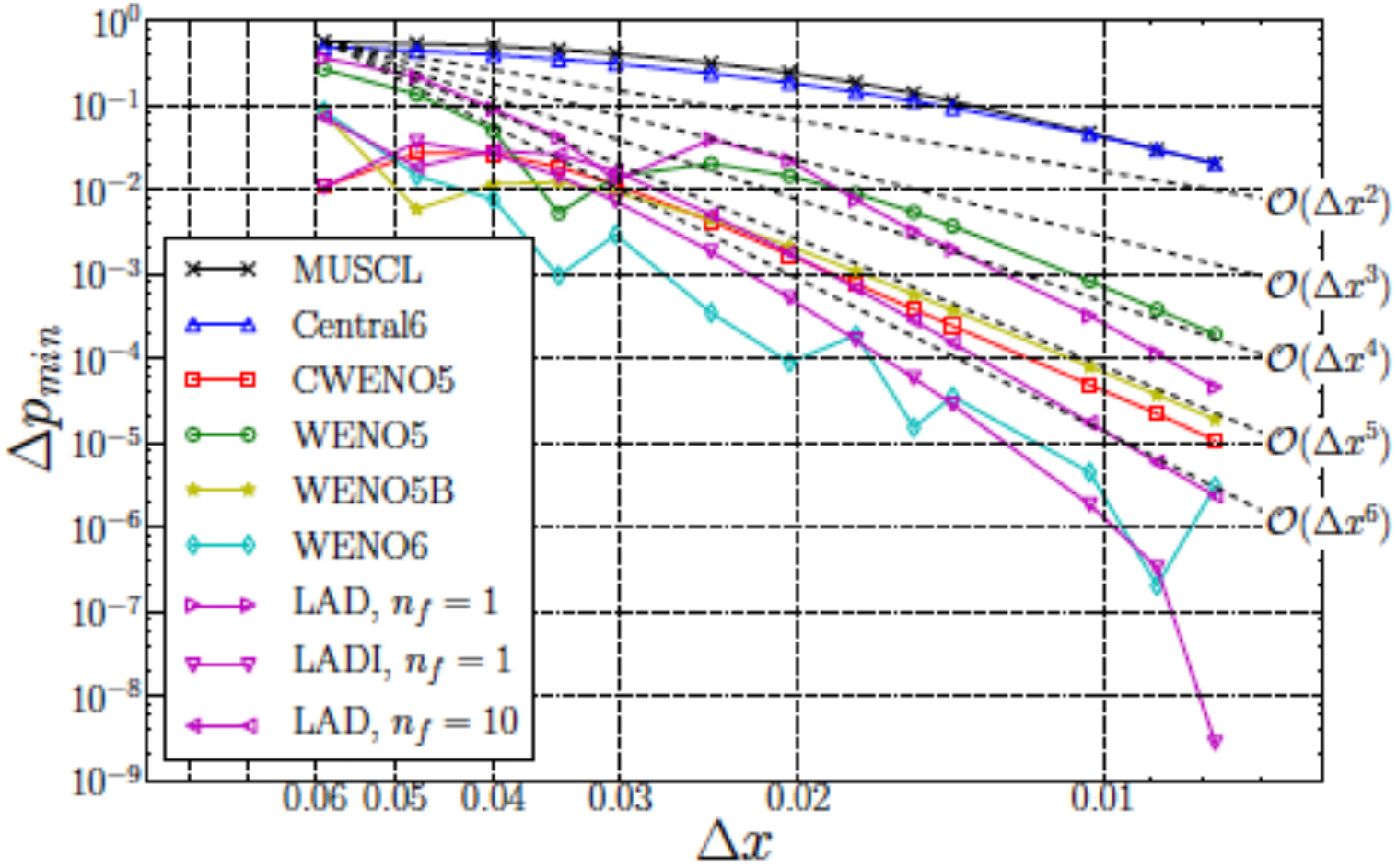



CFL=6.5×10$^{-2}$, Vs=0.5

Propagation of Vortical Structures:

# Vortex-Propagation

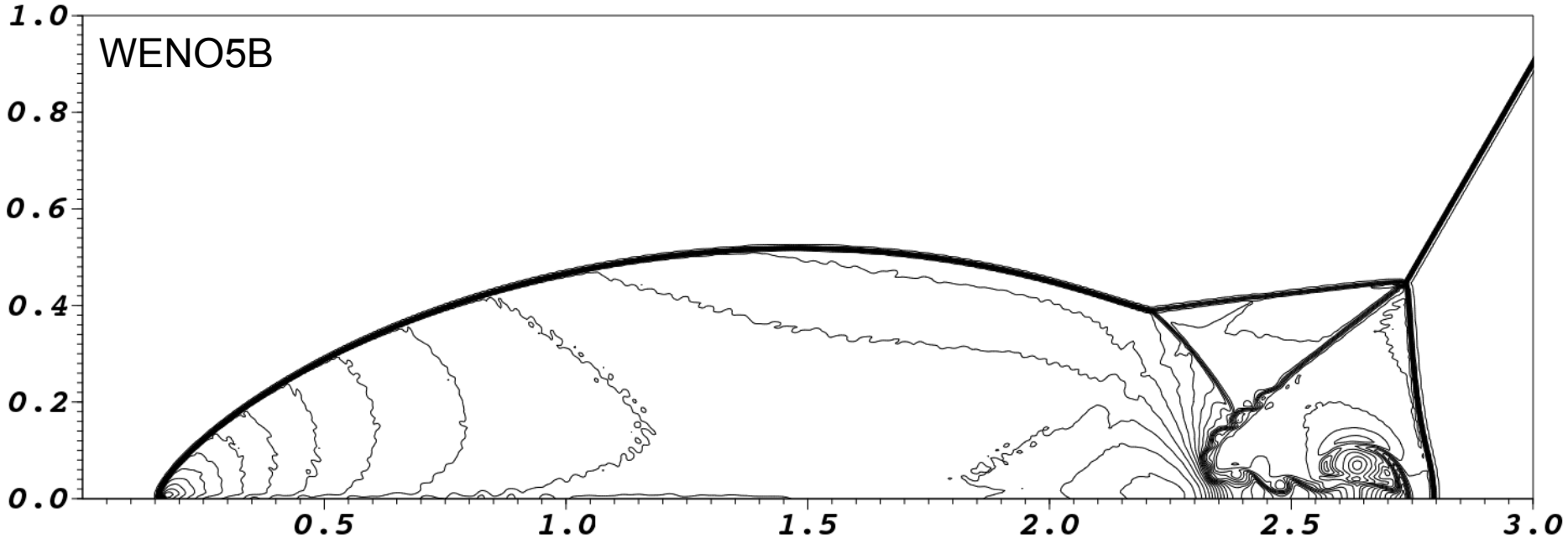
Error convergence study for minimum pressure extracted at t/T=2:




CFL=6.5×10$^{-2}$, Vs=5.0

Vortical Structures:

# Double-Mach Reflection

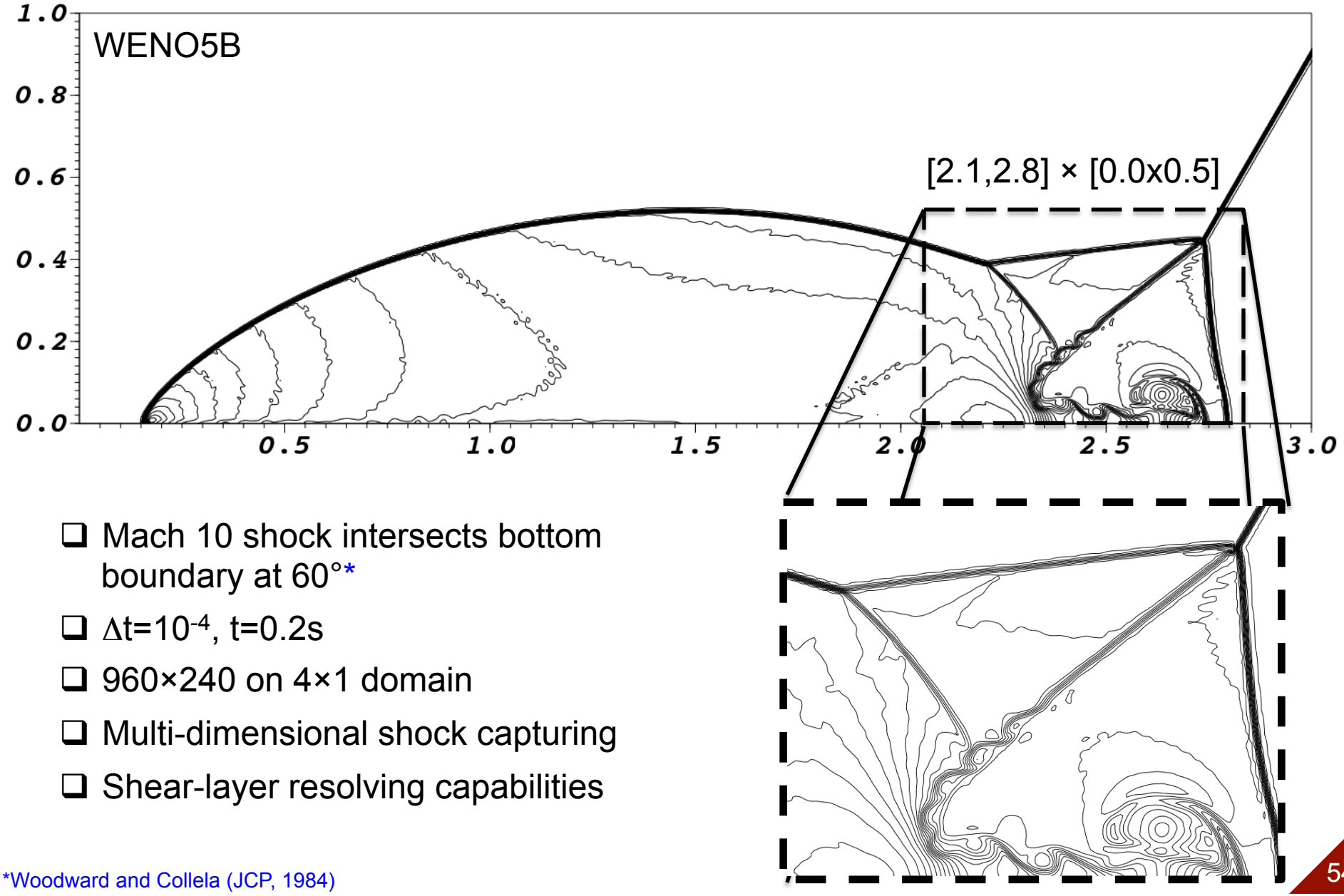



- Mach 10 shock intersects bottom boundary at 60°*
- $\Delta t=10^{-4}$, t=0.2s
- 960×240 on 4×1 domain
- Multi-dimensional shock capturing
- Shear-layer resolving capabilities

*Woodward and Collela (JCP, 1984)

Vortical Structures:

# Double-Mach Reflection

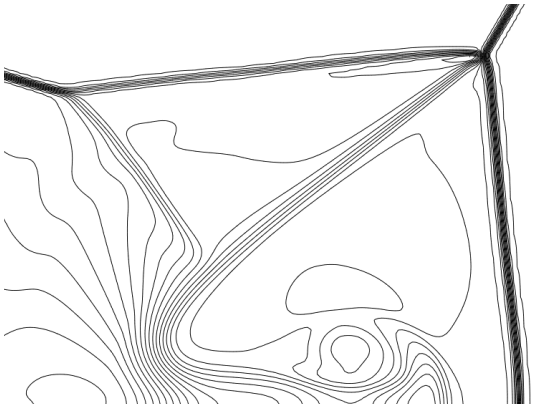



- Mach 10 shock intersects bottom boundary at 60°*
- $\Delta t=10^{-4}$, t=0.2s
- 960×240 on 4×1 domain
- Multi-dimensional shock capturing
- Shear-layer resolving capabilities

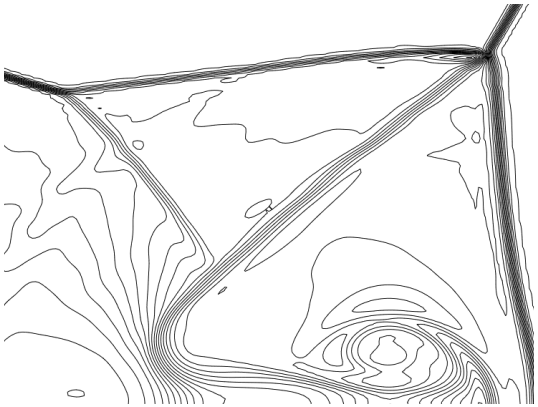
*Woodward and Collela (JCP, 1984)

Vortical Structures:

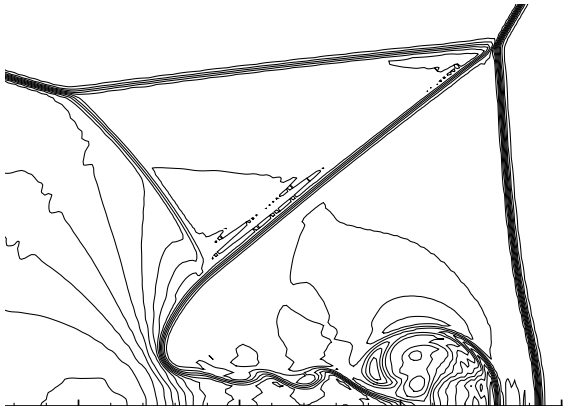
# Close-up Comparison



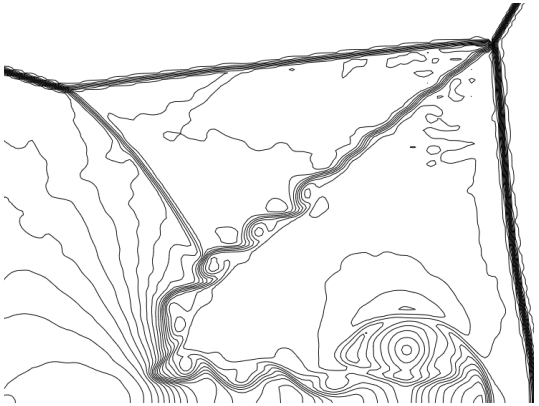
MUSCL



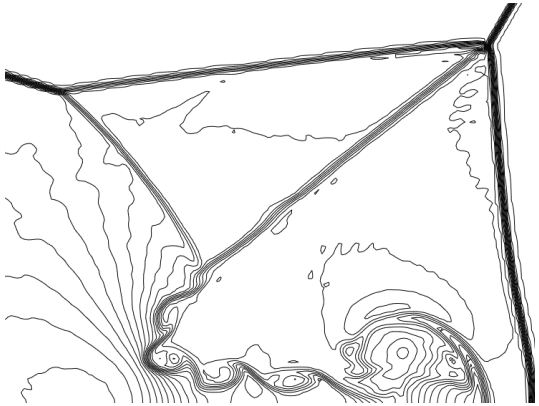
Central6D2



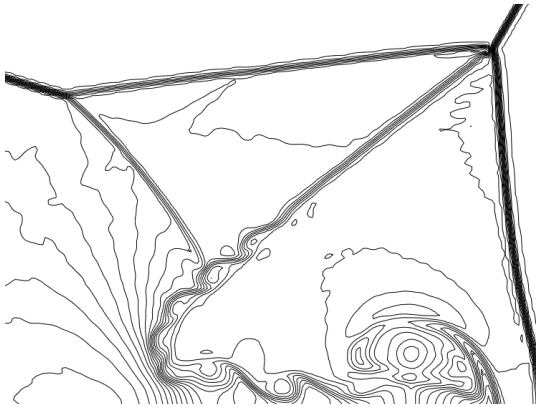
LAD



CWENO5



WENO6



WENO5B

[960×240] on [4×1] domain

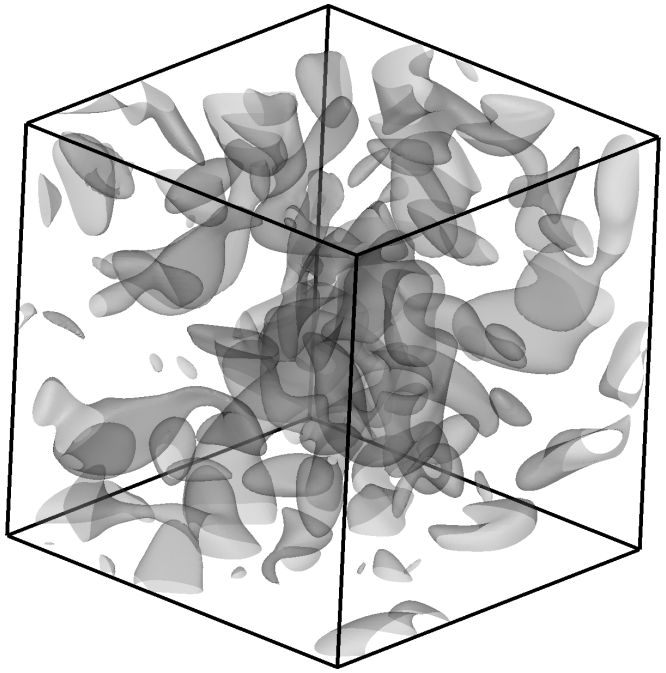
Spectral Resolution:

# Isotropic Turbulence

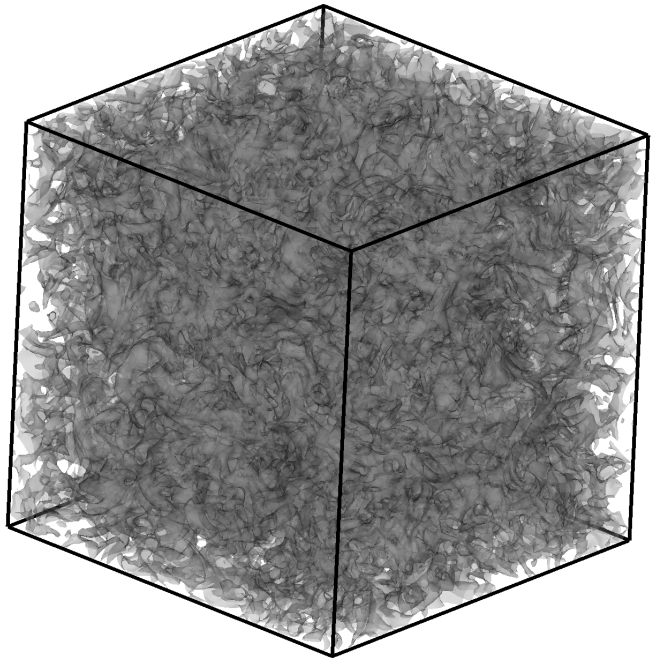
Computational setup

- $T_o=\rho_o=u_{rms,o}=1$, Pr=0.7, $\gamma$=1.4, $M_t$=0.5, Re $\rightarrow \infty$
- Eddy turn-over time, $\tau=L_I/u'$ (integral length scale / turbulent fluctuating velocity)
- Occurrence of shocklets (Lee *et al.* 1990, Samtaney *et al.* 2001, Thornber *et al.* 2007)

Iso-Vorticity Contours |w|=5 ($128^3$)



t/$\tau$=0.



t/$\tau$=4.0625

Spectral Resolution:

# Isotropic Turbulence

Initial Condition

❑ Use Helmholtz decomposition to generate I.C. with $RMS_{comp}/RMS_{sol}=1/10$ (Hu and Adams, 2011):

$$\boldsymbol{u}(\boldsymbol{k}) = \boldsymbol{u}_s(\boldsymbol{k}) + \boldsymbol{u}_d(\boldsymbol{k})$$

$$\boldsymbol{u}_s(\boldsymbol{k}) = \boldsymbol{u}(\boldsymbol{k}) - \frac{\boldsymbol{k}\cdot\boldsymbol{u}(\boldsymbol{k})}{|\boldsymbol{k}|^2}\boldsymbol{k}$$

(solenoidal)

$$\boldsymbol{u}_d(\boldsymbol{k}) = \boldsymbol{u}(\boldsymbol{k}) - \boldsymbol{u}_s(\boldsymbol{k})$$

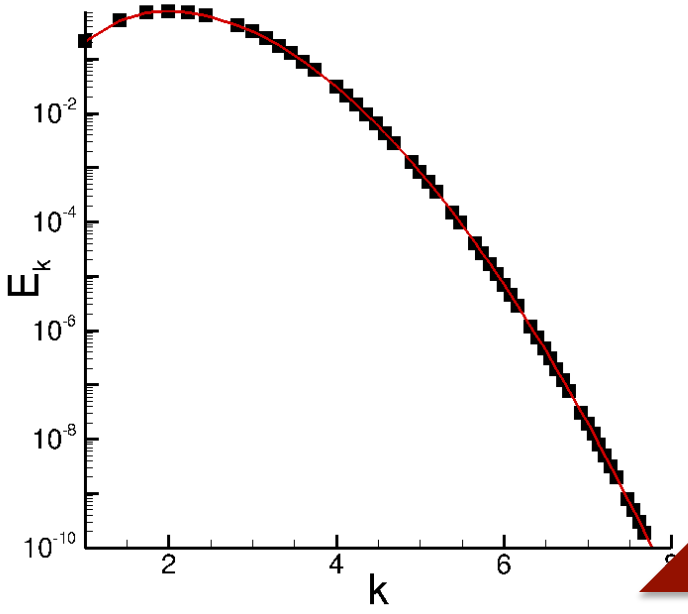
(dilatational)

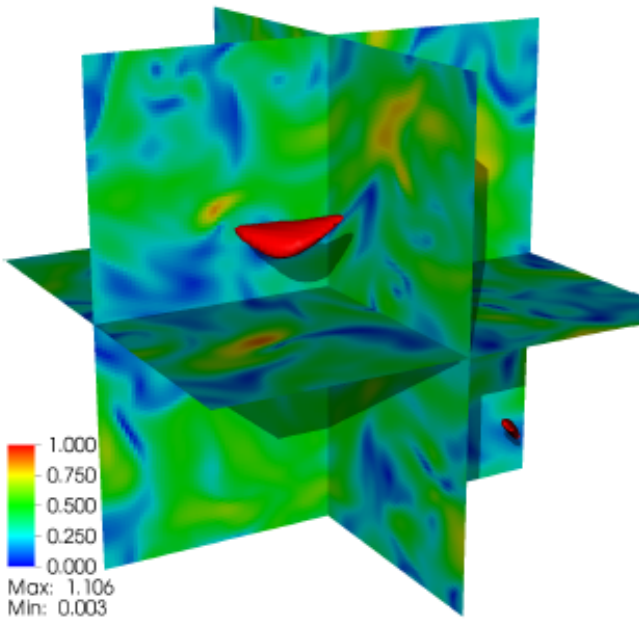
❑ Initial kinetic energy distribution:

$$E(k) = Ak^4 \exp\left(-k^2/k_p^2\right)$$

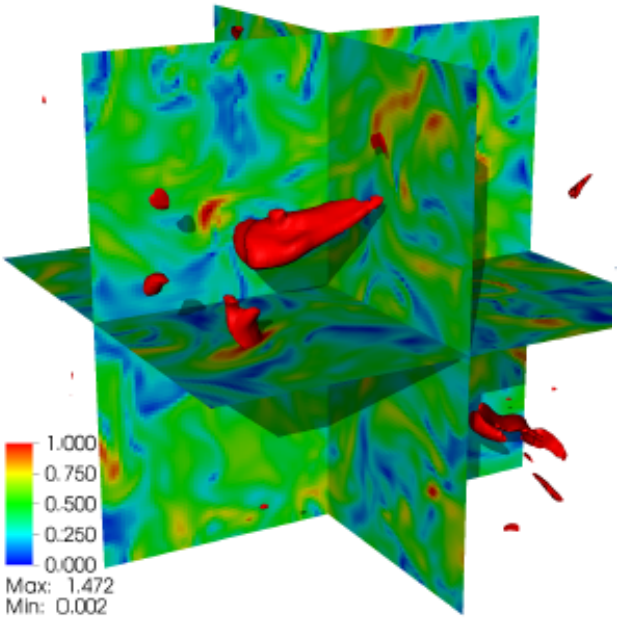
- Randomly oriented, sinusoidal sound and shear waves, $k_P=2$, r'=p'=0 (Ristorcelli and Blaisdell, 1997)
  - $k_P=2$, ρ'=p'=0
  - ➔ no acoustic equilibrium initial transient

initial kinetic energy spectrum

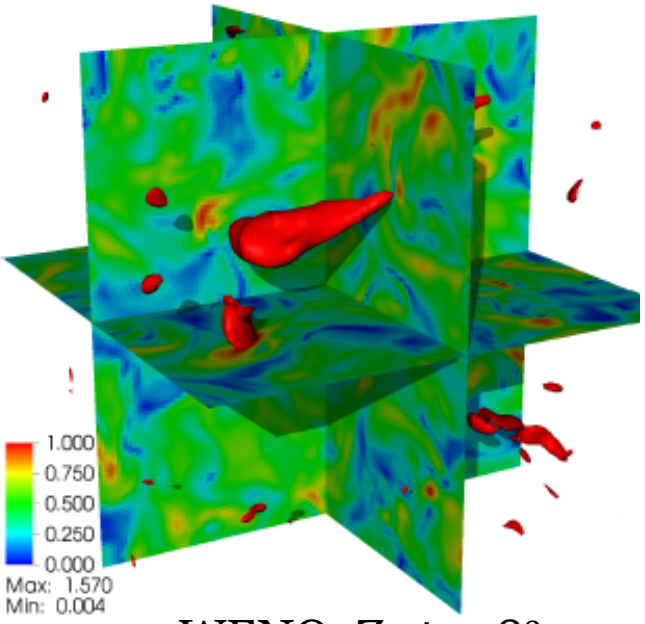




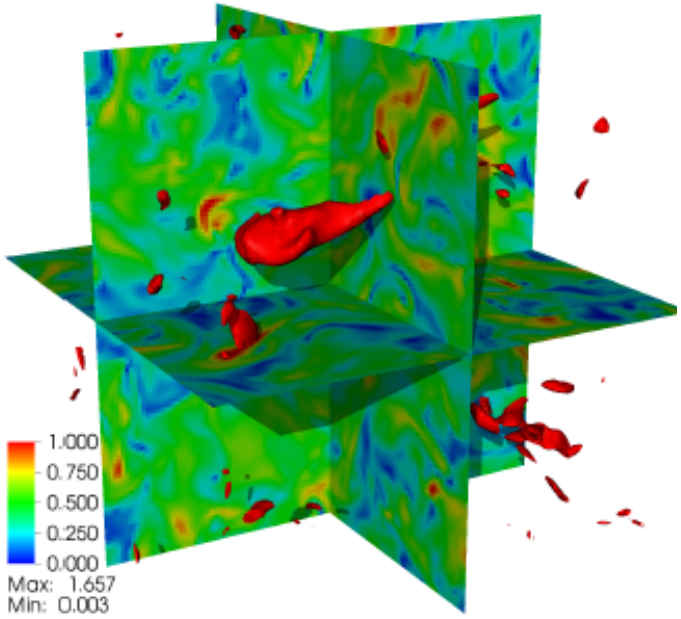

MUSCL at $128^3$



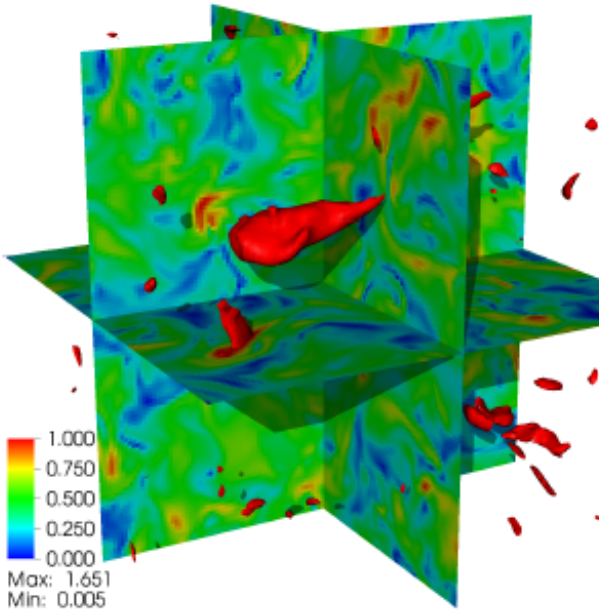

Central6 at $128^3$



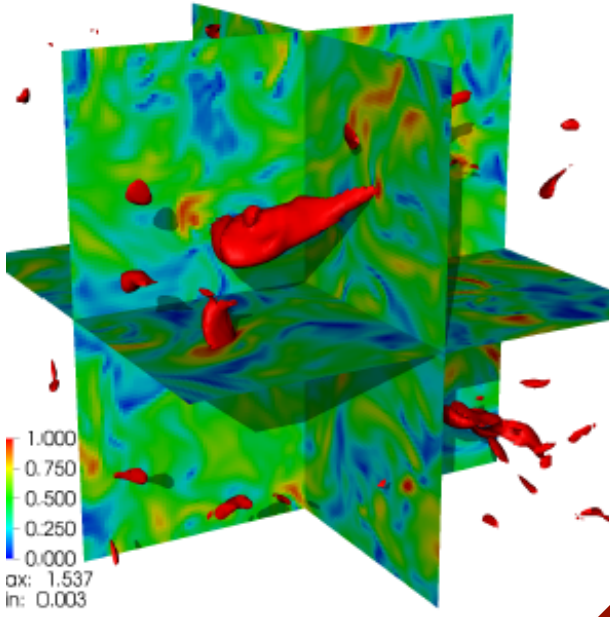

WENO5Z at $128^3$




CWENO5JS at $128^3$



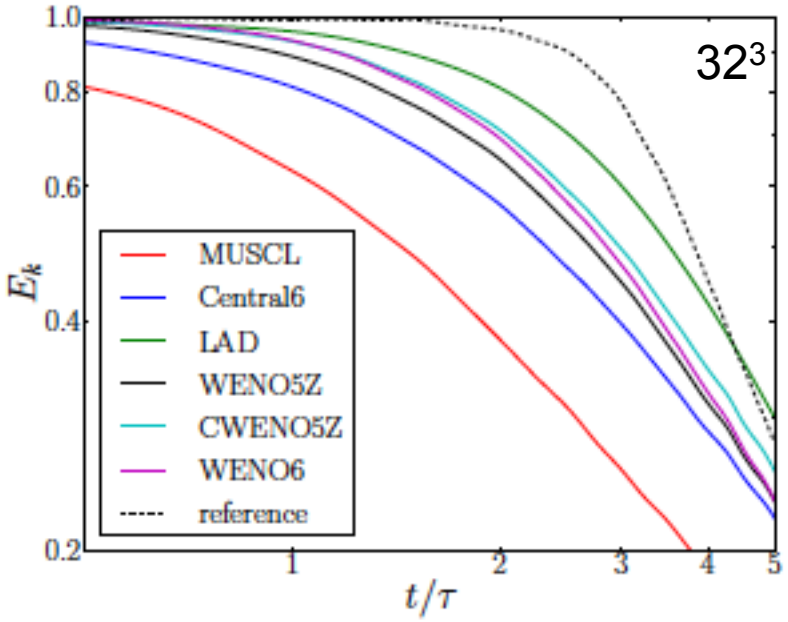

WENO6 at $128^3$

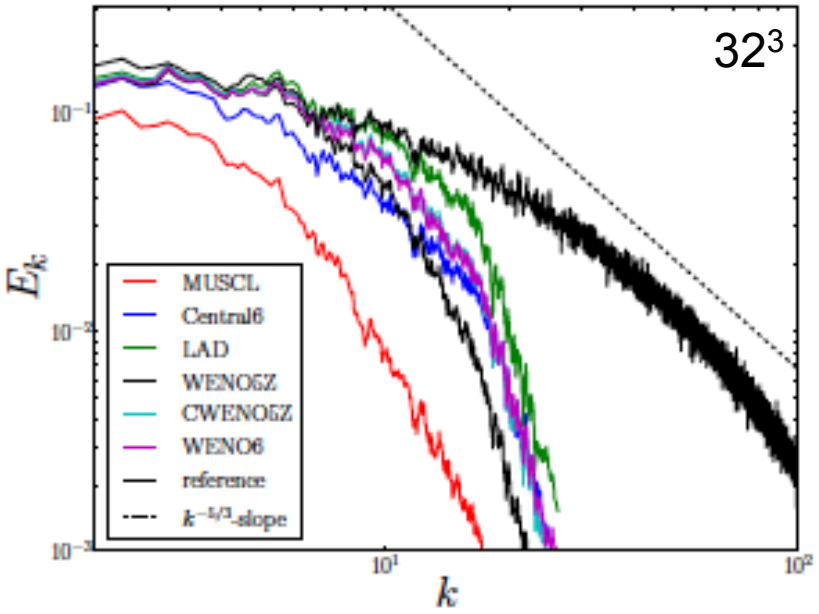


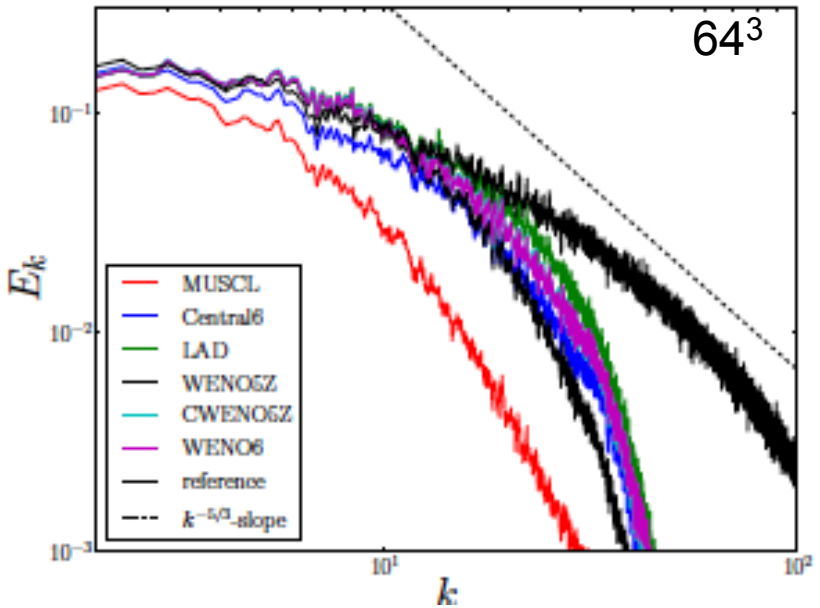

LAD at $128^3$

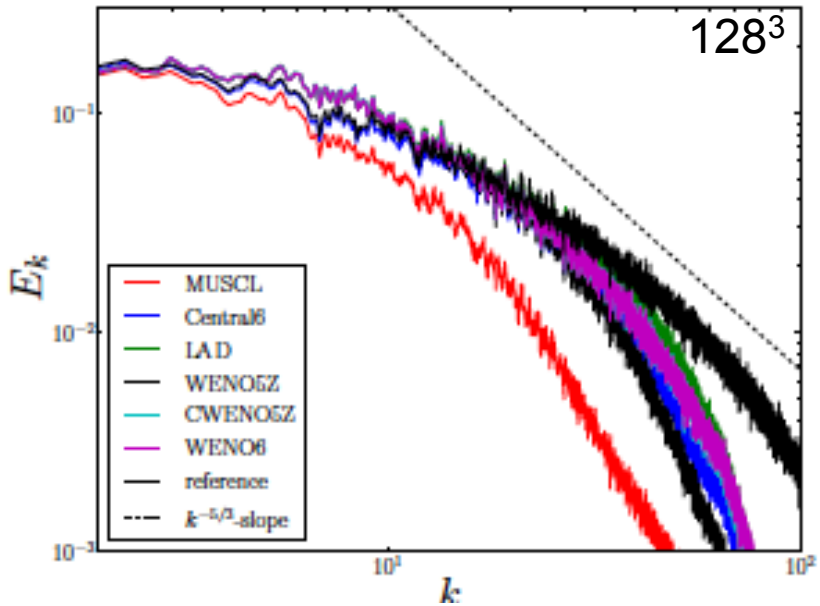
Spectral Resolution:

# Kinetic Energy Spectrum



# Outline




Motivation/Introduction

Higher-Order Shock Capturing Schemes

Accuracy

Test Problems

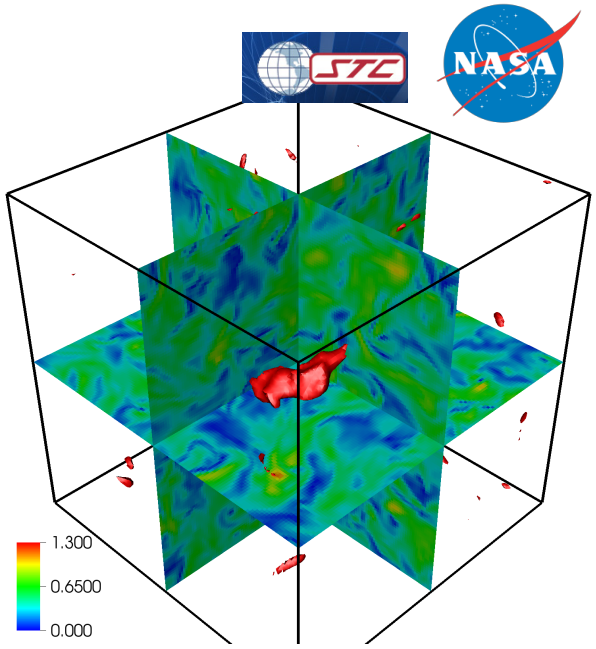
Computational Performance
*Analysis and comparison of computational cost.*

Summary & Future Work

Performance Comparison:

# Cost Breakdown

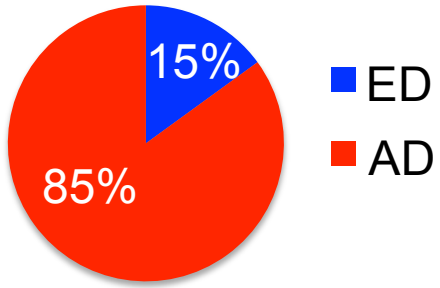
- Break down cost for different schemes individually
- Use homogeneous turbulence case
- Identify most costly parts of the scheme
- Single processor performance
- Performance of numerical schemes strongly depends on actual implementation of the numerical schemes, compiler, architecture, etc.




Isotropic Turbulence ($128^3$)
Mach number contours

# Central:

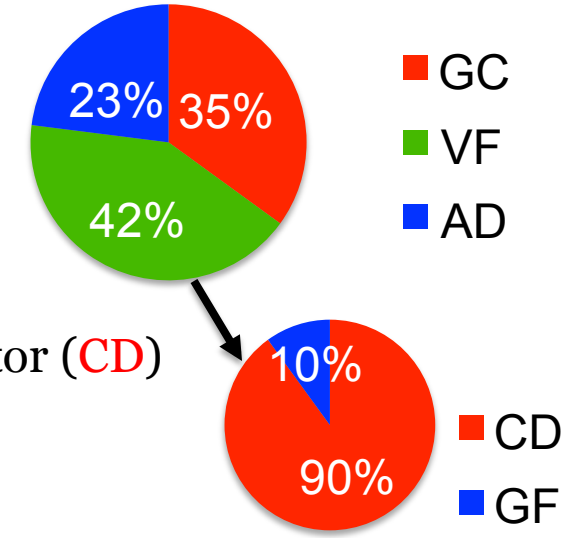
- Central FD with artificial dissipation
  - Explicit differentiation of physical flux [$9\times N^3\times V\times D$] (ED)
  - Computation of artificial dissipation term (AD)
- Comments:
  - Very lean numerical scheme
  - $\Gamma_p$ not needed for ideal gas



Performance Comparison:

# LAD: Cost Breakdown

- LAD
  - RHS Computations
    - Gradient Computation (GC)
    - Calculate viscous flux and differentiate fluxes (VF)
    - Determine artificial diffusivities (AD)
      - Compute $F_\nu$, $F_\beta$, and $F_\kappa$ + polyharmonic operator (CD)
      - Apply Gaussian filter (GF)



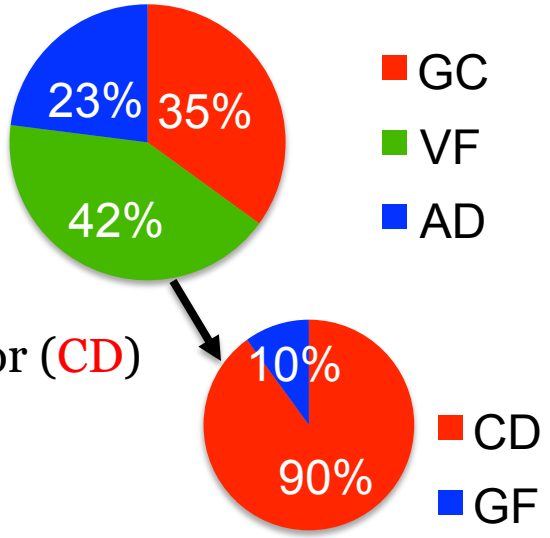

  - Apply implicit filter to conservative variables [10% of rhs]

- Variations:
  - Explicit vs implicit computation of gradients (for viscous terms)
    - 25% vs 35% of RHS computation
    - $[9\times N^3\times V\times D]$ vs $[(6+8)\times N^3\times V\times D]$ ➔ explicit is 40% cheaper
  - Explicit vs implicit differentiation of fluxes
    - 34% vs 41% of RHS computation
    - $[9\times N^3\times V\times D]$ vs $[(6+8)\times N^3\times V\times D]$ ➔ explicit is 45% cheaper
  - Explicit vs implicit filter

Performance Comparison:

# LAD: Cost Breakdown

- LAD
  - RHS Computations
    - Gradient Computation (GC)
    - Calculate viscous flux and differentiate fluxes (VF)
    - Determine artificial diffusivities (AD)
      - Compute $F_\nu$, $F_\beta$, and $F_\kappa$ + polyharmonic operator (CD)
      - Apply Gaussian filter (GF)
  - Apply filter to conservative variables [10% of rhs]




- Variations:
  - Explicit vs implicit computation of gradients
    - 25% vs 35% of RHS computation
    - $[9\times N^3\times V\times D]$ vs $[(6+8)\times N^3\times V\times D]$

almost no effect on accuracy

  - Explicit vs implicit computation of flux
    - 34% vs 41% of RHS computation
    - $[9\times N^3\times V\times D]$ vs $[(6+8)\times N^3\times V\times D]$

some effect on accuracy

  - Explicit vs implicit filter

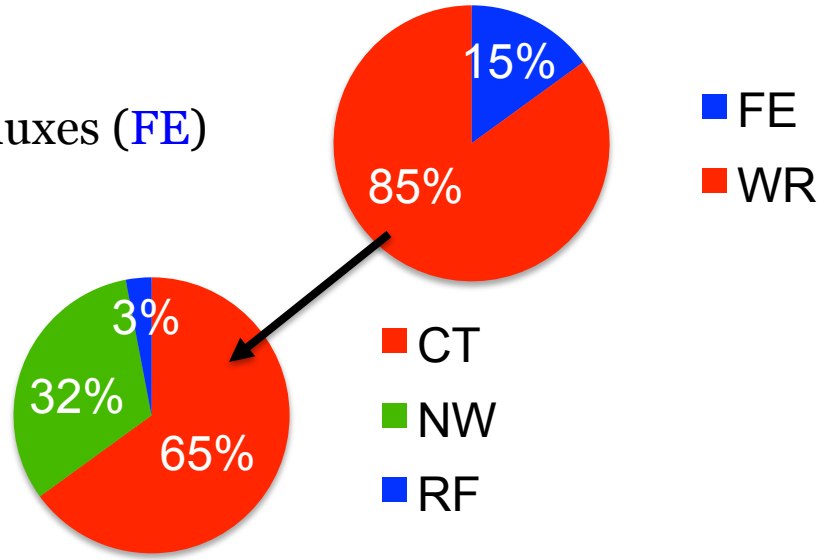
some effect on accuracy

Performance Comparison:

# WENO: Cost Breakdown



- WENO5 and CWENO5
  - Flux evaluation and differentiation of face fluxes (FE)
  - WENO reconstruction (WR)
    - Characteristic transform (CT)
    - Compute nonlinear weights (NW)
    - Calculate reconstructed flux, etc. (RF)

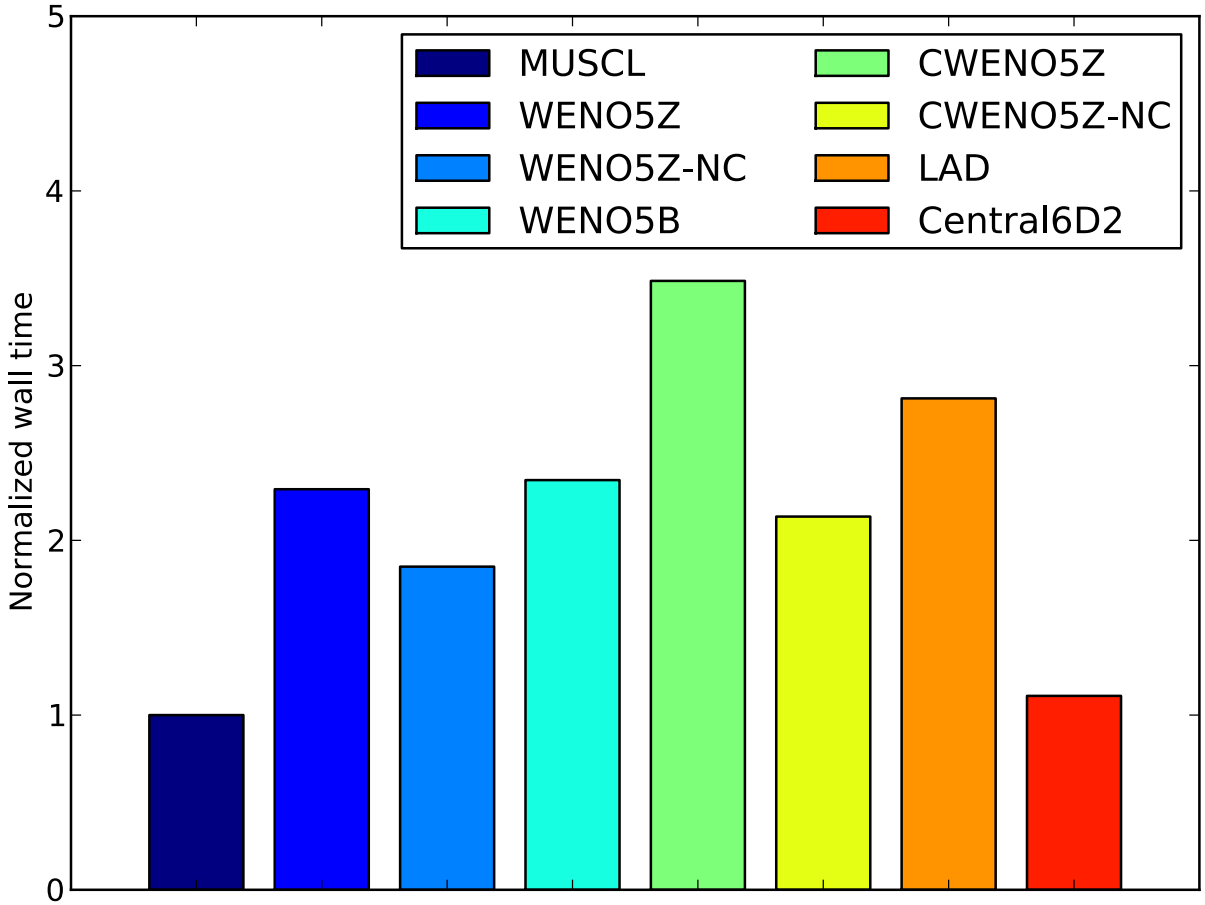



- Variations:
  - Characteristic transform
    - approximate characteristic transform* ➔ ~40% cheaper
  - WENO-Z
    - almost same cost as WENO5-JS
  - WENO6
    - slightly higher cost due to additional candidate stencil
  - CWENO5
    - higher cost due to compact reconstruction

*Su et al.(JSFM, 2011)

Performance Comparison:

# Relative Cost Comparison




- Parallel inviscid computation with $128^3$, box size $16^3$, and 20 cores
- All results are based on MUSCL2
- LAD scheme designed for viscous flows

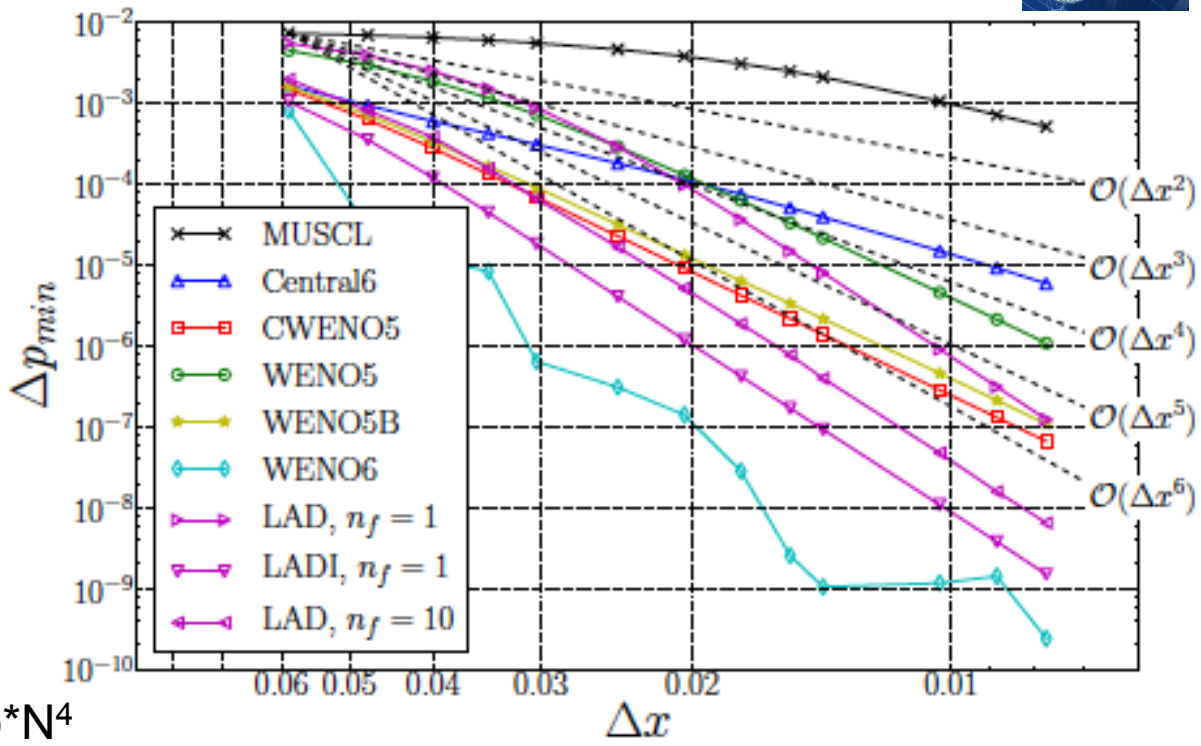
Performance Comparison:

# Cost Comparison: Isentropic Vortex

- Isentropic vortex

$$
\begin{aligned}
T &= T_\infty - \frac{V_s^2(\gamma-1)}{16 G_s \gamma \pi^2} e^{2G_s(1-r^2)} \\
\rho &= T^{\frac{1}{(\gamma-1)}} \\
u &= M_\infty - \frac{V_s}{2\pi}(y-y_0) e^{G_s(1-r^2)} \\
v &= \frac{V_s}{2\pi}(x-x_0) e^{G_s(1-r^2)}
\end{aligned}
$$

- smaller amplitude ($V_s$=0.5)
- periodic BCs [10x10]
- after ~13 rotations
- Estimated cost = cost per step*$N^4$




| $\Delta p_{min}$ | MUSCL | Central6 | CWENO5 | WENO5Z | WENO6 | LAD |
|---|---|---|---|---|---|---|
| $V_s = 0.5$ | | | | | | |
| 1E-4 | 1. /250. | 2E-3 /51.3 | 7.9E-4 /30.7 | 4.23E-3 /51.8 | 8.9E-5 /19.6 | 3.1E-4 /25.7 |
| 1E-5 | 1. /598. | 1.3E-3 /110. | 1.4E-4 /47.6 | 8.3E-4 /82.6 | 9.7E-6 /27. | 3.7E-5 /35.9 |

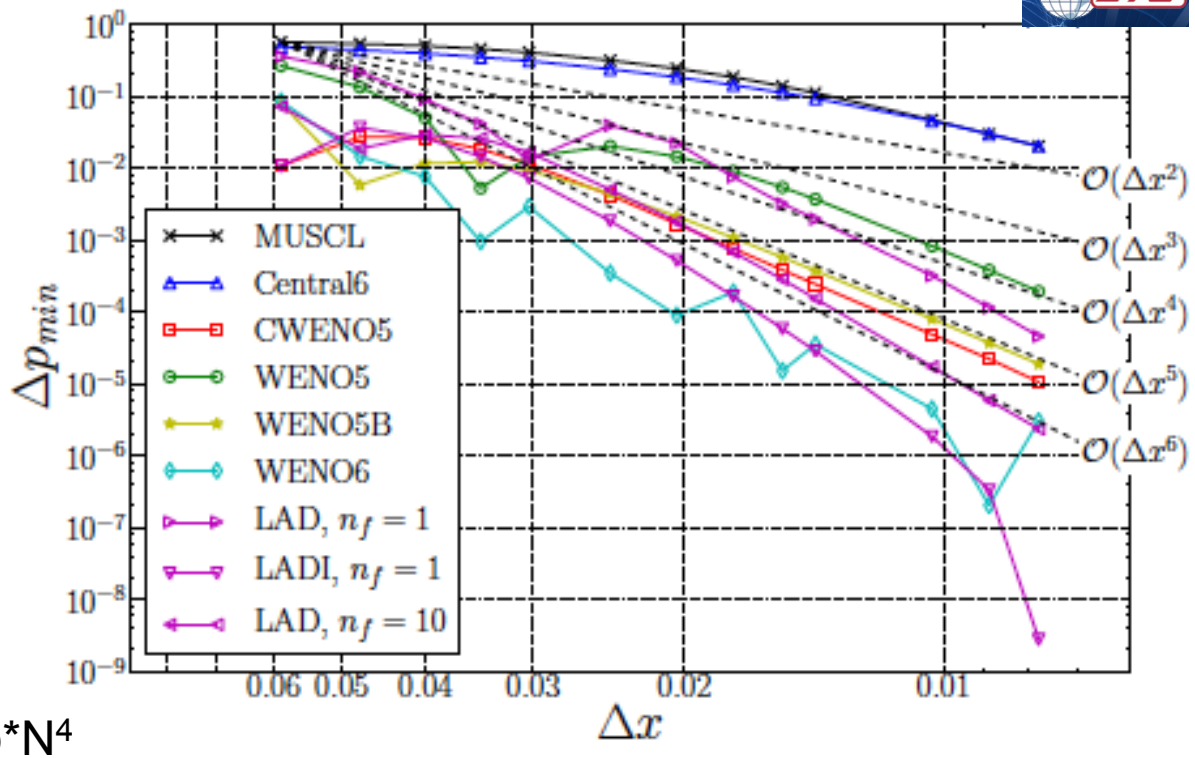
Performance Comparison:

# Cost Comparison: Isentropic Vortex

- Isentropic vortex

$$
\begin{aligned}
T &= T_\infty - \frac{V_s^2(\gamma-1)}{16 G_s \gamma \pi^2} e^{2G_s(1-r^2)} \\
\rho &= T^{\frac{1}{(\gamma-1)}} \\
u &= M_\infty - \frac{V_s}{2\pi}(y-y_0) e^{G_s(1-r^2)} \\
v &= \frac{V_s}{2\pi}(x-x_0) e^{G_s(1-r^2)}
\end{aligned}
$$

- larger amplitude ($V_s$=5)
- periodic BCs [10x10]
- after ~13 rotations
- Estimated cost = cost per step*$N^4$




| $\Delta p_{min}$ | MUSCL | Central6 | CWENO5 | WENO5Z | WENO6 | LAD |
|---|---|---|---|---|---|---|
| $V_s = 5.$ | | | | | | |
| 1E-3 | 1. /386. | 0.76 /350. | 1.4E-3 /54.3 | 7.9E-3 /93.5 | 1.9E-4 /36.8 | 5E-4 /44.6 |
| 1E-4 | 1. /892. | 0.58 /757. | 2.7E-4 /84. | 1.7E-3 /147. | 2E-5 /48.3 | 6E-5 /60.6 |

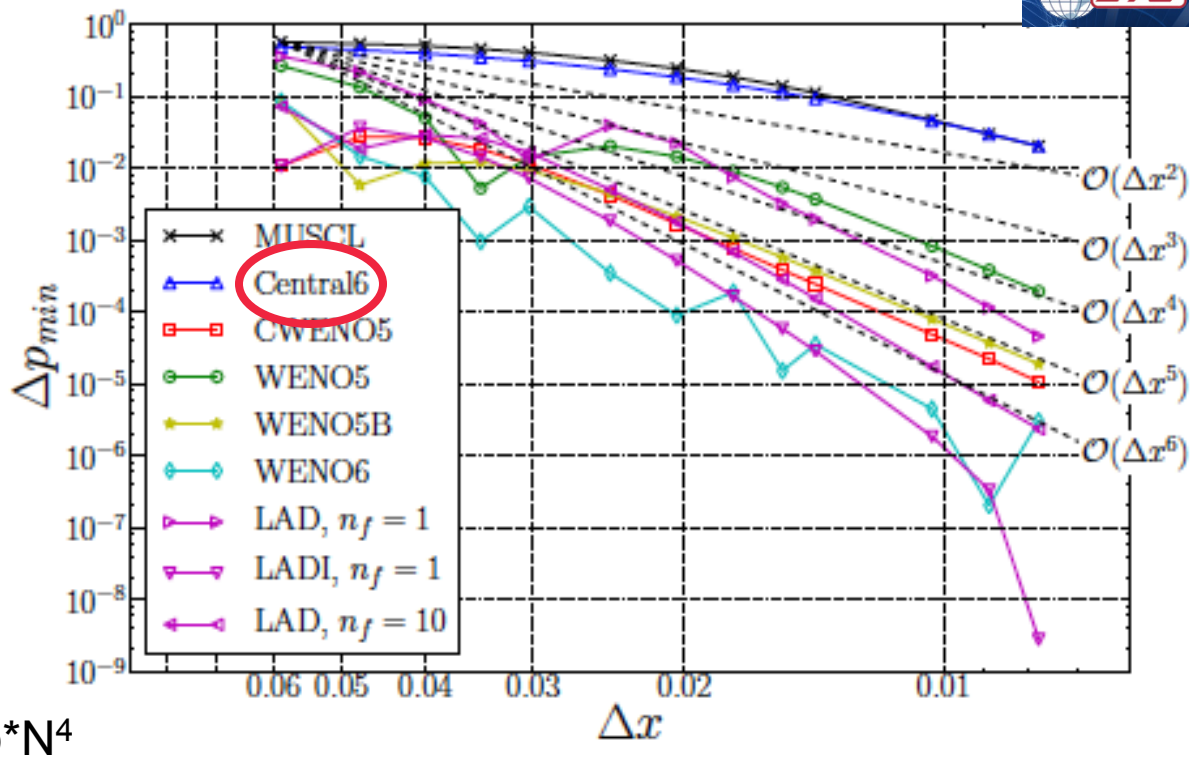
Performance Comparison:

# Cost Comparison: Isentropic Vortex

- Isentropic vortex

$$
\begin{aligned}
T &= T_\infty - \frac{V_s^2(\gamma-1)}{16 G_s \gamma \pi^2} e^{2G_s(1-r^2)} \\
\rho &= T^{\frac{1}{(\gamma-1)}} \\
u &= M_\infty - \frac{V_s}{2\pi}(y-y_0) e^{G_s(1-r^2)} \\
v &= \frac{V_s}{2\pi}(x-x_0) e^{G_s(1-r^2)}
\end{aligned}
$$

- larger amplitude ($V_s$=5)
- periodic BCs [10x10]
- after ~2 rotations
- Estimated cost = cost per step*$N^4$




| $\Delta p_{min}$ | MUSCL | Central6 | CWENO5 | WENO5Z | WENO6 | LAD |
|---|---|---|---|---|---|---|
| $V_s = 5.$ | | | | | | |
| 1E-3 | 1. /386. | 0.76 /350. | 1.4E-3 /54.3 | 7.9E-3 /93.5 | 1.9E-4 /36.8 | 5E-4 /44.6 |
| 1E-4 | 1. /892. | 0.58 /757. | 2.7E-4 /84. | 1.7E-3 /147. | 2E-5 /48.3 | 6E-5 /60.6 |

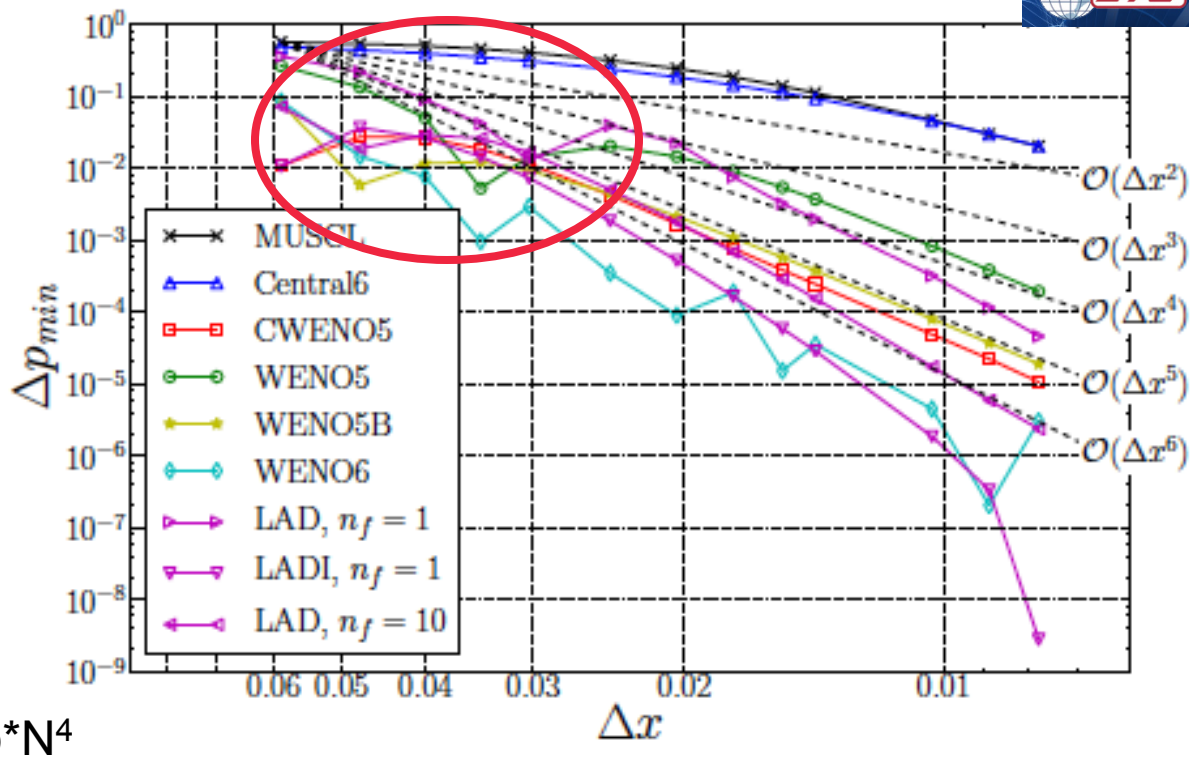
Performance Comparison:

# Cost Comparison: Isentropic Vortex

- Isentropic vortex

$$
\begin{aligned}
T &= T_\infty - \frac{V_s^2(\gamma-1)}{16 G_s \gamma \pi^2} e^{2G_s(1-r^2)} \\
\rho &= T^{\frac{1}{(\gamma-1)}} \\
u &= M_\infty - \frac{V_s}{2\pi}(y-y_0) e^{G_s(1-r^2)} \\
v &= \frac{V_s}{2\pi}(x-x_0) e^{G_s(1-r^2)}
\end{aligned}
$$

- larger amplitude ($V_s$=5)
- periodic BCs [10x10]
- after ~2 rotations
- Estimated cost = cost per step*$N^4$




| $\Delta p_{min}$ | MUSCL | Central6 | CWENO5 | WENO5Z | WENO6 | LAD |
|---|---|---|---|---|---|---|
| $V_s = 5.$ | | | | | | |
| 1E-3 | 1. /386. | 0.76 /350. | 1.4E-3 /54.3 | 7.9E-3 /93.5 | 1.9E-4 /36.8 | 5E-4 /44.6 |
| 1E-4 | 1. /892. | 0.58 /757. | 2.7E-4 /84. | 1.7E-3 /147. | 2E-5 /48.3 | 6E-5 /60.6 |

# Outline

Motivation/Introduction

Higher-Order Shock Capturing Schemes

Accuracy

Test Problems

Computational Performance

**Summary & Future Work**

*Summary of results and what tasks lie ahead.*

# Summary

- Central:
  - Current implementation did not perform well
  - Better spectral resolution than MUSCL
  - Attractive due to its low computational expense

- LAD:
  - High spectral resolution accuracy
  - Significant oscillations at discontinuities
  - Not as robust as WENO schemes, well suited for weak shocks
  - Time-step restriction due to high diffusivities (stretched meshes)

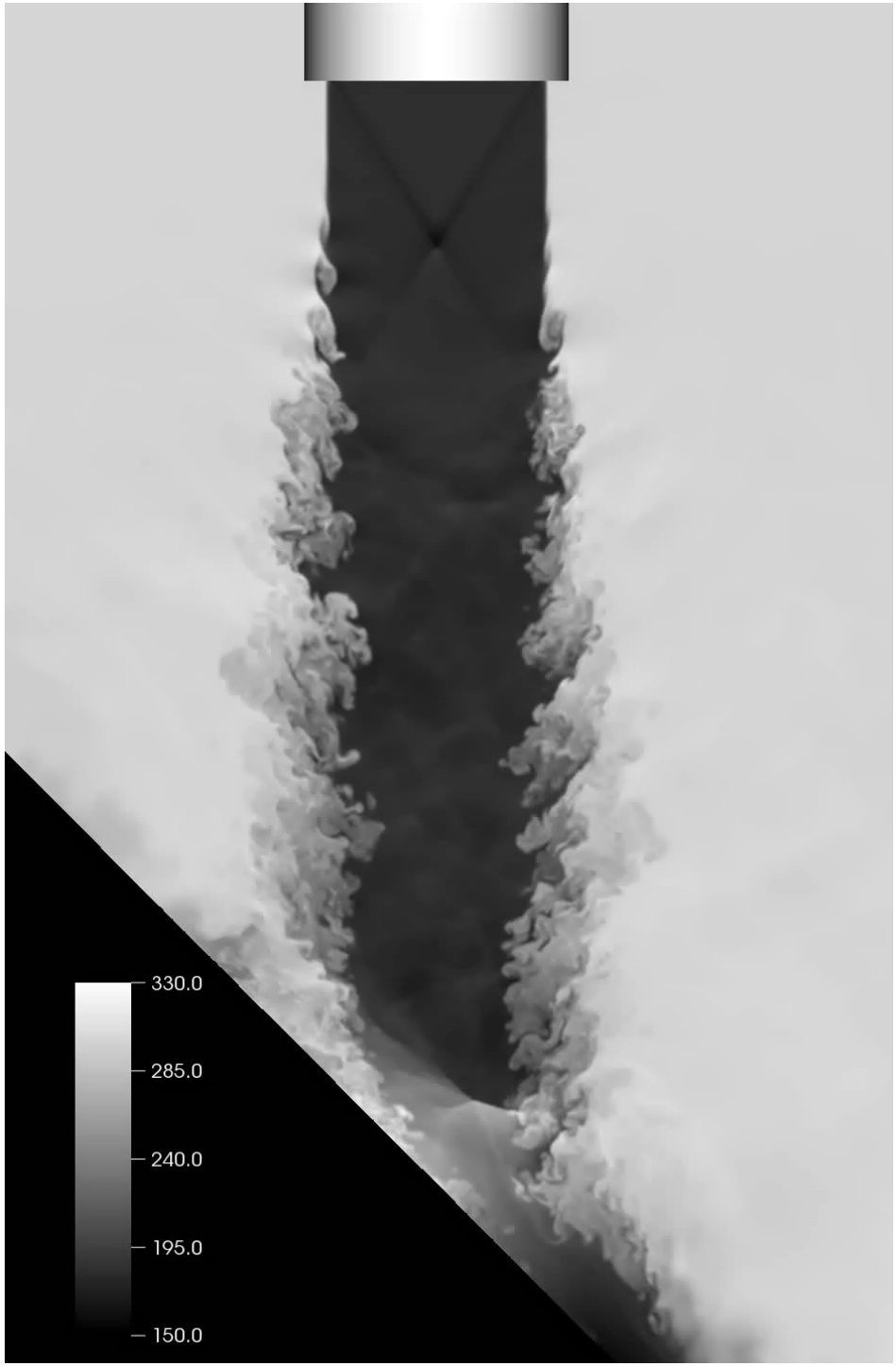
- WENO:
  - Great advances to WENO5 scheme by improved nonlinear weights and employing optimal schemes with higher spectral resolution
  - Presented new boundary treatment for compact WENO scheme
  - Most robust schemes

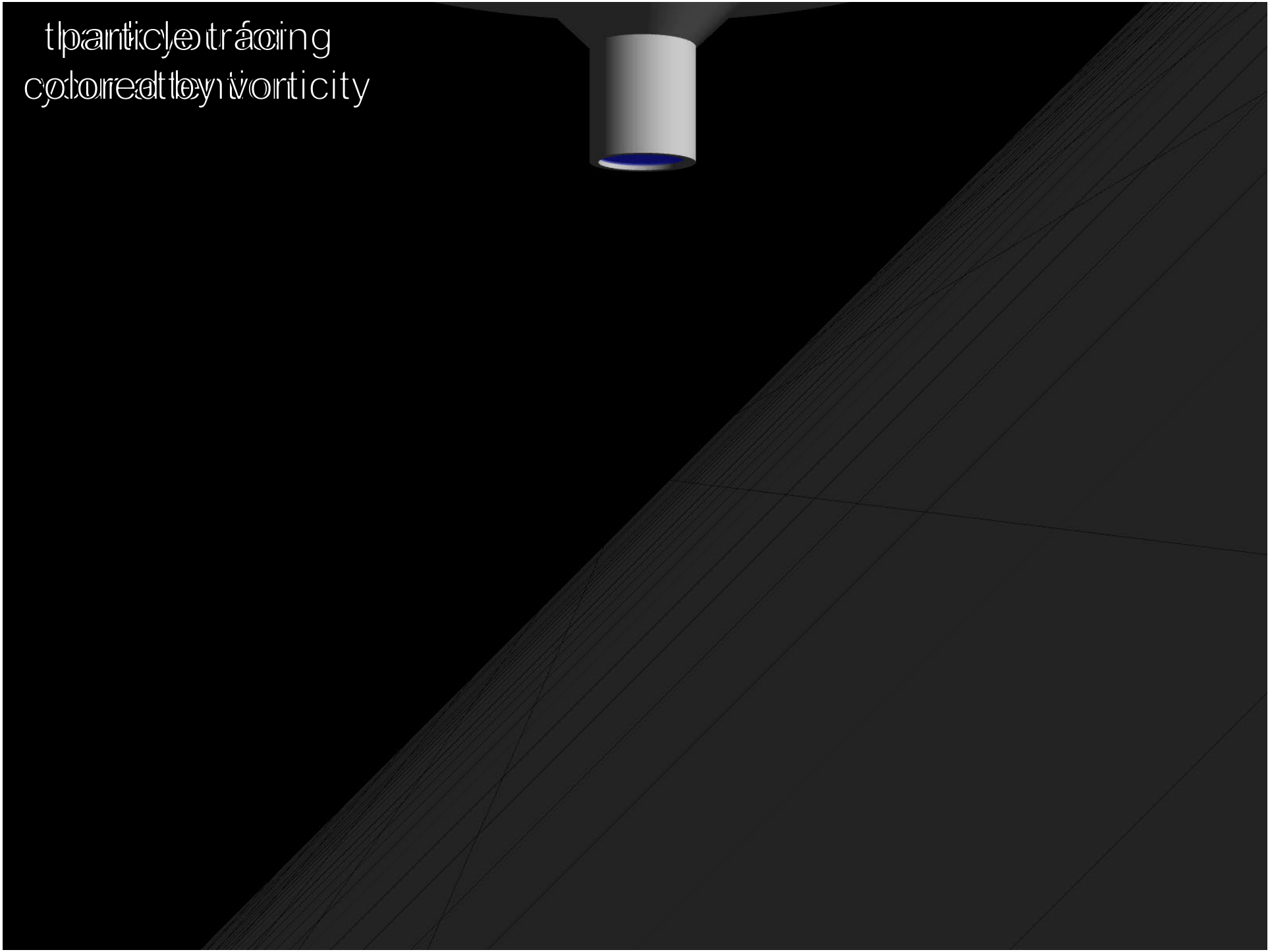
Summary and Outlook:

# Outlook

- Higher-Order Shock Capturing Scheme:
  - Working on more efficient higher-order compact scheme
  - Higher-order inter-level operators for block-structured Cartesian AMR (via Chombo) with limiting at shocks
  - Implementation of schemes for curvilinear meshes (metric terms)

- Higher-order immersed boundary method (AIAA-2014, Atlanta, Georgia)
  - Extension of work in Brehm *et al.* (2012,2013)
  - Viscous wall extension




particle tracing
colored by vorticity